

Fall 2022

Study Of Stochastic Market Clearing Problems In Power Systems With High Renewable Integration

Saumya Sakitha Sashrika Ariyarathne
Southern Methodist University, sakitha.shsu@gmail.com

Follow this and additional works at: https://scholar.smu.edu/engineering_management_etds

 Part of the Business Administration, Management, and Operations Commons, Electrical and Electronics Commons, Industrial Engineering Commons, Nonprofit Administration and Management Commons, Operational Research Commons, Operations and Supply Chain Management Commons, Power and Energy Commons, Strategic Management Policy Commons, and the Systems Engineering Commons

Recommended Citation

Ariyarathne, Saumya Sakitha Sashrika, "Study Of Stochastic Market Clearing Problems In Power Systems With High Renewable Integration" (2022). *Operations Research and Engineering Management Theses and Dissertations*. 16.
https://scholar.smu.edu/engineering_management_etds/16

This Dissertation is brought to you for free and open access by the Operations Research and Engineering Management at SMU Scholar. It has been accepted for inclusion in Operations Research and Engineering Management Theses and Dissertations by an authorized administrator of SMU Scholar. For more information, please visit <http://digitalrepository.smu.edu>.

STUDY OF STOCHASTIC MARKET CLEARING PROBLEMS IN POWER
SYSTEMS WITH HIGH RENEWABLE INTEGRATION.

Approved by:

Harsha Gangammanavar
(Operations Research and Engineering
Management)
Dissertation Committee Chairperson

Sila Çetinkaya
(Operations Research and Engineering
Management)

Eojin Han
(Operations Research and Engineering
Management)

Raanju R. Sundararajan
(Department of Statistical Science)

Jianhui Wang
(Department of Electrical and Computer
Engineering)

STUDY OF STOCHASTIC MARKET CLEARING PROBLEMS IN POWER
SYSTEMS WITH HIGH RENEWABLE INTEGRATION.

A Dissertation Presented to the Graduate Faculty of the

Lyle School of Engineering

Southern Methodist University

in

Partial Fulfillment of the Requirements

for the degree of

Doctor of Philosophy

with a

Major in Operations Research

by

Saumya Sakitha Sashrika Ariyarathne

M.S., Statistics, Sam Houston State University

B.S., Statistics and Operations Research, University of Peradeniya

December 09, 2022

Copyright (2022)

Saumya Sakitha Sashrika Ariyarathne

All Rights Reserved

Ariyarathne, Saumya Sakitha Sashrika M.S., Statistics, Sam Houston State University, 2018

B.S., Statistics and Operations Research, University of Peradeniya, 2015

Study of stochastic market clearing problems in power systems with high renewable integration.

Advisor: Harsha Gangammanavar

Doctor of Philosophy conferred December 09, 2022

Dissertation completed December 09, 2022

Integrating large-scale renewable energy resources into the power grid poses several operational and economic problems due to their inherently stochastic nature. The lack of predictability of renewable outputs deteriorates the power grid's reliability. The power system operators have recognized this need to account for uncertainty in making operational decisions and forming electricity pricing. In this regard, this dissertation studies three aspects that aid large-scale renewable integration into power systems. 1. We develop a nonparametric change point-based statistical model to generate scenarios that accurately capture the renewable generation stochastic processes; 2. We design new pricing mechanisms derived from alternative stochastic programming formulations of the electricity market clearing problem under uncertainty; 3. We devise a novel approach to coordinate strategic operations of multiple noncooperative system operators.

The current industry practices are based on deterministic models that do not account for the stochasticity of renewable energy. Therefore, the solutions obtained from these deterministic models will not provide accurate measurements. Stochastic programming (SP) can accommodate the stochasticity of renewable energy by considering a set of possible scenarios. However, the reliability of the SP model solution depends on the accuracy of the scenarios. We develop a nonparametric statistical simulation method to develop scenarios for wind generation using wind speed data. In this method, we address the nonstationarity issues that come with wind-speed time-series data using a nonparametric change point detection

method. Using this approach, we retain the covariance structure of the original wind-speed time series in all the simulated series.

With an accurate set of scenarios, we develop alternative two-stage SP models for the two-settlement electricity market clearing problem using different representations of the non-anticipativity constraints. Different forms of non-anticipativity constraints reveal different hidden dual information inside the canonical two-stage SP model, which we use to develop new pricing mechanisms. The new pricing mechanisms preserve properties of previously proposed pricing mechanisms, such as revenue adequacy in expectation and cost recovery in expectation. More importantly, our pricing mechanisms can guarantee cost recovery for every scenario. Furthermore, we develop bounds for the price distortion under every scenario instead of the expected distortion bounds. We demonstrate the differences in prices obtained from the alternative mechanisms through numerical experiments.

Finally, we discuss the importance of distributed smart grid operations inside the power grid. We develop an information and electricity exchange system among multiple distribution systems. These distribution systems participate/compete in common markets where electricity is exchanged. We develop a standard Nash game treating each distribution system (DS) as an individual player who optimizes their strategies separately. We develop proximal best response (BR) schemes to solve this problem. We present results from numerical experiments conducted on three and six DS settings.

TABLE OF CONTENTS

LIST OF FIGURES	ix
LIST OF TABLES	x
ACKNOWLEDGMENTS	xi
CHAPTER	
1. Introduction	1
1.1. Electricity Market	2
1.1.1. Market Operations and Models	5
1.1.2. Electricity Pricing Models	6
1.1.2.1. Deterministic Models	7
1.1.2.2. Stochastic Models	7
1.2. Brief Overview of Stochastic Programming	8
1.2.1. Two-stage SP Models	8
1.2.2. Non-anticipativity	9
1.2.3. Algorithms	10
1.3. Contributions	10
1.4. Dissertation Outline	11
2. Change Point-based Statistical Model of Wind Time Series	13
2.1. Introduction	13
2.2. Methodology	17
2.2.1. Change Point Detection	23
2.2.2. Stationary Process Simulation	25
2.2.2.1. Parametric	25
2.2.2.2. Nonparametric	26

2.2.3. Estimation	26
2.3. Application	28
2.3.1. Economic Dispatch Problem	28
2.3.2. Experiments	30
2.3.3. Change Point Detection	30
2.3.4. Simulation of Wind Speeds	32
2.3.5. Performance in Economic Dispatch Problem	35
2.4. Conclusions	38
3. New Models, Pricing Mechanisms, and Interpretations for Stochastic Market Clearing Problem	40
3.1. Introduction	40
3.2. Stochastic Market Clearing	42
3.2.1. Market Setting	42
3.2.1.1. Model Elements	42
3.2.2. Market Metrics	45
3.3. Models and Pricing Mechanisms	47
3.3.1. Canonical Stochastic Programming Model	48
3.3.1.1. Pricing Mechanism 1	49
3.3.2. Mean-vector Stochastic Programming Model	51
3.3.2.1. Pricing Mechanism 2	55
3.3.3. State-vector Stochastic Programming Model	61
3.3.4. Pricing Mechanism 3	65
3.4. Experiments	71
3.4.1. Test System	71
3.4.1.1. Relationships Between Dual Optimal Solutions	72

3.4.1.2. Performance of Pricing Mechanism \mathcal{R}^m	73
3.4.1.3. Performance of Pricing Mechanism \mathcal{R}^s	74
3.5. Conclusion	76
4. Multiagent Optimization for Coordinated Transmission-distribution System	78
4.1. Introduction	78
4.1.1. Multiagent markets	79
4.1.2. Best Response Schemes	79
4.2. Market Setting and Models	81
4.2.1. DS optimization problem	82
4.2.2. Mathematical Structure	84
4.3. Proximal BR Algorithms	87
4.3.1. Cyclic Order Coordinated Updates	88
4.3.2. Cyclic Order Immediate Updates	89
4.3.3. Random Order Immediate Updates	90
4.4. Experiments	91
4.4.1. Problem Settings	91
4.4.2. Performance of the Algorithms	92
4.4.3. Convergence of Inter Connections	93
4.4.4. Market Prices	94
4.5. Conclusions	95
5. Conclusion	97
BIBLIOGRAPHY	100

LIST OF FIGURES

Figure	Page
1.1. Electricity market setting.	4
2.1. Work flow to utilize NWP forecast for decision making in power systems using deterministic and stochastic approaches.	15
2.2. Autocovariance plots of sub-hourly residual data for February 19 th , 2011.	21
2.3. Autocovariance plots of hourly averaged residual data from February 19 th , 2011.	22
2.4. September 15, 2011.	31
2.5. Results from the Rolling Horizon Economic Dispatch model.	37
3.1. Network diagram of six-node system.	72
3.2. Results illustrating cost recovery in expectation under \mathcal{R}^m	74
3.3. State-vector cost recovery by scenario.	75
3.4. State-vector price distortion by scenario.	76
4.1. Market setting	81
4.2. Demand inverse curve	85
4.3. Convergence of Interconnections	94
4.4. Market prices.	95

LIST OF TABLES

Table	Page
2.1. Correlation matrix of the residual series \mathbf{r}_t (Feb. 19, 2011).	18
2.2. The p-values from multivariate stationarity test for the five wind farm locations in Oklahoma.	19
2.3. Change point analysis: Series length, significance level, number of series. Starting day: September 15 th , 2011.	33
2.4. Correlation comparison of the NWP forecasted original series vs. simulated series. (Feb. 19, 2011).	34
3.1. Summary of dual solutions from different SP models.	73
4.1. Three DSs setting interconnection setting.	91
4.2. Six DSs setting interconnection setting.	92
4.3. Summary of performance of cyclical order coordinated updates (CC), cyclical order immediate updates (CI), and random order immediate updates (RI).	93

ACKNOWLEDGMENTS

Firstly, I would like to express my sincere gratitude to my advisor Prof. Harsha Gangammanavar for the continuous support of my Ph.D. study and related research, his patience, motivation, and immense knowledge. His guidance helped me in all the research and writing this thesis. I could not have imagined having a better advisor and mentor for my Ph.D. study.

Besides my advisor, I would like to thank the rest of my thesis committee: Prof. Sila Çetinkaya, Prof. Eojin Han, Prof. Raanju R. Sundararajan, and Prof. Jianhui Wang for their insightful comments and encouragement. Last but not the least, I would like to thank my family: my wife, parents, and my brothers for supporting me spiritually throughout writing this thesis.

Chapter 1

Introduction

Electricity usage has significantly increased over years all over the world from the household level to the industry level. Electricity has almost become a basic need of human life. The reason behind this influx in demand for electricity is the increased use of electronic devices that serve two purposes: 1. they save either money or time, and 2. they make life comfortable. On the other hand, electricity generation disrupts human life by emitting greenhouse gases that cause global problems such as climate change and global warming.

Fossil fuel is the primary resource for electricity generation. According to the US Energy Information Agency (EIA), fossil fuel was the leading contributor to U.S. electricity production in 2021, accounting for more than 60%. Burning fossil fuels is extremely harmful to the environment. Further, electricity generation has to compete with other industries, such as transportation, for the same depleting resource, fossil fuels. Therefore, consumers must pay a premium price for electricity to keep up with other sectors [1]. To make matters worse, the recent decision of the Organization of the Petroleum Exporting Countries (OPEC) to reduce oil production by 2 million barrels per day has already impacted these price increases [2,3].

Moreover, electricity generation is also one of the most significant contributors to greenhouse gas emissions. The transportation industry has been the biggest over the past years, accounting for about 27%. However, with the introduction of electric vehicles, the rate of greenhouse gas emissions is slowly declining in the transportation industry. On the other hand, the electricity needed for these vehicles adds up to the already fast-growing electricity demand. Therefore, electricity generation is in dire need of a sustainable solution.

Renewable energy resources such as geothermal, hydroelectric, wave, tidal, biofuel, solar thermal, and wind have been gaining much attention since the late twentieth century as viable and environmentally friendly solutions to this energy crisis. The U.S. EIA reported that renewable energy resources contributed about 20% of the total electricity generation

in 2021 [4]. Further, by 2050 the renewable contribution is projected to be around 42% of the U.S. electricity generation [5]. Therefore, authorities have mandated using renewable energy in the electricity generation portfolios. Wind energy is one of the most economical renewable energy resources out of the bunch [6]. In the United States, electricity production from wind resources contributes to over 7.3% of the total electricity generation. Solar is another excellent resource that accounts for about 2.8% of the total electricity generation in the United States. These resources are cheap and address the environmental issues raised by fossil fuel burning.

Integrating large-scale renewable energy resources into the power grid poses several operational and economic challenges. These challenges are attributed to the inherently stochastic nature of these resources. In addition to uncertainty, wind energy resources also exhibit significant fluctuation in their output in a short duration of time. Such stochastic and intermittent nature is also a common characteristic in solar generation. These characteristics also exacerbate the difficulty of obtaining an accurate forecast of wind and solar generation. To address these fluctuations, system operators must incorporate large amounts of operating reserves in the power network [7]. These expensive operating reserves result in an overall increase in operational costs negating the cost benefits of renewable wind and solar generation.

1.1 Electricity Market

The Western, Eastern, and Texas power grids combine to form the United States power grid. Within these interconnections, there are vertically integrated markets and wholesale markets. The vertically integrated market is governed by a single body that oversees all electricity generation, transmission lines, distribution lines, and delivery decisions within its geographic borders. Since this is a centralized monopoly, there are many issues, especially regarding reliability. Despite these issues, vertically integrated still exist in the U.S. power grids. The federal government intervened to address these problems founding Federal Energy Regulatory Commission(FERC) in 1977 to overlook the electricity market at the federal level. The primary responsibility of the FERC is to deploy policies, maintain the markets' reliability, and develop wholesale markets to sell and transport electricity across borders.

This intervention did not sit well with the private sector, and hence in 1990, they came to the consensus of developing Independent System Operators (ISO), non-profit organizations. ISO allows privately owned generators, transmission lines, and distribution lines to compete to sell their products to customers. This deregulated retail market incentivizes market participants to keep their prices low and innovate operations. There are seven ISOs in the U.S. power grid; 1. California Independent Service Operator (CAISO), 2. Electric Reliability Council of Texas (ERCOT), 3. Independent Service Operator New England (ISO-NE), 4. Midcontinent Independent System Operator (MISO), 5. New York Independent Service Operator (NYISO), 6. PJM Interconnection (PJM), 7. Southwest Power Pool (SPP).

The power grids mentioned above have many entities separated by their geographical locations and are extremely large to handle using a single authority. Therefore, the U.S. power grid operates on several levels. Each level operates at different voltages to reduce power losses during electricity transportation. Voltages are converted using transformers at each level for safety before finally reaching the end users. This complex system is too large to model as a single decision-making process. Thus, there are separate decision-making entities at each level. Since the decisions of one level depend on the other's decisions, overlapping optimization models are implemented over several periods to give enough time to make necessary adjustments.

Electricity market operations start at the Transmission System (TS) level (see Figure 1.1). A dedicated ISO controls the whole operation in the TS. The responsibility of the TS is to ensure fast, safe, reliable, and economical electricity transportation from suppliers to distributors/loads. To aid these transactions and to connect all TS entities, there are substations known as buses. Typically, generators, large-scale power storage units, and distributors are connected to their nearest substation depending on the distance and cost. There are transmission lines connecting these buses, and altogether this is known as the TS network.

Typically, large-scale generators are in remote areas. Therefore, the electricity must travel long distances to meet the distributors. When electricity travels long distances, the losses increase due to power flow phenomena. Thus, the TS network works at high voltages to reduce these power losses. These voltages may vary between 11kV and 33kV depending

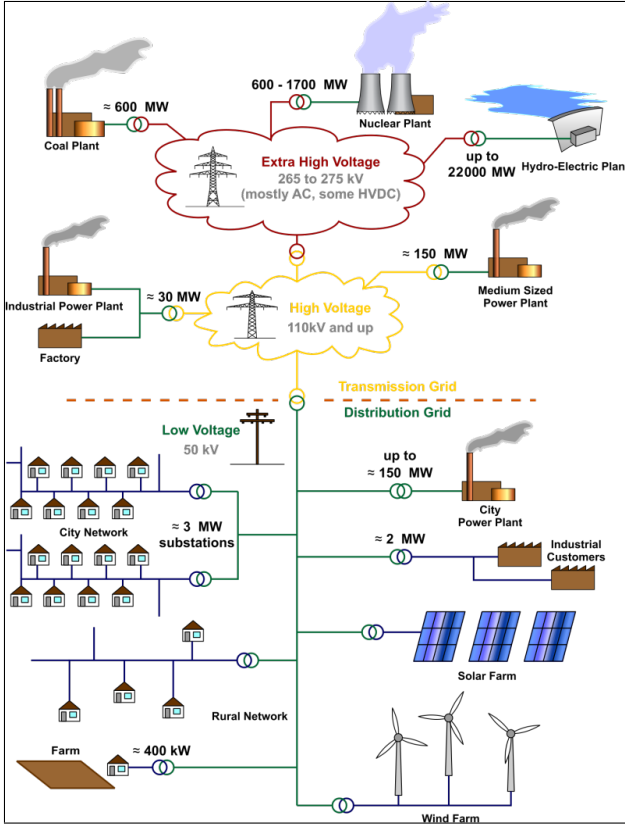


Figure 1.1: Electricity market setting.¹

on the distance.

The next level of the power grid is the Distribution System (DS). The decision at the DS level mainly depends on the TS decisions, and hence typically, they make their decisions after TS decisions. DSs also have access to small generators, which usually produce cheaper electricity than buying from the TS. Therefore, it is safe to assume that these generators consistently generate the maximum capacities. Similar to the TS, DS also has buses and distribution lines to create the distribution network. However, these networks are small compared to the transmission network and closer to the consumers. Therefore, the network is operated at lower voltage levels.

¹Source: By MBizon - Own work Originally derived from de:Datei:Stromversorgung.png, CC BY 3.0, <https://commons.wikimedia.org/w/index.php?curid=9676556>

1.1.1 Market Operations and Models

To start the operations, the ISO solves an optimization model known as the day-ahead Unit Commitment (UC) problem [8]. The day-ahead UC decisions are available to the market participants a day before the actual dispatch. Similarly, there is a real-time UC problem which solves hours before the actual market. The real-time UC decisions fine tunes the day-ahead UC decisions. The exact nature of problems (day-ahead, real-time UC, etc.) differs among various ISO [9, 10]. The UC problem determines the most economical order of power-generating unit operations while meeting the demand forecast. The UC model decisions allow the ISO to select or switch on cost-effective generators and switch off expensive generators while maintaining the system's reliability. Generators' start-up costs, shutdown costs, and ramping capabilities affect these on-off decisions. Hence, these are modeled as constraints in the UC problem. The UC problem contains both continuous and binary variables resulting in a MIP.

We can find extensive work on the UC problem in the literature. An integer programming (IP) approach has been proposed in [11] to decide UC decisions. A mixed-integer programming (MIP) formulation for the UC problem has been discussed in [12] and [13]. A two-stage stochastic programming model has been employed to handle the uncertainty in wind generation in [14]. The authors have discussed the benefits of combining reserves with stochastic decisions that can lead to more robust solutions. A similar approach has been taken in [15], where they discuss the importance of reserves with large-scale wind generation by ignoring transmission network constraints. A mixed-integer stochastic programming model and a progressive-hedging algorithm based solution method with tractable solving time have been developed for the UC problem in [16]. In [17], the authors have discussed the advantages of stochastic programming (SP) models over the deterministic models for the UC problem. A SP-based UC model for a single bus system has propped in [18]. Including sub-hourly dispatch constraints, a SP UC model has been developed in [19]. To ease computational difficulties with added constraints, authors have used a modified Benders decomposition method to solve the model. In [20], a chance constraint SP model has been developed for the UC problem. The model exhibits both chance constraints SP and two-stage SP features. A robust optimization approach has been proposed for the UC problem in [21]. A comprehensive

review of the UC problem can be found in [22], and different UC models can be found in [23].

Once the UC decisions are fixed, the ISO solves another optimization problem known as the economic dispatch (ED) model. The objective of this model is to decide the most economical generation amounts for each generator while meeting the demand. The capacity limits and power flow laws restrict these decisions. Similar to the UC problem, the ISO solves a day-ahead ED model and a real-time ED model. For instance, California ISO (CAISO) releases the day-ahead dispatch schedule at 1:00 PM on the prior day of the actual trading and real-time results 45 minutes prior to the start of the trading hour. The current practice in the industry is to solve a deterministic model using forecasted generation amounts for renewable generation. We provide a thorough review of renewable energy forecasting in section 2.

To coordinate the day-ahead and real-time decisions, a deterministic approach has been discussed in [24, 25]. In [25], the day-ahead model provides economical operating direction, and the real-time model provides optimal dispatch decisions. The benefits of using SP models over deterministic ones for ED problems have been discussed in [26, 27].

A SP framework has been proposed in [28] to address the uncertainty in the ED model with renewable energy. The authors have shown that solving the SP model in different time scales can significantly improve the quality and the cost of the dispatch. A two-stage stochastic convex program has been introduced in [29]. The model includes frequency constraints that incorporate under-frequency load shedding. An adaptive multi-period robust ED model has been discussed in [30]. The authors model the dispatch operations using a two-stage structure with a rolling horizon framework. A quadratically constrained quadratic program for the ED problem has been proposed in [31] with an efficient solution framework. A mixed-integer quadratic constrained model has been employed in [32].

1.1.2 Electricity Pricing Models

After solving the ED problem, the ISO must compensate all generators to cover their costs. In most other industries, a separate pricing model determines the pricing solutions, especially in manufacturing [33]. However, in the electricity market, developing a separate pricing model is complicated due to physical limitations. Therefore, the ISO utilizes the dual

information of the ED model to develop prices for the market participants. The ISO has little to no control over the resulting prices. Hence, to cover the costs of market participants, the ISO often has to make payments that are not necessarily supported using dual prices. These are known as the up-lift payments, and achieving zero up-lift payments is known as cost recovery [34]. These properties are important in attracting investors to the market [35]. Furthermore, it is desirable to have enough payments from the loads to cover the costs of generators. This is known as the revenue adequacy for the ISO. Therefore, designing an accurate pricing mechanism is an essential task. The presence of uncertainty in the ED model makes developing an accurate pricing mechanism more difficult.

1.1.2.1 Deterministic Models

There have been many attempts at developing pricing mechanisms in the literature. Operating characteristics of generators result in nonconvex models for the clearing prices. [36] has discussed the properties of prices with deterministic nonconvex markets. Failure to achieve cost recovery has dangerous long-term consequences. A pricing structure for two suppliers with nonconvex costs is discussed in [37]. Electricity market clearing prices are affected by both UC, and ED problems [38]. Therefore, locational marginal prices (LMP) are sensitive to UC commitment solutions. Biasness toward a set of participants results in lower average prices. The inefficiencies of suboptimal UC solutions are discussed using several test systems in [39, 40]. In [41], the authors have used different algorithms to obtain ED solutions and discussed the role of up-lift payments for each algorithm.

1.1.2.2 Stochastic Models

Furthermore, we have discussed the SP models for ED problems, and hence there are studies conducted to develop pricing mechanisms using two-stage SP models. Stochastic linear programming based pricing mechanism has been proposed in [42]. The proposed pricing mechanism achieves revenue adequacy in expectation. However, there are separate price schemes for generators and loads. This discontinuation could result in undesirable prices for a set of market participants. A two-stage SP based pricing model has been proposed in [43, 44] that achieves cost recovery and revenue adequacy in expectation. The properties of the proposed pricing mechanism have been further discussed in [45]. The authors have shown

bounds for the unit price deviations in the day-ahead and real-time markets. In [46], cost recovery by scenario is achieved by compensating for the maximum and minimum deviations in each scenario. A scenario-wise revenue-adequate pricing mechanism has been proposed in [47]. With the use of virtual bids, [48] has shown cost recovery for every scenario. However, this is only achievable in a convex setting. Given the extensive role of SP in designing operations and prices in power systems, we provide a brief overview of SP next.

1.2 Brief Overview of Stochastic Programming

Stochastic programming (SP) is a mathematical optimization framework for modeling decisions-making problems involving uncertainty. In SP problems, some or all parameters of the optimization model can be uncertain but with known probability distributions. In addition to power systems, SP models are applied in quite a range of applications. These include fleet assignment problem in airline industry [49], production planning problem [50], and water management problems [51]. The textbooks by [52] and [53] serve as excellent resources for SP. We refer the reader to [54] for elaborate presentation of SP applications. We review some key SP elements relevant in this dissertation here.

We can write a generic stochastic programming model as follows:

$$\min_x \left\{ \mathbb{E}[F(x, \tilde{\omega}), x \in \mathcal{X}(\omega) \text{ a.s.}] \right\}, \quad (1.1)$$

where $x \in \mathbb{R}^n$ is the n dimensional decision vector and $\tilde{\omega} \in \mathbb{R}^d$ is a random vector. We capture the associated uncertainty through the random vector $\tilde{\omega}$ defined on a probability space. A realization of this random vector, denoted by ω is known as a scenario.

1.2.1 Two-stage SP Models

Two-stage SP models are applicable when decision variables of the first stage affect the second-stage decisions. Usually, the two stages are apart in time, and hence the second stage parameters are uncertain at the time first-stage decisions are made. We can extend

the generic SP formulation in (1.1) to state the two-stage SP model as follows:

$$\min_{x \in \mathcal{X}} f(x) = F_0(x) + \mathbb{E}\{F(x, \omega)\}, \quad (1.2a)$$

$$F(x, \omega) = \min_y g(y, \omega), \quad (1.2b)$$

$$\text{s.t. } y \in \mathcal{Y}(x, \omega). \quad (1.2c)$$

Here, function $g(y, \omega)$ depends on a realization of the random vector $\tilde{\omega}$, and the decision variable y in a set \mathcal{Y} which depends on the first-stage decision and the random vector. The first-stage decisions x must be made here-and-now before the realization of the random vector. Therefore, they are also known as non-anticipative decisions. The second-stage decisions are made in the future depending on the realization of the random vector. Hence, they are anticipative. Furthermore, a two-stage stochastic linear programming problem is a relatively complete recourse if the second stage problem is feasible for all $x \in \{x | Ax = b\}$ and $\omega \in \Omega$.

1.2.2 Non-anticipativity

When we solve a deterministic model, the decisions are fixed. The same applies to the SP models when we know all the realizations of the random vector (scenario) at the time first-stage decisions are made. That is, the SP model reduces to a deterministic model known as the extensive scenario or the deterministic-equivalent problem. For each scenario, we can also solve a deterministic problem, known as the scenario problem in the SP literature. However, the first-stage solutions of these scenario problems are unimplementable since each scenario problem will result in a different first-stage solution. That is because the scenario problem anticipates the realization of the random variables.

To achieve an implementable first-stage solution, we must have a single solution for the first-stage decisions despite the realization of the random vector. In the canonical two-stage SP model, this non-anticipativity is achieved by modeling all the first-stage decisions independent of the scenarios. There are two more modeling approaches, mean-vector and state-vector, to achieve non-anticipativity. For these approaches, the first-stage decisions are modeled as scenario-dependent variables. Then a restriction is imposed on the scenario-

dependent first-stage variables to have the same value despite the scenario. The mean-vector formulation imposes that all first-stage decisions must equal their mean value, and the state vector imposes this restriction using auxiliary variables. In our studies, we discuss all three types of two-stage SP models with the added linearity restriction.

1.2.3 Algorithms

SP models are one of the most challenging classes of optimization models to solve, especially with a large number of scenarios, which is the case in most practical situations. Therefore, formulating the extensive scenario form and using off-the shelf deterministic optimization algorithms are not suitable for solving SP models. There are a few efficient algorithms to solve SP models available in the literature.

The SP solution methods fall under two broad categories, stage decomposition and scenario decomposition methods. The L-shaped method is a stage decomposition algorithm. The L-shaped method introduced in [55] is the most widely used SP algorithm. The algorithm starts with a feasible solution to the master problem. Then solves the subproblems for one scenario at a time, fixing the first-stage decisions. Depending on the subproblem solution, a feasibility cut or an optimality cut is added to the model.

On the other hand, the progressive Hedging Algorithm (PHA) is another SP algorithm that takes advantage of scenario decomposition. The algorithm was introduced in [56]. The algorithm starts with solving scenario problems by treating the first-stage decisions as a scenario-dependent decision vector. Since the first stage is non-anticipative, it is not necessary to have feasible first-stage decisions. Once all scenario-dependent first-stage decisions are determined, we compute the expected first-stage decision to obtain a non-anticipative first-stage decision vector. Note that the mean-vector formulation supports this process as it has scenario-dependent first-stage decisions and non-anticipativity constraints that set first-stage decisions to their mean value.

1.3 Contributions

This dissertation is aimed at studying three aspects that aid large-scale renewable integration into power systems. The main contributions are as follows.

1. *Wind-speed simulation.* In chapter 2, we introduce parametric and nonparametric

statistical methods to simulate wind-speed time series. We discuss the nonstationarity of wind-speed time series and how it plays a crucial role in developing simulations. We use a nonparametric change point detection method to identify stationary segments within the nonstationary series. We apply the method to simulate wind speeds and solve an electricity market-clearing model to show the price changes with the wind speeds.

2. *Pricing mechanisms.* In chapter 3, we develop two new pricing mechanisms using alternative stochastic programming models based on two different representations of non-anticipativity. The first mechanism utilizes the mean-vector formulation of non-anticipativity that has an efficient algorithm to obtain numerical solutions. The pricing mechanism achieves cost recovery and revenue adequacy in expectation and has bounds for price distortion under every scenario. The second pricing mechanism uses the state-vector form of non-anticipativity. The pricing mechanism achieves revenue adequacy in expectation and cost recovery under every scenario. We also show the bounds for the price distortion under every scenario. Finally, we prove the relationships to obtain the state-vector formulation results using the computationally efficient mean-vector solutions. We demonstrate our results using a six-bus test example.
3. *Coordination system.* We develop a system to coordinate operations between the transmission (market) and distribution systems to accommodate smart grid operations in chapter 4. We discuss a market setting with multiple markets and distribution systems that perform as a standard nash game. We develop algorithms to achieve a Nash equilibrium using proximal best response schemes that guarantee convergence. Using numerical experiments, we evaluate the performance of three algorithms and interpret the results from distribution systems, markets, policymakers, and customer perspectives.

1.4 Dissertation Outline

In section 2.1, we introduce wind speed modeling for renewable electricity generation and the nonstationarity of the wind speed time series. Then we propose a method to tackle the

nonstationarity using a nonparametric change point detection method to separate the time series into stationary segments in section 2.2. Then we use an electricity market clearing model to show the effects, especially pricing, using the change point based model in section 2.3. We dedicate chapter 3 to discuss different modeling approaches to the electricity market clearing problem. In section 3.2, we describe the market setting and move on to section 3.3 to discuss SP approaches to the electricity market clearing problem. In this section, we develop two alternative models to the two-settlement electricity market clearing problem using non-anticipativity constraints. We also develop two new pricing mechanisms from each newly built model and analyze their properties. We illustrate our findings in our numerical experiments for the new pricing mechanisms in section 3.4. In chapter 4, the discussion is on developing a coordination system for the power systems. In section 4.2, we describe the market setting considered in this study and build the optimization model. We present different algorithms to solve the developed model in section 4.3, and finally, in section 4.4, we illustrate the numerical results of the study.

Chapter 2

Change Point-based Statistical Model of Wind Time Series

2.1 Introduction

Wind energy is one of the most economical renewable energy resources [6]. In the United States, electricity production from wind resources contributes to over 7.3% of the total electricity generation. However, the integration of a large amount of wind energy resources in power systems poses several operational and reliability challenges. These challenges are attributed to the inherently stochastic nature of wind generation. In addition to uncertainty, the wind energy resources also exhibit large fluctuation in their output in a short duration of time. These characteristics also exacerbate the difficulty to obtain accurate forecast of wind generation. To address this issue, system operators are forced to incorporate large amounts of operating reserves in the power network [7]. The use of expensive operating reserves results in an overall increase in operational costs negating the cost benefits of wind generation.

The determining element of wind energy generation is wind speed. Since this is a natural phenomenon, factors that affect wind speed are not easy to recognize. Modeling wind speed accurately has been a well-researched area among both statistics and power systems communities [57]. Wind speed modeling methods in the literature are predominantly based on using historical data. That is, they use wind speed data from similar periods of time (seasons, weather conditions, etc.) to build a model. Such modeling approaches can be classified into three categories. 1) Persistence methods; these models assume that the present wind speed stays consistent in the future. That is, wind speed at time t is used as the prediction of wind speed at $t + \Delta t$. Even though this technique outperforms most of the other sophisticated models for very short-term predictions, its performance diminishes very quickly as the prediction length increases. 2) Artificial Intelligence (AI) methods; these models use a

large amount of historical data to identify patterns between input features and wind speeds. These techniques include Artificial Neural Networks (ANN) [58, 59], Support Vector Machine (SVM) [60], multi-layered perceptron [61], among others. The prediction power of these models also diminishes quickly with the prediction time horizon. 3) Statistical methods; these are data-driven models that are easily applicable, interpretable and yield computationally efficient methods that can produce accurate short-term predictions. The statistical methods include time series analysis techniques such as Autoregressive (AR), Autoregressive Moving Average (ARMA), and autoregressive integrated moving average (ARIMA) models [62]. An ARMA model has been used in [63] to simulate wind speed scenarios using Monte Carlo simulation. A time-shifting technique has been used in [64] to simulate wind speeds using an AR model. Hourly wind speed data was modeled using an ARMA model in [65]. A vector AR model (VAR) [66] has been developed using spatio-temporal data of several nearby wind farms in [67]. 5) Hybrid methods; Any combination of the above approaches can be classified as a hybrid method. For instance, a NN model has been employed with a filter to deal with non-linearity of wind speed data to improve ARIMA model in [59].

Contrary to historical data dependent modeling approaches, the physics-based methods utilize Numerical Weather Prediction (NWP) data to predict short-term wind speeds. These models rely on physical phenomenon like temperature, pressure, surface roughness, precipitation, and geographical obstacles to determine the predictions. For this reason, in stable weather conditions, these models can produce highly accurate predictions. However, the high computational burden that comes with solving these complex mathematical models limits their usefulness in real-time power systems operations. For instance, [68] reports that generating a single hourly NWP forecast would require 28 hours on standard 8-core machines or a 500-CPU cluster to generate within an hour. In light of this, one can only employ deterministic optimization methods for power systems planning and operations. To harness the benefits of integrating NWP and SP (see Figure 2.1), in this chapter we present an approach to generate a set of scenarios that share similar statistical properties with the NWP forecast. Using our approach, new scenarios can be generated within a fraction of the time required to generate an NWP forecast. A similar approach has been taken in [69] to simulate hourly wind speed time series interpolating from 6hr NWP forecasts. In this chapter, we focus

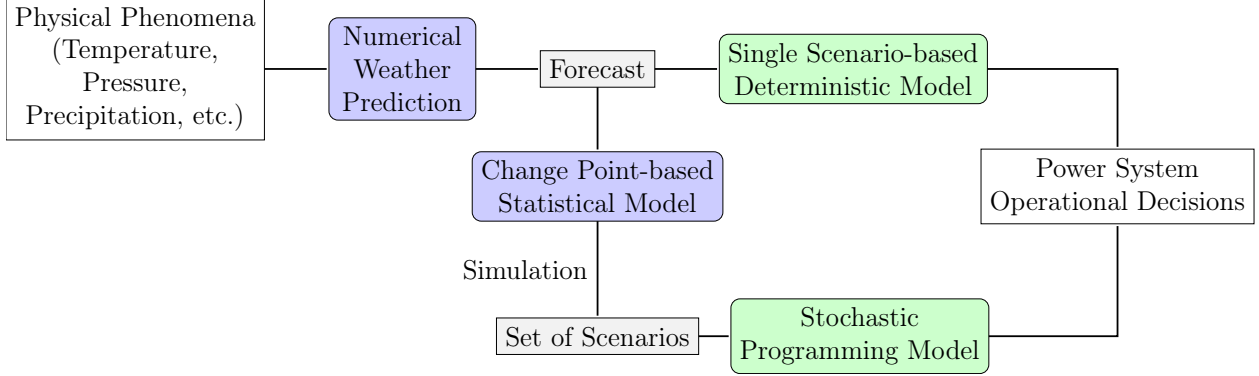


Figure 2.1: Work flow to utilize NWP forecast for decision making in power systems using deterministic and stochastic approaches.

on applying statistical methods to model the NWP forecasted wind speed time series. Our choice is motivated by the fact that our statistical models are supported by sound theoretical properties while retaining computational requirements within acceptable limits. However, there are few obstacles to applying statistical methods to wind time series. Wind farms located in close proximity share common spatio-temporal properties. The statistical models employed for power systems problems have predominantly involved univariate analysis. Such time series models (e.g., AR, ARMA, and ARIMA) fail to capture the spatial relationships. Therefore, the first challenge pertains to capturing spatio-temporal information by treating wind speed time series from nearby locations as a multivariate time series. Such models have been employed in power systems, for instance, [70, 71] present vector autoregressive (VAR) models.

When either univariate or multivariate time series analysis is employed, the standard modeling approaches, including those mentioned above, largely require stationarity of the underlying stochastic process. However, for wind speed data, there is no guarantee that this assumption is satisfied. The most common approach to address the requirement of stationarity is to standardize the original data using the mean and the variance of the entire time series [72, 73]. This approach does not make the time series stationary in terms of variance and temporal dependence (covariance). This leads to statistical inconsistencies between the original time series and those simulated based on models built using standardized data. An-

other way of addressing nonstationarity is to segment the entire series into stationary pieces. However, this segmenting cannot be done arbitrarily. The traditional way of identifying points where an abnormality occurs is using control charts. The approach is more suitable in finding isolated major changes in an ongoing process. In an effort to transform nonstationary data into stationary, [74] apply a transformation based on t -location-scale distribution to achieve standard normal distribution for the wind speed residuals. [75] uses a Weather Research and Forecasting (WRF) data to simulate wind speed time series combined with a stochastic model to add fluctuations to the forecast time series.

Finally, most existing time series methods for modeling wind speeds require certain distributional assumptions. That is, to apply these methods, the data, or at least the residual or error terms obtained after removing the trend and seasonal components, is required to follow a Gaussian distribution. For instance, [76, 77] claim that wind speed data is more likely to follow an approximately Gaussian distribution as the time resolution of the time series increases. To address the distributional requirement, previous works (e.g., [72]) propose different pre-processing techniques, like filtering, to achieve Gaussianity.

In light of these observations, the main contributions of this chapter are as follows.

1. *Change point detection.* We propose a nonparametric change point detection method for the NWP forecasted wind speed data. Our approach is based on a recent work [78], and treats this wind speed data as a multivariate nonstationary time series. This data-driven technique identifies stationary segments of the entire series using change points. The change points are detected based on differences in the covariance structure measured using spectral density matrices [79]. The method is nonparametric and does not make distributional assumptions.
2. *Simulation of wind speed, parametric vs nonparametric approaches.* We discuss parametric and nonparametric time series methods for simulating sub-hourly wind speed data. These simulation methods are applied to all the stationary segments identified using the change point detection method. The proposed simulation methods retain statistical properties of the original time series (the series generated by the NWP) and this is witnessed in the computational experiments involving the NWP forecasted time

series and the simulated wind speed time series.

3. *Application to a power systems operations problem.* We demonstrate the application of time series simulated using our proposed approaches to the economic dispatch problem used for power systems operations planning. Our computational experiments illustrate that the distributional changes, at identified change points, in the NWP generated wind speed time series, result in distributional changes at around the same time points in time series corresponding to conventional generation and location marginal prices. Our approach provides systematic tools to analyze power systems both from the operations and market stability perspectives.

The rest of the chapter is organized as follows. In Section 2.2, we present the change point method to detect changes within wind speed time series. We also discuss parametric and nonparametric approaches to simulate new wind speed scenarios. In Section 2.3, we introduce an economic dispatch problem to illustrate the application of our wind speed modeling method to an important problem in power systems operations. In Section 2.3.2, we present the computational experiments conducted on wind time series data and the behavior of the economic dispatch problem outputs. The concluding remarks are in Section 2.4.

2.2 Methodology

In this section, we present the statistical methods for modeling wind speed time series. We provide a description of the change point method and then discuss the parametric and nonparametric simulation techniques. We start with the model assumption and the motivation to study wind speed data as a multivariate nonstationary time series.

Let $\{\mathbf{w}_t\}_{t=1}^T$ denote the L -dimensional wind speed time series. This series can be decomposed into three L -dimensional terms: trend (\mathbf{x}_t), seasonal (\mathbf{s}_t), and residual (\mathbf{r}_t) terms. That is,

$$\mathbf{w}_t = \mathbf{x}_t + \mathbf{s}_t + \mathbf{r}_t, \quad t = 1, 2, \dots, T. \quad (2.1)$$

We postpone the discussion on estimating the trend and the seasonal terms to the end of

this section. Observe that the model in (2.1) assumes presence of trend and seasonal terms for each component (or variate) of the multivariate series. The serial and contemporaneous dependence among the L components of \mathbf{w}_t is assumed to be driven exclusively by the L -dimensional residual series \mathbf{r}_t . If this series $\{\mathbf{r}_t\}$ is stationary, application of conventional time series models, such as VARMA, is appropriate. The model components would then be estimated by minimizing the least squares error [66].

As an illustration, we present the correlation matrix of the residual series \mathbf{r}_t in Table 2.1 for a randomly selected day (Feb. 19, 2011¹). The $L = 5$ component series here are sub-hourly wind speed data gathered at 5 wind farm locations in Oklahoma. Note that the presence of trend and/or seasonal characteristics in the NWP forecasted original series \mathbf{w}_t makes it inappropriate for an analysis using the standard correlation coefficient and hence, we only present the correlation results based on the residual series \mathbf{r}_t . Furthermore, the model assumption in (2.1) implies that the dependence among components of \mathbf{w}_t is captured entirely by dependence among components in \mathbf{r}_t . The results from Table 2.1 indicate a strong linear relationship among individual components of the multivariate series \mathbf{r}_t , suggesting a multivariate consideration of the wind speed time series.

Table 2.1: Correlation matrix of the residual series \mathbf{r}_t (Feb. 19, 2011).

	Series 1	Series 2	Series 3	Series 4	Series 5
Series 1	1.00	0.55	0.60	0.72	0.52
Series 2	0.55	1.00	0.43	0.29	0.14
Series 3	0.60	0.43	1.00	0.67	0.62
Series 4	0.72	0.29	0.67	1.00	0.55
Series 5	0.52	0.14	0.62	0.55	1.00

Next, an application of a multivariate stationarity test [80] on the residual series \mathbf{r}_t

¹Data source: <https://www.nrel.gov/grid/wwsis.html>

suggests that the stationarity assumption does not hold for every wind speed time series. As an illustration, we present the p-values from this test on hourly and sub-hourly wind speed data gathered at the same $L = 5$ wind farm locations in Oklahoma. The analysis here was conducted on day-long sub-hourly wind speed data for five randomly selected days and week-long hourly wind speed data² starting on the same randomly selected days. The test checks for covariance stationarity of the multivariate time series with a null hypothesis that the given multivariate series is stationary. The p-values in the table provide strong evidence to reject the null hypothesis, leading us to conclude that both the sets of sub-hourly and hourly time series exhibit nonstationarity.

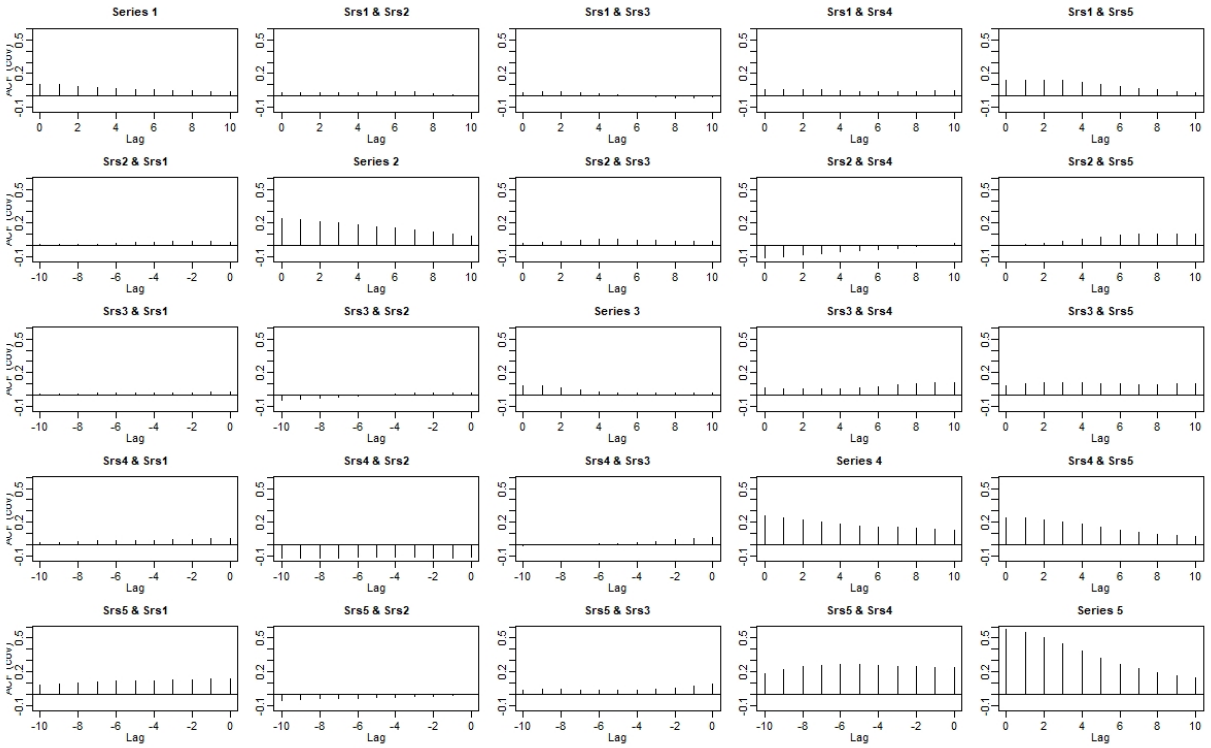
Table 2.2: The p-values from multivariate stationarity test for the five wind farm locations in Oklahoma.

Day	Hourly	Sub-hourly
Feb. 19, 2011	$1.211e - 03$	$< 1e - 06$
Apr. 21, 2011	$8.633e - 04$	$< 1e - 06$
Aug. 07, 2011	$3.185e - 04$	$< 1e - 06$
Nov. 01, 2011	$8.069e - 06$	$< 1e - 06$
Dec. 04, 2011	$1.347e - 06$	$< 1e - 06$

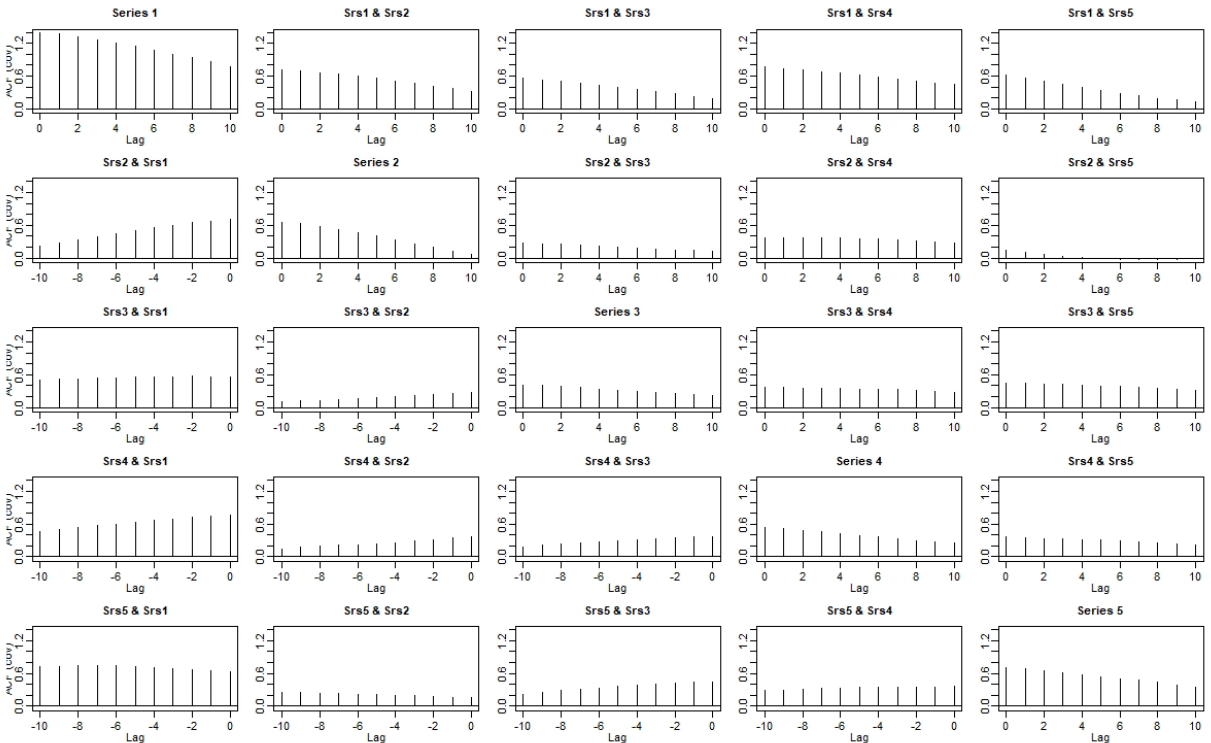
Nonstationarity in the wind speed time series can also be witnessed by checking the autocovariance over different segments in time. Figure 2.2 depicts the changes in the covariance structure of sub-hourly data recorded on February 19 over time. In Figure 2.2a, the covariance patterns of the first 100 observations are entirely different from the last 100 observations in Figure 2.2b. For instance, the first 100 observations of series 1 and 3 (Figure 2.2a) suggest a small relation over different lags while the last 100 observations (Figure 2.2b)

²The choice of selecting 7 consecutive days for hourly data is to ensure that sufficient data is available for model parameter estimation. The hourly data has $24 \times 7 = 168$ data points and sub-hourly data has $12 \times 24 = 288$.

suggest otherwise. Even the univariate plots along the diagonal in both Figures 2.2a and 2.2b show their variance structure change over time. Similar changes were also observed in the covariance structure for sub-hourly wind speed data for other days listed in Table 2.2. Figure 2.3 depicts the covariance structural changes of hourly averaged data. A significant change in the covariance structure between the first 68 observations and the last 68 observations is observable in series 2 and 5. This highlights the prominence of covariance nonstationarity in wind speed data. These preliminary analyses not only emphasize the need to pursue multivariate analysis, but also illustrate that the direct application of stationary VARMA models is not suitable due to inherent nonstationarity.

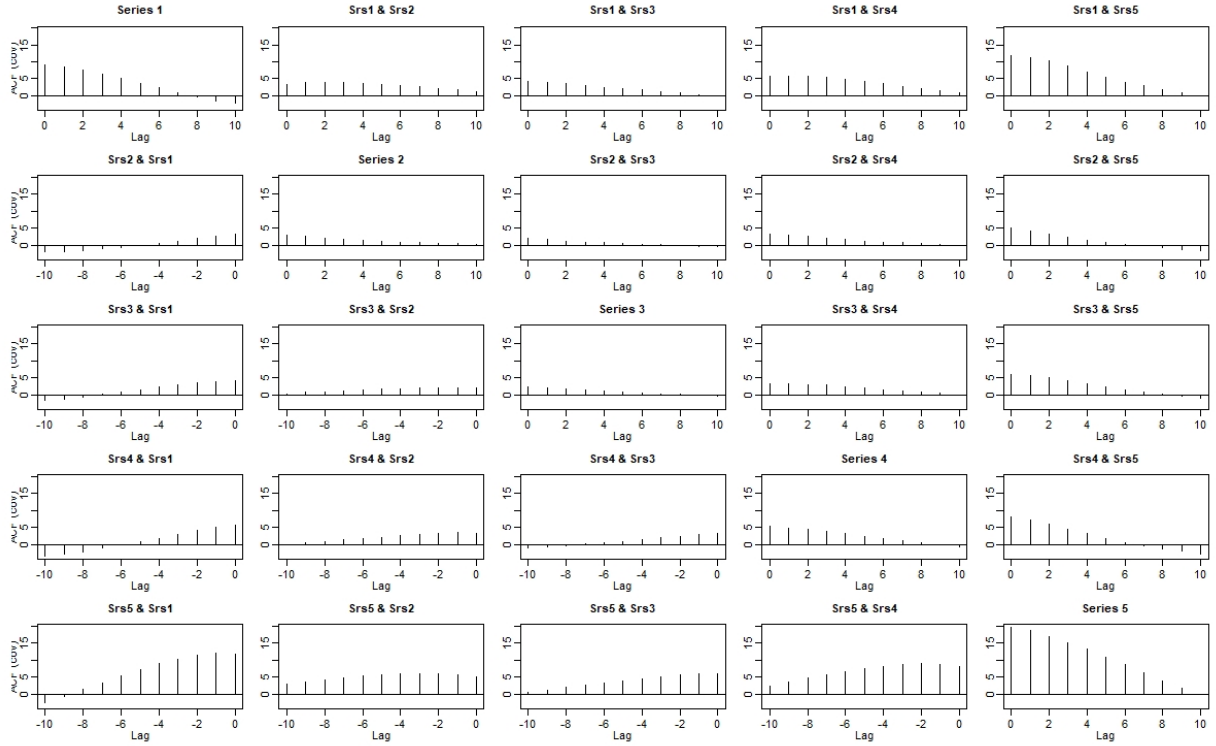


(a) First 100 observations.

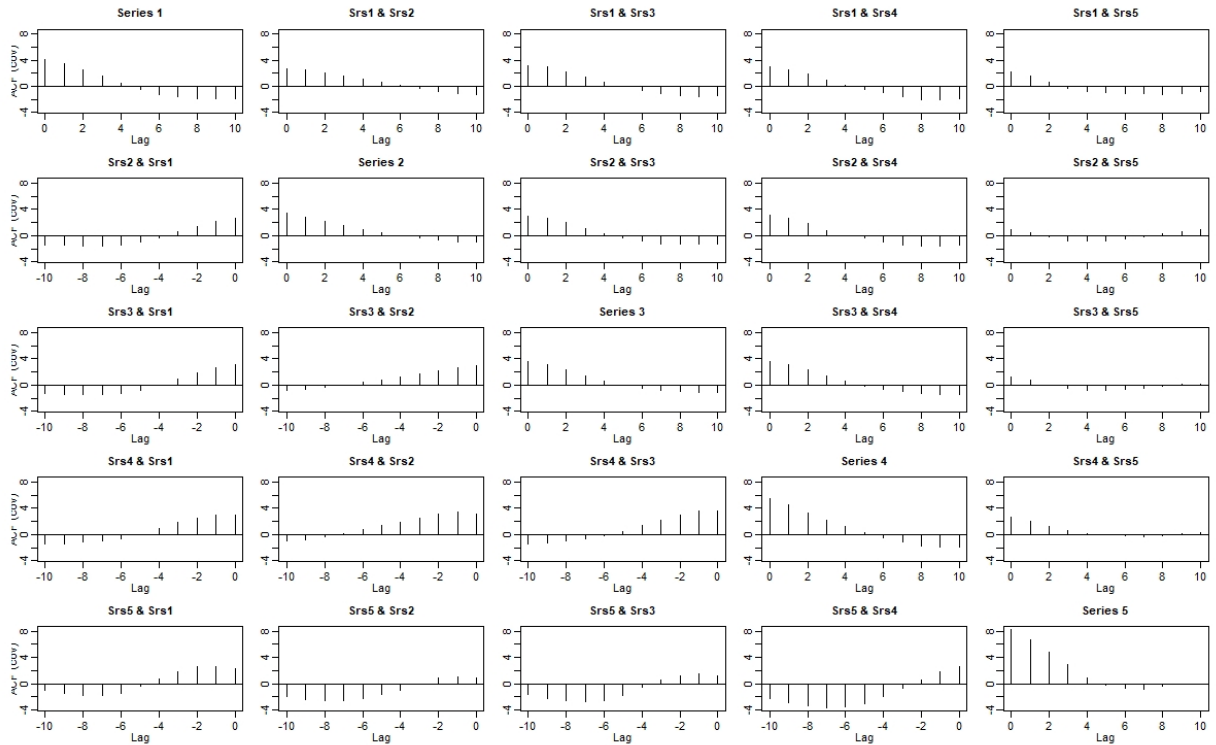


(b) Last 100 observations.

Figure 2.2: Autocovariance plots of sub-hourly residual data for February 19th, 2011.



(a) First 68 observations.



(b) Last 68 observations.

Figure 2.3: Autocovariance plots of hourly averaged residual data from February 19th, 2011.

2.2.1 Change Point Detection

Change point analysis identify changes in the statistical properties of nonstationary time series data. Applications of change point analysis are widespread; see [81–84] for examples. Change point analysis can be performed in parametric [85] and nonparametric [86] settings. Parametric methods assume the data arises from a certain distribution and change points are obtained by tracking changes in the parameters of that distribution across time. Nonparametric methods work without such assumptions and we resort to this approach to identify change points in wind speed data.

A time point $\tau \in (1, T)$ is regarded as a change point when the statistical properties of the series \mathbf{r}_t on either side of that time point τ are different. For instance, if the covariance $Cov(\mathbf{r}_t, \mathbf{r}_{t+h})$ for $t \in (\tau - \delta, \tau]$ at some lag $h \geq 0$ is different from $Cov(\mathbf{r}_t, \mathbf{r}_{t+h})$ for $t \in (\tau, \tau + \delta]$ for some neighborhood length $\delta > 0$, then τ is a change point. The same concept can be extended to $M > 1$ change points at $\tau_1, \tau_2, \dots, \tau_M \in (1, T)$ and we let $\tau_0 = 0$ and $\tau_{M+1} = T$. In this case, the original time series can be split into $M + 1$ *stationary segments* indexed by $I^k := (\tau_k, \tau_{k+1}]$, for $k = 0, 1, \dots, M$. Notice that the above procedure requires the knowledge of the number and locations of change points τ_k , for $k = 1, \dots, M$.

In many practical settings, it is unreasonable to expect that either the number or the location of change points is known a priori. We resort to a nonparametric method for detecting changes in the covariance structure of the residual time series \mathbf{r}_t . Our approach is based on the recently developed nonparametric method in [78]. We provide a brief overview of this approach here and refer the reader to [78, 87, 88] for detailed exposition and analysis.

Let $f(s, \omega)$ for $\omega \in [-\pi, \pi]$, be the $L \times L$ spectral density matrix of the residual series \mathbf{r}_t at frequency ω and time s . Note that the spectral matrix, at different frequencies, carries all the information about the covariance structure of the series \mathbf{r}_t . The key tool for locating change points is a deviation metric that serves as a measure of departure from stationarity. More precisely, for any candidate change point τ , we consider $D(\tau)$ as the integrated squared Euclidean norm of the vectorized difference of the spectral density matrices in a neighborhood

around point τ . We have

$$D(\tau) = \frac{1}{2\pi} \int_{-\pi}^{\pi} \|\text{vec}\left(f_L(\tau, \omega) - f_R(\tau, \omega)\right)\|^2 d\omega. \quad (2.2)$$

where, $f_L(\tau, \omega)$ and $f_R(\tau, \omega)$ are the spectral matrices evaluated over the neighborhoods $(\tau - \delta, \tau)$ and $(\tau, \tau + \delta)$, respectively. Here, $\delta > 0$ is the size of the local neighborhood and $\omega \in [-\pi, \pi]$ is the frequency. While estimating $D(\tau)$, we consider N observations on either side of the candidate change point τ and this N serves as a proxy for δ . Then, an estimate of $f_L(\tau, \omega)$ can be defined using the discrete Fourier transform (DFT) and the periodogram of the series \mathbf{r}_t :

$$J_L(\omega) = \frac{1}{\sqrt{2\pi N}} \sum_{s=\tau-N+1}^{\tau} \mathbf{r}_s e^{-it\omega}, \quad I_L(\omega) = J_L(\omega) J_L^*(\omega), \quad (2.3)$$

where $J_L^*(\omega)$ is the conjugate transpose of $J_L(\omega)$. The estimated $L \times L$ spectral density matrix for $\omega \in [-\pi, \pi]$ is given by

$$\hat{f}_L(\omega) = \frac{1}{N} \sum_{j=-\lfloor \frac{N-1}{2} \rfloor}^{\lfloor \frac{N}{2} \rfloor} K_h(\omega - \omega_j) I_L(\omega_j), \quad (2.4)$$

where $\omega_j = \frac{2\pi}{N} j$ and $K_h(\cdot) = \frac{1}{h} K(\frac{\cdot}{h})$. Here, $K(\cdot)$ is a nonnegative symmetric kernel function and h is the bandwidth. An estimate for $f_R(\tau, \omega)$ can be obtained similarly. Finally, an estimate for $D(\tau)$ in (2.2) can be defined as

$$\hat{D}(\tau) = \frac{1}{2\pi} \int_{-\pi}^{\pi} \|\text{vec}\left(\hat{f}_L(\tau, \omega) - \hat{f}_R(\tau, \omega)\right)\|^2 d\omega. \quad (2.5)$$

The method operates in a sequential manner wherein the point with maximal value in $\hat{D}(\cdot)$ is identified first and tested for significance. To test the significance of this candidate change point at level α , the estimate in (2.5) serves as a test statistic. The method then moves to the time point with the next biggest value in $\hat{D}(\cdot)$. The significant change points are identified sequentially until there are no more time points deemed as change points by the

test. This procedure yields the number M and location of the change points.

Once we identify the M change points, we are left with $M + 1$ stationary segments and the time series within these segments can be treated as stationary series. Our goal then is to mimic this segmentation by simulating stationary time series in each of these segments, thereby producing a realization of the entire series that is statistically consistent with the original time series. Producing accurate simulations of the original series helps greatly in power systems operations and this application is discussed in Section 2.3.

2.2.2 Stationary Process Simulation

In this Section, we present parametric (Section 2.2.2.1) and nonparametric (Section 2.2.2.2) methods to simulate from a stationary time series. These are the methods that will be used to simulate time series data within each of the $M + 1$ identified segments.

2.2.2.1 Parametric

Modeling a stationary time series can be achieved using the *Vector Autoregression* (VAR) model. The p^{th} order VAR model for the residual vector \mathbf{r}_t in segment $I^k := (\tau_k, \tau_{k+1}]$, for $k = 0, 1, \dots, M$, can be written as

$$\mathbf{r}_t = W_{1,k} \mathbf{r}_{t-1} + \cdots + W_{p,k} \mathbf{r}_{t-p} + \Psi_{t,k}, \quad (2.6)$$

where $W_{1,k}, W_{2,k}, \dots, W_{p,k}$ are the $L \times L$ coefficient matrices, and $\Psi_{t,k}$ is the L -dimensional noise term. Selecting the model order p is an important step in VAR model estimation and can be achieved through selection methods such as Akaike information criterion (AIC) or Bayesian information criterion (BIC) [66].

After fitting VAR models in each of the $M + 1$ stationary segments, the fitted models can be used to simulate stationary series for each segment, thereby resulting in a realization of the entire series [89]. The parametric bootstrap method described above requires specification of the distribution of the noise term $\Psi_{t,k}$. Typically, the noise term is assumed to follow Gaussian distribution.

In finite sample situations, fitting VAR models, especially those with high model orders p , can be a challenging estimation problem. In the next section, we describe a nonparametric

approach to simulate a stationary time series. This approach avoids fitting parametric models such as VAR and its associated problems such as model order estimation and error term distribution specification.

2.2.2.2 Nonparametric

The block bootstrap technique is one of the nonparametric methods that can be used to simulate from a stationary time series [90]. In this method, blocks of the original time series are created using a block length parameter. The simulated series is obtained by resampling blocks of observations as opposed to resampling individual observations. The block length is an important parameter choice and the technique in [91] can be utilized to identify the optimal block length. Though the previous method is developed for univariate time series, one can obtain optimal block lengths for each component series in the multivariate series and compute an average block length in the end. The block bootstrap method does not require the distribution of the error terms, avoids small sample estimation problems in parametric models such as VAR. Instead, it requires selecting a single block parameter. In practice, the choice between a parametric or nonparametric simulation technique depends on the length of the $M + 1$ segments discovered by the change point method in Section 2.2.1 and also the estimated model order p of the VAR model described in Section 2.2.2.1. Parametric resampling methods face estimation issues when there are many parameters to be estimated with few observations and this is further discussed in Section 2.3.5.

2.2.3 Estimation

Our model assumption in (2.1) includes a trend term \mathbf{x}_t and a seasonal term \mathbf{s}_t . Popular approaches to estimating the trend term \mathbf{x}_t are smoothing techniques such as moving average, exponential smoothing, and local least squares. The sub-hourly and hourly wind speed data do not exhibit linear nor monotone trend behavior. We thus utilize the *Loess regression algorithm* [92] to estimate the trend term wherein the algorithm fits regression models over local time windows.

The seasonal component \mathbf{s}_t is the repeating pattern of a time series at regular intervals. After removing the trend term, plots of the spectral density [79] and autocorrelation of the univariate components of \mathbf{s}_t provide an initial idea of presence of seasonality in the time

series. To identify seasonal periods and estimate the seasonal term \mathbf{s}_t , one can resort to the additive models and state space modeling framework suggested in [93, 94]. In modeling sub-hourly wind speed data over individual days, seasonality is not an issue due to the small time period under consideration.

The entire procedure of modeling and simulating wind speed time series is summarized in Algorithm 1. The procedure accepts a L -dimensional time series as input, preprocesses the time series (Step 1), identifies the change points at user-defined significance level α (Step 2), and returns the desired number of simulated time series (Step 4). The simulated series are generated using either parametric or nonparametric approaches (Step 3).

Algorithm 1 Simulating wind speeds

- 1: **Input:** L -dimensional time series from nearby wind farm \mathbf{w}_t , $t = 1, 2, \dots, T$; significance level α ; number of simulations N .
 - 2: **Step 1:** Identify trend \mathbf{x}_t and seasonal \mathbf{s}_t components. Obtain residual series $\mathbf{r}_t = \mathbf{w}_t - \mathbf{x}_t - \mathbf{s}_t$. (Section 2.2.3)
 - 3: **Step 2:** Run the change point detection method on \mathbf{r}_t for the input significance level α to obtain change points $\tau_0, \tau_1, \dots, \tau_{M+1}$ where $\tau_0 = 0$ and $\tau_{M+1} = T$. Separate \mathbf{r}_t into segments indexed by $I^k := (\tau_k, \tau_{k+1}]$ (Section 2.2.1)
 - 4: **Step 3:** Obtain time series model for each segment.
 - 5: **for** $k = 0, \dots, M$ **do**
 - 6: Use parametric method, $VAR(p)$ to obtain model for the segment I^k . (Section 2.2.2.1)
 - 7: **if** $p < 5$ **then**
 - 8: Simulate N time series using the $VAR(p)$ model.
 - 9: **else**
 - 10: Use nonparametric method, block bootstrap to obtain N simulated time series. (Section 2.2.2.2)
 - 11: **end if**
 - 12: **end for**
 - 13: **Step 4:** Append all the simulated segments to obtain a time series of length T . Add trend \mathbf{x}_t and seasonal \mathbf{s}_t components. This is done separately for each of the N simulations.
 - 14: **Output:** N simulated wind speed time series.
-

2.3 Application

With large-scale integration of renewable energy resources for electricity generation, the planning and operations problems in power systems face several challenges that stem from the inherent stochasticity in these resources. The deterministic optimization tools employed by the system operators raise several concerns regarding reliable operations as well as consistency in electricity prices. Stochastic programming provides a suitable framework to address both these issues when optimization model parameters are uncertain. However, the effect of nonstationarity on system operations has been an issue. In light of this, we present a critical power systems operations problem to illustrate how nonstationarity in input parameters (wind speed time series) impacts optimization output (conventional generation and electricity prices).

2.3.1 Economic Dispatch Problem

Consider a power system with the set of lines \mathcal{L} , buses \mathcal{B} , generators \mathcal{G} , and load \mathcal{D} . The following mathematical program is a deterministic quadratic programming model of the economic dispatch problem for time period t . The decision variables of the model are as follows: g_{it} is the generation of $i \in \mathcal{G}$ generator, d_{it} is the demand met at $i \in \mathcal{D}$ load, f_{ijt} is the power flow on line $(i, j) \in \mathcal{L}$, and θ_i is the angle at bus $i \in \mathcal{B}$. The model for time period t is given by:

$$\min \sum_{i \in \mathcal{G}} a_i g_{it}^2 + b_i g_{it} - \sum_{i \in \mathcal{D}} \beta_i d_{it} \quad (2.7a)$$

$$\text{s.t. } \sum_{j:(j,i) \in \mathcal{L}} f_{ jit} - \sum_{j:(i,j) \in \mathcal{L}} f_{ijt} + \sum_{j \in \mathcal{G}_i} g_{jt} - \sum_{j \in \mathcal{D}_i} d_{jt} = 0 \quad \forall i \in \mathcal{B}, \quad (2.7b)$$

$$\underline{\Delta}_i + g_{i(t-1)}^* \leq g_{it} \leq \overline{\Delta}_i + g_{i(t-1)}^* \quad \forall i \in \mathcal{G}, \quad (2.7c)$$

$$f_{ijt} = \frac{V_i V_j}{X_{ij}} (\theta_{it} - \theta_{jt}) \quad \forall (i, j) \in \mathcal{L}, \quad (2.7d)$$

$$\underline{G}_i \leq g_{it} \leq \overline{G}_i \quad \forall i \in \mathcal{G}, \quad (2.7e)$$

$$0 \leq d_{it} \leq D_i \quad \forall i \in \mathcal{D}, \quad (2.7f)$$

$$\underline{F}_{ij} \leq f_{ijt} \leq \overline{F}_i \quad \forall (i, j) \in \mathcal{L}. \quad (2.7g)$$

In the above, a_i and b_i are the cost coefficients, $\underline{G}_i/\bar{G}_i$ are the production capacity limits, and $\underline{\Delta}_i/\bar{\Delta}_i$ are the ramp-down/ramp-up limits of the generator $i \in \mathcal{G}$. The bidding price and demand of the load $i \in \mathcal{L}$ is denoted by β_i and D_i , respectively. V_i is the voltages at bus $i \in \mathcal{B}$; X_{ij} is the line impedance and $\underline{F}_{ij}/\bar{F}_{ij}$ are the line capacities of the line $(i, j) \in \mathcal{L}$. In addition, we used a simple linear regression model to transform the wind speed into wind power.

The objective of the model, (2.7a) minimizes the negative of total revenue of the entire power system. The first term in the objective function represents the total power generating cost and the second term represents the total income from the consumers. The first constraint, (2.7b) captures the power flow balancing constraints. That is, the total power inflow of a bus $b \in \mathcal{B}$ is equal to the total outflow. The second set of constraints, (2.7c) are the ramping limitations of generators in the system and the third set, (2.7d) represent the direct-current (linear) approximation of power flow on line $(i, j) \in \mathcal{L}$. Constraints (2.7e), (2.7f), and (2.7g) are the bounds on the respective decision variables. The optimization model is stated for a given generation amount $(g_{i(t-1)}^*)_{i \in \mathcal{G}}$ for the previous time period $(t-1)$ that affects the current generation amount through the ramping constraints (2.7c). Notice that, (2.7) is a quadratic program with affine equality constraints and bounded variables.

Since the input to the optimization model follows a stochastic process, its output, the optimal primal and dual solutions, can also be viewed as stochastic processes. To capture these output stochastic processes, the model is solved iteratively in a rolling-horizon manner. That is, at time period t , a model instance with wind generation corresponding to wind speed \mathbf{w}_t is setup and solved. The resulting optimal generation amount (denoted g_{it}^* for $i \in \mathcal{G}$), along with wind generation amount corresponding to \mathbf{w}_{t+1} is used to setup the next instance of the model at time period $t+1$. The process is repeated until the end of the horizon. At a given time period t , the optimal dual solution of (2.7b), denoted by π_{it}^* , is the location marginal price at bus $i \in \mathcal{B}$. We denote the generation and location marginal prices at time period t by $\mathbf{g}_t = (g_{it})_{i \in \mathcal{G}}$ and $\boldsymbol{\pi}_t = (\pi_{it})_{i \in \mathcal{B}}$. In our computational study, we investigate the behavior of generation $\{\mathbf{g}_t\}$ and price $\{\boldsymbol{\pi}_t\}$ stochastic processes.

2.3.2 Experiments

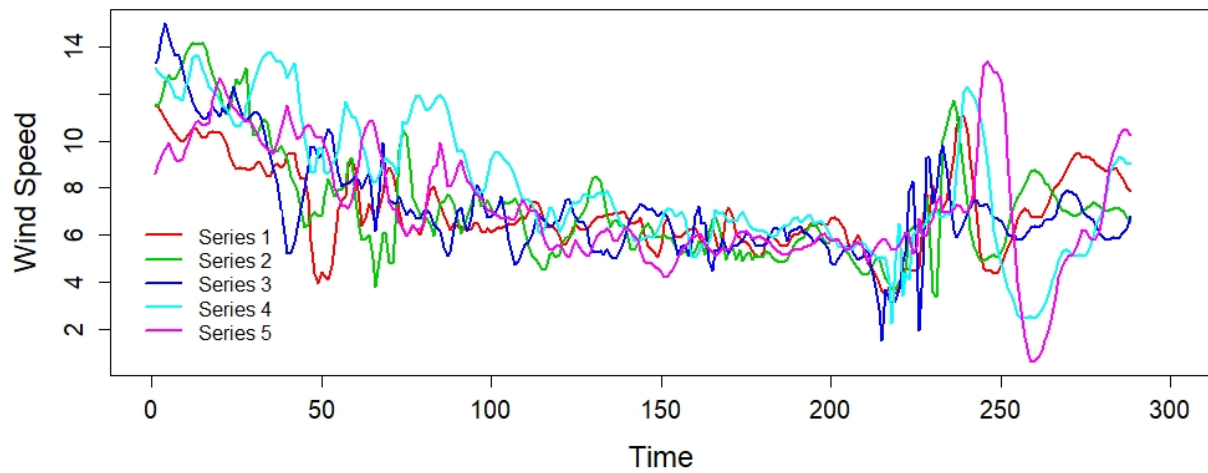
In this section, we present the numerical results of the change point detection method presented in Section 2.2.1. The experiments were conducted on five wind farm locations in Oklahoma. The data was collected from the National Renewable Energy Laboratory (NREL) website (<https://www.nrel.gov/>). All the experiments were conducted on Intel Core i3 CPU 2.2 GHz processor and 8 GB RAM with SSD storage. Statistical modeling and the simulations were implemented using R, version 3.5.1. The optimization model was implemented in C++ and solved using CPLEX 12.9.

The five wind farm locations considered are in close proximity to maintain the spatio-temporal properties, as demonstrated in Section 2.2. Five-minutes apart sub-hourly data was gathered for each location. Figure 2.4a depicts wind speed time series data for the selected five wind farms for September 15 2011. The speeds are varying from 0.613 ms^{-1} to 15.014 ms^{-1} . These wind speeds result in energy generation that range between 0 MWh to 21.02 MWh.

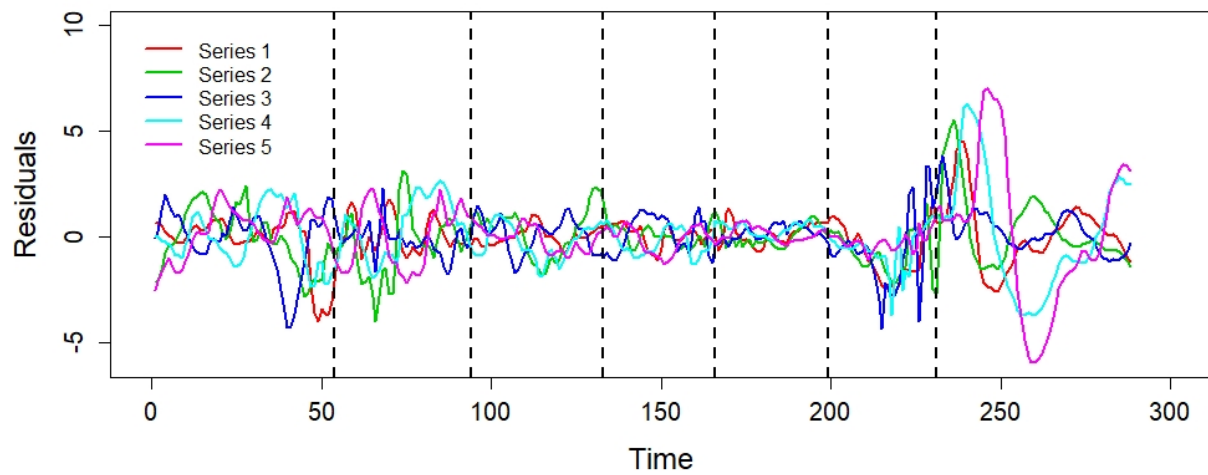
2.3.3 Change Point Detection

To illustrate the potential of the change point detection method presented in Section 2.2, we conducted experiments on different sets of multivariate wind speed time series based on different choices of length of series and number of variables. Sub-hourly data for 12, 24, and 48 hour time periods were obtained using $T = 144, 288, \text{ and } 576$ data points of wind speed time series starting at midnight of September 15, 2011. The variates or components of the multivariate time series correspond to wind farm locations selected at random from the available dataset. We use two, three, four, and five-dimensional time series in our experiments.

For each component of the wind speed time series, we used the method proposed in [94] to verify the presence of seasonal components in the NWP forecasted series. The tests indicated that the time series did not exhibit any seasonal patterns. Therefore, the residuals time series were obtained by removing the trend from the NWP forecasted original series, using the Loess algorithm. The residual series are depicted in Figure 2.4b. The change point method was then applied on this residual series and the results are summarized in Table 2.3.



(a) Observed wind speed time series at five locations.



(b) Residual series

Figure 2.4: September 15, 2011.

For instance, the change point method detected six change points at $\tau = 54, 94, 133, 166, 199$, and 231 in the 5-dimensional sub-hourly time series. These change points are identified using the vertical lines in Figure 2.4b.

A critical parameter for the change point detection method is the significance level α . A smaller value of α imposes a stringent requirement for determining a candidate point to be affirmed as a change point. We recommend using $\alpha = 0.05$ or $\alpha = 0.01$ for wind speed time series. Table 2.3 presents the results for different sets of time series at these two significance levels. The impact of the choice of significance level was revealed in the results for 12-hours long, two-dimensional sub-hourly time series. When $\alpha = 0.05$, the change point method detected three change points at $58, 75$, and 102 . However, the change point at $\tau = 102$ was not significant at $\alpha = 0.01$. Similar observation was also made for the 7 days long, 5-dimensional hourly time series.

The length of the series also has an impact on the change point detection method. Table 2.3a shows that when series length increases the number of change points identified increases. For instance, the 12 hours long, three-dimensional time series has two change points at $\alpha = 0.01$, whereas, the 24 hours long series has four change points, and 48 hours long series has five change points.

2.3.4 Simulation of Wind Speeds

The detected change points lead to the stationary segments, and then, parametric and nonparametric approaches from Sections 2.2.2.1 and 2.2.2.2, respectively, can be used for simulation. The parametric approach involves, at each segment, identifying the appropriate VAR model order, estimating the model parameters and simulating time series using the estimated model. The nonparametric approach, on the other hand, is based on block bootstrap carried out on each segment. The entire procedure to simulate wind speeds is summarized in Algorithm 1. For a given NWP forecast, the process involves identifying the change points, estimating model parameters when using the parametric approach, and simulating new time series. The process takes 7.20 and 7.68 seconds when parametric and nonparametric approaches are employed, respectively.

For the sub-hourly time series in Figure 2.4b, the change point detection method indicates

Table 2.3: Change point analysis: Series length, significance level, number of series. Starting day: September 15th, 2011.

(a) Sub-hourly time series.

Significance level(α)	Length of the series	Number of time series				
		2	3	4	5	
0.01	12hrs	58, 75	58, 103	42, 58, 83	41, 58, 83	
	24hrs	89, 224	54, 103, 145, 224	89, 231	54, 94, 133, 166, 199, 231	
	48hrs	89, 224, 256, 371, 436	89, 224, 256, 341, 435	89, 231, 264, 359, 436	89, 231, 302, 368, 435	
0.05	12hrs	58, 75, 102	58, 103	42, 58, 83	41, 58, 83	
	24hrs	89, 224	54, 103, 145, 224	89, 231	54, 94, 133, 166, 199, 231	
	48hrs	89, 224, 256, 371, 436	89, 224, 256, 341, 435	89, 231, 264, 359, 436	89, 231, 264, 359, 435	

(b) Hourly averaged time series.

Significance level(α)	Length of the series	Number of time series				
		2	3	4	5	
0.01	7days	55, 71	55, 71	55, 71	54, 71	
	14days	99, 257	99, 257	99, 257	99, 164, 257	
	21days	99, 257	98, 257	98, 257	98, 257	
0.05	7days	55, 71	55, 71	55, 71	54, 71, 90	
	14days	99, 257	99, 257	99, 257	99, 164, 257	
	21days	99, 257	98, 257	98, 257	98, 257	

the presence of six change points. Thus, we decompose the time series into seven stationary segments index by the intervals [1, 54], [55, 94], [95, 133], [134, 166], [167, 199], [200, 231], and [232, 288]. Segment-wise VAR model order p was estimated using the Akaike information criterion (AIC) resulting in orders $p = 9, 6, 6, 5, 5, 5$, and 10 respectively. The number of VAR parameters depends on the dimension of the series (L) and model order (p), and is given by $pL^2 + L$. Unless the series length in each segment far exceeds the number of parameters to be estimated, the quality of estimated parameters is suspect. For all the series considered in our experiments, this was found to be the case. For daily wind speed data at 5 minute resolution, we do not recommend using the parametric approach for wind speed when the model order is five or higher. In such cases, we recommend the nonparametric block bootstrap approach for simulation.

Once the change points are estimated for the NWP forecasted original wind speed time series, we conduct multiple replications of the block bootstrap simulation. We compute the correlation matrix for the original and all the simulated time series. Table 2.4 presents the correlation matrix for the original and the average correlation matrix of 30 simulations along with their 95% confidence intervals. Across all the replications, the average distance, computed using the Frobenius Norm, between the correlation matrices corresponding to the original and a simulated time series was 0.28 with the standard deviation of 0.09. These results indicate the simulated time series retain the correlation structure of the NWP forecasted original time series.

Table 2.4: Correlation comparison of the NWP forecasted original series vs. simulated series. (Feb. 19, 2011).

(a) NWP forecasted original series.

	Series 1	Series 2	Series 3	Series 4	Series 5
Series 1	1.00	0.73	0.61	0.58	0.36
Series 2	0.73	1.00	0.74	0.61	0.41
Series 3	0.61	0.74	1.00	0.60	0.53
Series 4	0.58	0.61	0.60	1.00	0.72
Series 5	0.36	0.41	0.53	0.72	1.00

(b) Average correlations of simulated series (Nonparametric)

	Series 1	Series 2	Series 3	Series 4	Series 5
Series 1	1.00 ± 0.00	0.72 ± 0.02	0.61 ± 0.02	0.57 ± 0.02	0.33 ± 0.02
Series 2	0.72 ± 0.02	1.00 ± 0.00	0.73 ± 0.01	0.63 ± 0.02	0.42 ± 0.02
Series 3	0.61 ± 0.02	0.73 ± 0.01	1.00 ± 0.00	0.61 ± 0.02	0.55 ± 0.01
Series 4	0.57 ± 0.02	0.63 ± 0.02	0.61 ± 0.02	1.00 ± 0.00	0.67 ± 0.03
Series 5	0.33 ± 0.02	0.42 ± 0.02	0.55 ± 0.01	0.67 ± 0.02	1.00 ± 0.00

2.3.5 Performance in Economic Dispatch Problem

To verify the impact of nonstationarity in wind speed time series on power systems operations, we implemented the rolling-horizon economic dispatch problem. For this experiment we considered a modified IEEE-30 test system [95]. The system comprises of 30 buses, 41 lines with a maximum capacity of $50MWh$, a total of 6 generators, and 21 loads. We considered hourly changes in the demand at each load.

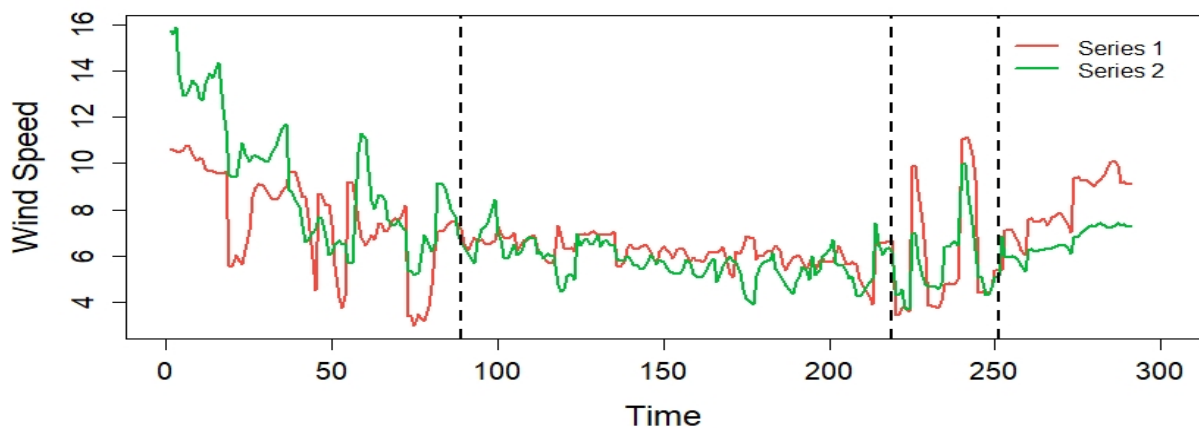
We considered generators at bus 8 and bus 13 to be wind generators located on farms that share similar wind patterns. From the available sub-hourly wind speed data, two locations were randomly picked to simulate the wind speed time series. The correlation between the selected locations' NWP forecasted original wind speed time series is 0.7265. The change point analysis detected three change points for the bivariate time series at $\tau = 87, 218, 250$, resulting in four stationary segments. When parametric modeling was used, the order of the VAR model for each stationary section was 10, 8, 6, and 5. Since these values are higher than the recommended model order of 5, the nonparametric approach was used for simulation.

The bivariate time series generated using the nonparametric simulation method is shown in Figure 2.5a. The correlation between the simulated time series is 0.6664. This indicates that the simulated time series retain the original linear relationship between the two variates. The change point method detected $\tau = 89, 219, 251$ as the change points (see Figure 2.5a) for the simulated time series indicating that the simulation preserves the structural properties of the NWP forecasted original series. Note that the asymptotic properties of change point detection method are well established, however, such behavior can only be observed when a very large number of observations are available. In small sample settings, as is our case, the method searches in a neighborhood of a point for potential locations for change points. Therefore, we expect to see mild discrepancies in change points between the original (e.g., $\tau = 87$) and the simulated ($\tau = 89$) time series.

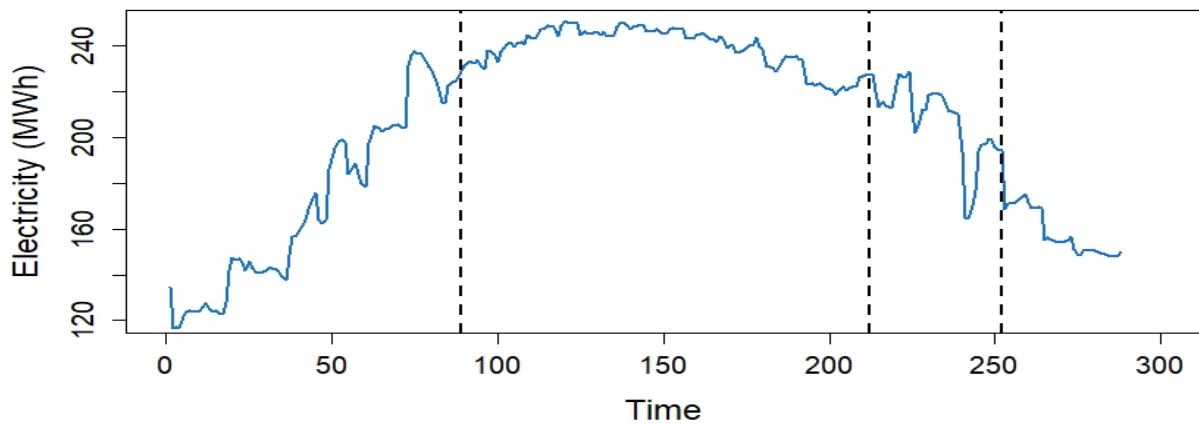
The wind generation corresponding to the simulated time series was input to the dispatch model (2.7). Notice that the input time series affects only the upper bound constraint (2.7e) corresponding to the wind generators. As wind generation is the cheapest out of all the generators in the system, wind generation is fully utilized, when possible, and the conventional generators are adjusted to meet the remaining demand. The total conventional

generation is depicted in Figure 2.5b. The change point analysis on the total conventional generation time series reveals three change points at $\tau = 89, 212$, and 252 . These change points are in the neighborhood of the change points identified for the simulated wind speed time series in Figure 2.5a.

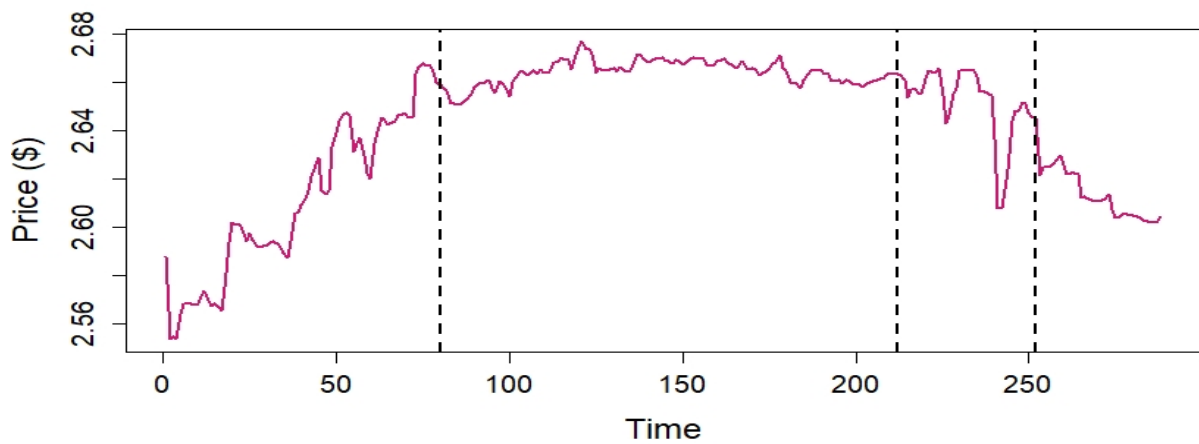
In addition to the primal optimal solution (conventional generation, etc.), we also monitored the dual optimal solutions of the optimization model in (2.7). Since line capacities are considered in the dispatch model, we observed some load-shedding in some buses. Load-shedding is penalized in the objective, and therefore, the prices at these buses are distorted by the load-shedding penalty. We conducted the change point analysis on the location marginal price time series at buses whose marginal prices was not distorted by the load-shedding penalty. For example, the marginal price time series and the detected change points at Bus-1 are depicted in Figure 2.5c. Change point analysis reveals similar change points (at $\tau = 80, 212$, and 252) for the price time series as in the input wind speed and the primal total conventional generation times series.



(a) Simulated wind speed.



(b) Total conventional generation.



(c) Location Marginal Price at Bus-1

Figure 2.5: Results from the Rolling Horizon Economic Dispatch model.

The primal and dual solutions to quadratic programs with affine constraints, such as (2.7), are known to be piecewise continuous in the right-hand side parameters. Since wind generation impacts the upper bound constraint in (2.7e), the observations in Figure 2.5b and 2.5c provide an empirical evidence for the piecewise relationship of quadratic programming solutions and its input. Furthermore, the neighborhood around the detected change points correspond to intervals that exhibit significant fluctuation in generation and prices. Therefore, the change point detection method can be used for power systems operation and market stability analyses. The piecewise relationship also allows the system operator to predict intervals of volatility, at desired level of significance, by conducting the change point analysis on a wind speed forecast time series.

2.4 Conclusions

In this chapter, we emphasized on two principal elements of wind speed modeling, viz., spatio-temporal correlation and nonstationarity. Analyzing wind speed at geographically separated wind farms in isolation (univariate analysis) fails to capture the spatial correlations. We also demonstrated the presence of the nonstationarity in both hourly and sub-hourly wind speed time series. Therefore, wind speed time series cannot be directly modeled by usual stationary time series modeling methods such as VAR. Ignoring spatial correlation and nonstationarity restricts the capabilities of power systems planning and operations models fail to realistically capture the stochastic processes that affect them.

To address this issue, we presented a change point detection method for multivariate nonstationary wind speed time series. The change point detection method allowed the nonstationary time series to be decomposed into stationary segments. The change point method sequentially identifies the time points where significant changes in the covariance structure occur. The presented change point detection method does not make any distributional assumptions and is supported by sound asymptotic consistency properties.

Once the stationary segments are identified, parametric and nonparametric approaches were presented to simulate new wind speed time series. Generally, the parametric method provides better results if the time series segments satisfy the distributional assumptions of the parametric model. However, parametric models can get computationally expensive and

require large amount of data for estimating the model parameters when the model order increases. Therefore, for wind speed data we recommend a nonparametric approach if the parametric model order is greater than five for at least one stationary segment. We presented a block bootstrap technique as a reliable nonparametric approach to simulate wind speed time series.

Finally, we demonstrated an application of the change point detection method and subsequent simulation techniques to the economic dispatch problem. We showed that the change points of the wind speed time series correspond to time intervals where the conventional generation and electricity prices also exhibit significant volatility. Such relationship between input time series (wind speed) and optimization model output (generation amounts and electricity prices) can play a critical role in detecting and predicting system instabilities.

Chapter 3

New Models, Pricing Mechanisms, and Interpretations for Stochastic Market Clearing Problem

3.1 Introduction

Due to various environmental and economic reasons, U.S. policymakers are aggressively integrating renewable energy into the power grid [5]. Even though there are many benefits to renewable energy, there are also many challenges to integrating large-scale renewable energy resources into the power grid. The inherent stochastic nature of these resources is the main cause of these issues. Since most of the renewable energy resources depending on weather conditions, these issues are out of the control of the system operators. Therefore, we must accommodate these fluctuations in market operation models.

The system operators face two major problems due to the stochasticity of renewable energy resources. Since we cannot have an accurate forecast for the renewable generation output, the system operator must rely on an estimate that changes with the weather conditions. This uncertainty causes damage to the power grids' reliability. The second conflict is economic in nature. Since the renewable generation output can change during electricity transactions, the system operator cannot provide accurate prices beforehand.

In this chapter, we attempt to address the latter using stochastic programming (SP) methods. In [44], the authors have proposed and shown the advantages of using SP to model the electricity market clearing problem over the current industry practice, deterministic methods. They also introduced a pricing mechanism for market participants with important properties such as revenue adequacy and cost recovery in expectation. [45] has further analyzed this price mechanism. [48] has proposed another SP-based pricing mechanism that proves revenue adequacy and cost recovery for every scenario at the expense of losing social surplus (non-economic dispatch).

In light of these observations, the main contributions of this chapter are as follows:

1. *New pricing mechanisms.* We develop two alternative models for the two-settlement electricity market that accounts for uncertainty in renewable generation and demand. These models are based on two-stage SP principles, particularly the notion of non-anticipativity. Based on the alternative approaches to capture the non-anticipativity requirement, we develop two separate models, mean-vector and state-vector formulations. In addition, we introduce two pricing mechanisms using the two alternative models and show the relationships between the models using linear programming duality. We show that both pricing mechanisms have improved pricing characteristics over the pricing mechanism proposed in [44].
2. *Analysis of pricing mechanisms.* We show that the new pricing mechanisms achieve revenue adequacy for the system operator in expectation. That is, the system operator does not face a financial deficit in the long run. We also prove that every participating generator achieves cost recovery without any out-of-market payments in expectation with mean-vector formulations' pricing mechanism. For the state-vector formulations' pricing mechanism, we prove that all generators achieve cost recovery under every scenario, a more significant result. Finally, we develop bounds on price distortion, the deviation between the first-stage unit price and the second-stage unit price for both pricing mechanisms. We illustrate these properties through numerical experiments.

In the following section 3.2, we describe the market setting we consider in this study. We introduce model elements in sub-section 3.2.1.1 and market metrics in section 3.2.2. Then we present optimization models for the clearing problem in section 3.3. We begin with the two-stage SP model in section 3.3.1 and proceed to alternative SP models from section 3.3.1. We present the first alternative SP model in section 3.3.2 and its' pricing mechanism. Then we present the second alternative SP formulation and its' pricing mechanism in section 3.3.3. Finally, in section 3.4, we use a small example to illustrate the findings of the previous sections.

3.2 Stochastic Market Clearing

In this section, we present the electricity market-clearing model formulations. We begin with a description of the market setting we consider in our study. We also present the metrics that we use to analyze and compare the pricing mechanisms.

3.2.1 Market Setting

We consider a two-settlement market setting where the market participants partake in a forward day-ahead market and a real-time balancing market. An Independent System Operator (ISO) manages and clears the markets centrally. We denote by \mathcal{P} the market participants who make offers separately in the day-ahead market and the real-time market. We assume that a market participant operates a single unit and does not cooperate with other market participants, thus ensuring perfect competition. Therefore, a participant either operates a generation unit or is a demand aggregator. We denote by \mathcal{G} and \mathcal{D} the set of generator and demand participants, respectively. Typically, the ISO clears the day-ahead market by first scheduling generators using a security-constrained unit commitment problem. Following the commitment problem, the ISO identifies optimal generation amounts and reserves using a security-constrained economic dispatch problem (see for example, [96] for details regarding market operations at PJM ISO). Our formulations assume that the unit commitment decisions are made a priori and are available as input. This market setting is also the subject of previous works on stochastic market clearing, particularly in [44] and [45].

3.2.1.1 Model Elements

The power network is captured by a set of nodes (buses) \mathcal{N} and a set of lines \mathcal{L} . The day-ahead market is cleared using the day-ahead offers that include price bids c_i for $i \in \mathcal{P}$. The offers also include estimates of available maximum/minimum capacity that we denote by x_i^{\max}/x_i^{\min} for $i \in \mathcal{P}$. We denote the day-ahead settlement/cleared amounts by the decision variable x_i for either type of participants $i \in \mathcal{P}$. A decision variable that corresponds to a generator satisfies $x_i \geq 0$, and that which corresponds to a demand satisfies $x_i \leq 0$. These constitute the principal elements of the consolidated first-stage decision vector $\mathbf{y}_1 \in \mathbb{R}^{n_1}$. In addition to the day-ahead clearing decisions, the decision vector \mathbf{y}_1 also includes the power flows f_{ij} for $(i, j) \in \mathcal{L}$ that support the cleared day-ahead quantities. Therefore, we define

$\mathbf{y}_1 := ((x_i)_{i \in \mathcal{P}}, (f_{ij})_{(i,j) \in \mathcal{L}})$. The capacity limits on these decision variables define the set \mathcal{C}_1 as:

$$\mathcal{C}_1 := \left\{ \mathbf{y}_1 \left| \begin{array}{ll} x_i^{\min} \leq x_i \leq x_i^{\max} & \forall i \in \mathcal{P}, \\ f_{ij}^{\min} \leq f_{ij} \leq f_{ij}^{\max} & \forall (i,j) \in \mathcal{L}, \\ (f_{ij})_{(i,j) \in \mathcal{L}} \in \mathcal{F}. \end{array} \right. \right\} \quad (3.1)$$

The first two constraints limit the first-stage decisions within their capacity limits. For a generator, these limits capture the min up-time generation (lower bound) and generation capacity (upper bound). On the other hand, for a load, the lower bound is set to the negative of demand forecast and the upper bound is set to zero. The third requirement ensures that the power flows satisfy the underlying physics. The description of the set \mathcal{F} depends on the nature of approximation (such as the direct-current approximation) or relaxations (such as second-order conic programming and semidefinite programming-based relaxations) adopted to describe the power flows on a line. We refer the reader to [97] for a detailed review on modeling power flows. We assume that $0 \in \mathcal{F}$. In addition to the above, the cleared day-ahead quantities and the power flows do satisfy the flow balance at all nodes. These are given by

$$\underbrace{\sum_{j:(j,n) \in \mathcal{L}} f_{jn} - \sum_{j:(n,j) \in \mathcal{L}} f_{nj}}_{:=\tau_n(f)} + \sum_{j \in \mathcal{P}(n)} x_j = 0 \quad \forall n \in \mathcal{N}. \quad (3.2)$$

The function $\tau_n(f) = \sum_{j:(j,n) \in \mathcal{L}} f_{jn} - \sum_{j:(n,j) \in \mathcal{L}} f_{nj}$ captures the net flow (difference between inflow and outflow) at bus n . For ease of exposition, we adopt an abstract form for power flow equations as $g_1(\mathbf{y}_1) = 0$. Finally, the day-ahead social deficit (negative social surplus; formally defined later in this section) is given by

$$f_1(\mathbf{y}_1) := \sum_{i \in \mathcal{P}} c_i x_i. \quad (3.3)$$

This constitutes the first-stage objective function.

The day-ahead and the real-time markets are cleared sequentially. The real-time mar-

ket conditions are uncertain at the time the day-ahead market is cleared. The uncertain conditions include (but not limited to) renewable generation, demand, transmission line capacities, and generator status. These uncertain elements are modeled by the random vector ω defined on a probability space $(\Omega, \mathcal{F}, \mathbb{P})$, where Ω is a set of all possible scenarios, \mathcal{F} is the sigma-algebra, and \mathbb{P} is the probability distribution. The real-time market is cleared only after observing a realization ω of the random vector ω . We will refer to individual realizations as scenarios. Therefore, the quantities cleared in the real-time market may deviate from those cleared in the day-ahead clearing. The market participants submit a separate generation and demand bids to address the deviation between the day-ahead and real-time conditions.

The real-time offers include the additional cost for positive $(\delta_i^+)_i \in \mathcal{P}$ and negative deviations $(\delta_i^-)_i \in \mathcal{P}$ incurred by the market participants. They also include maximum and minimum capacity bounds given by X_i^{\max}/X_i^{\min} for $i \in \mathcal{P}$. Analogous to the day-ahead settlements, we denote real-time settlements/cleared amounts under realization ω by $X_i(\omega)$ for $i \in \mathcal{P}$ that satisfy $X_i(\omega) \geq 0$ for generators and $X_i(\omega) \leq 0$ for loads. We collectively denote the real-time decisions by the vector $\mathbf{y}_2(\omega) := ((X_i(\omega))_{i \in \mathcal{P}}, (F_{ij}(\omega))_{(i,j) \in \mathcal{L}}) \in \mathbb{R}^{n_2}$, where $F_{ij}(\omega)$ for $(i, j) \in \mathcal{L}$ denote the power flows that support real-time amounts. In the real-time market, the day-ahead amount of a participant $i \in \mathcal{P}$ is adjusted by either $(X_i(\omega) - x_i)_+$ or $(X_i(\omega) - x_i)_-$. We assume that both these operations incur costs that we denote by δ_i^+ and δ_i^- , respectively. These deviation costs are a small fraction of the day cost c_i (we use 1%-5% in our experiments). Therefore, the day-ahead cost is adjusted by

$$f_2(\mathbf{y}_1, \mathbf{y}_2(\omega), \omega) := \sum_{i \in \mathcal{P}} \left[(c_i + \delta_i^+)(X_i(\omega) - x_i)_+ - (c_i - \delta_i^-)(X_i(\omega) - x_i)_- \right]. \quad (3.4)$$

The above constitutes the second-stage objective function. We define the real-time counter-

parts of \mathcal{C}_1 and flow-balance equations for $\omega \in \Omega$ as

$$\mathcal{C}_2(\omega) := \left\{ \mathbf{y}_2(\omega) \left| \begin{array}{l} \max\{X_i^{\min}, -X_i^{\text{avail}}(\omega)\} \leq X_i(\omega) \leq \min\{X_i^{\max}, X_i^{\text{avail}}(\omega)\} \quad \forall i \in \mathcal{P}, \\ F_{ij}^{\min} \leq F_{ij}(\omega) \leq F_{ij}^{\max} \quad \forall (i, j) \in \mathcal{L}, \\ (F_{ij}(\omega))_{(i,j) \in \mathcal{L}} \in \mathcal{F} \end{array} \right. \right\} \quad (3.5)$$

and

$$\tau_n(F(\omega)) - \tau_n(f(\omega)) + \sum_{j \in \mathcal{P}(n)} X_j(\omega) - x_j(\omega) = 0 \quad \forall n \in \mathcal{N}, \quad (3.6)$$

respectively. As before, we will use $g_2(\mathbf{y}_2(\omega)) = 0$ to succinctly represent the flow-balance equations. The quantity $X_i^{\text{avail}}(\omega)$ used in (3.5) denotes the observed quantity of i^{th} participant under realization ω . Notice the explicit dependence of the cleared real-time quantities, power flows, and the cost function upon the realization, ω .

3.2.2 Market Metrics

The next section presents pricing mechanisms based on the alternative SP formulations and their properties. For each pricing mechanism, we analyze the payment received by market participants and the revenue earned by the ISO. In our analyses, we use the notion of revenue adequacy for the ISO and cost recovery for the participating generators. Price consistency was identified as an appropriate metric for stochastic market settings in [45] as they help achieve appropriate incentives. The authors define price consistency as when the deviations between the day-ahead unit price and the expected real-time unit price is zero. We adopt this distortion as an additional metric to assess our pricing mechanisms. Before presenting the model formulations and pricing mechanisms, we introduce these metrics of interest.

Under a scenario ω , a market participant realizes a value given by

$$\varphi_i(\omega) := -c_i x_i(\omega) - (c_i + \delta_i^+)(X(\omega) - x_i)_+ + (c_i - \delta_i^-)(X_i(\omega) - x_i)_- \quad \forall i \in \mathcal{P}. \quad (3.7)$$

Recall that $X_i, x_i \geq 0$ for generators, $X_i, x_i \leq 0$ for loads, and $\delta_i^+, \delta_i^- > 0$ (typically a small

fraction of c_i). Therefore, the realized value is negative for the generators and must be viewed as the generator's cost. On the other hand, the realized value is positive for loads which can be interpreted as the value gained by meeting their demand. The *social surplus* is defined as the value realized across all the market participants under $\omega \in \Omega$. That is,

$$\varphi(\omega) := \sum_{i \in \mathcal{P}} \varphi_i(\omega). \quad (3.8)$$

The stochastic market clearing problem aims to minimize the negative of expected social surplus (for instance, see the objective function of (3.13)). The above form of social surplus can be derived from the definition of the day-ahead cost f_1 in (3.3), and the real-time adjustment cost f_2 in (3.4) through simple algebraic operations. It is worth noting that the expected social surplus is a systemwide measure viewed from the ISO's perspective. For individual participants, we denote by $\rho_i(\omega)$ the payment made to a generator (when $\rho_i(\omega) \leq 0$) by the ISO or received from a load (when $\rho_i(\omega) \geq 0$) under scenario ω .

Definition 1. A participating generator i achieves scenario-specific cost recovery when,

$$\rho_i(\omega) - \varphi_i(\omega) \leq 0, \quad (3.9a)$$

under scenario ω . The participating generator achieves cost recovery in expectation when,

$$\mathbb{E}[\rho_i(\omega)] - \mathbb{E}[\varphi_i(\omega)] \leq 0. \quad (3.9b)$$

Notice that the cost recovery metric is defined for only the participating generators. When a generator achieves cost recovery, it can cover its short-run costs through its payments from the ISO. This case, also known as making whole, encourages the generators to participate in the market. In the absence of this feature, the payment mechanism has to incorporate additional side payments known as *uplift payments*. Uplifts become essential under three cases (i) when approximations/relaxations are employed for the optimal power flow equations, (ii) the inclusion of binary-valued commitment decision, and (iii) when an approximate representation of uncertainty is utilized. In this study, we focus our attention on the latter. From the ISO's perspective, the following metric is useful.

Definition 2. *The ISO achieves scenario-specific revenue adequacy when,*

$$\sum_{i \in \mathcal{P}} \rho_i(\omega) \geq 0, \quad (3.10a)$$

under scenario ω . The ISO achieves revenue adequacy in expectation when,

$$\mathbb{E} \left[\sum_{i \in \mathcal{P}} \rho_i(\omega) \right] \geq 0. \quad (3.10b)$$

When we achieve revenue adequacy under a specific payment mechanism, the ISO receives sufficient payment from the loads to make payments to generators and does not run into a financial deficit. Finally, we use the following definition to capture the deviation of price signals in the day-ahead and real-time.

Definition 3. *The scenario-specific price distortion, denoted by $\mathbb{M}_n(\omega)$ for all $n \in \mathcal{N}$ and $\omega \in \Xi$, is the difference between the day-ahead and real-time prices. Furthermore, the prices are said to be consistent at a node n if $\mathbb{E}[\mathbb{M}_n(\omega)] = 0$.*

Notice that we introduce metrics in scenario-specific and expectation forms. While the scenario-specific statements provide relatively stronger metrics, providing such strong guarantees may not always be possible, as we illustrate in the next section.

3.3 Models and Pricing Mechanisms

In this section, we present alternative SP problem formulations of the stochastic clearing problem. For each formulation, we present the general primal form and develop the dual form. We also present the extended two-settlement marker-clearing problem for each model. In identifying the alternative formulations, we place a particular emphasis on our ability to computationally solve these problems to optimality.

Notice that, when we employ direct-current approximation (which is the case in our numerical study), the constraints we defined in Section 3.2.1.1 are linear. Further, we allow generation and load shedding in the second stage as the real-time quantities are only required to be within specified bounds; see (3.5). This implies that we achieve relatively complete recourse for the two-settlement market problem. Therefore, the sets \mathcal{C}_1 and \mathcal{C}_2 are bounded

polyhedrons, and hence they are convex, closed, and nonempty. We also assume finite support for the probability set. Therefore, f_1 and f_2 are linear, and hence they are convex, everywhere-defined, and finite. Before presenting the new formulations, we present the two-settlement problem in the canonical SP form.

3.3.1 Canonical Stochastic Programming Model

The general form of the two-stage SP program is typically stated as follows:

$$\text{Primal: } \min c^\top x^c + \sum_{\omega \in \Omega} p(\omega) d^\top y^c(\omega), \quad (3.11a)$$

$$\text{s.t. } Ax^c = b, \quad (3.11b)$$

$$Cx^c + Dy^c(\omega) = r(\omega) \quad \forall \omega \in \Omega. \quad (3.11c)$$

Using the dual multipliers $(\pi^c, \Pi^c(\omega))$ of (3.11b) and (3.11b), respectively, now we can state the dual program of (3.11) as follows:

$$\text{Dual: } \max b^\top \pi^c + \sum_{\omega \in \Omega} r(\omega)^\top \Pi^c(\omega), \quad (3.12a)$$

$$\text{s.t. } A^\top \pi^c + \sum_{\omega \in \Omega} C^\top \Pi^c(\omega) = c, \quad (3.12b)$$

$$D^\top \Pi^c(\omega) = p(\omega)d \quad \forall \omega \in \Omega. \quad (3.12c)$$

Now, we can expand the above primal model,(3.11) for the two-settlement problem as follows:

$$\min \sum_{i \in \mathcal{P}} c_i x_i + \mathbb{E}[(c_i + \delta_i^+)(X_i(\omega) - x_i)_+ - (c_i - \delta_i^-)(X_i(\omega) - x_i)_-], \quad (3.13a)$$

$$\text{s.t. } x_i^{\min} \leq x_i \leq x_i^{\max} \quad \forall i \in \mathcal{P}, \quad (3.13b)$$

$$f_{ij}^{\min} \leq f_{ij} \leq f_{ij}^{\max} \quad \forall (i, j) \in \mathcal{L}, \quad (3.13c)$$

$$(f_{ij})_{(i,j) \in \mathcal{L}} \in \mathcal{F}, \quad (3.13d)$$

$$\tau_n(f) + \sum_{j \in \mathcal{P}(n)} x_j = 0, \quad \forall n \in \mathcal{N}, \quad (3.13e)$$

$$\max\{X_i^{\min}, -X_i^{\text{avail}}(\omega)\} \leq X_i(\omega) \leq \min\{X_i^{\max}, X_i^{\text{avail}}(\omega)\} \quad \forall i \in \mathcal{P}, \omega \in \Omega, \quad (3.13f)$$

$$F_{ij}^{\min} \leq F_{ij}(\omega) \leq F_{ij}^{\max} \quad \forall (i, j) \in \mathcal{L}, \omega \in \Omega, \quad (3.13g)$$

$$(F_{ij}(\omega))_{(i,j) \in \mathcal{L}} \in \mathcal{F}, \quad \forall \omega \in \Omega, \quad (3.13h)$$

$$\tau_n(F(\omega)) - \tau_n(f) + \sum_{j \in \mathcal{P}(n)} (X_j(\omega) - x_j) = 0, \quad \forall n \in \mathcal{N}, \omega \in \Omega. \quad (3.13i)$$

Notice the explicit dependence of second-stage decisions on the random variable ω . We assume Ξ is finite, and therefore, the above perspective on two-stage SP problems can be solved using by the L-shaped method [55]. This decomposition-based approach provides a computationally viable path for large-scale implementation. The previous studies (e.g., [44] and [45]) on stochastic market clearing problems utilize this two-stage perspective.

3.3.1.1 Pricing Mechanism 1

The first pricing mechanism is based on the properties of the canonical form (3.13) of the SP problem. This payment mechanism was proposed in [44] and further analyzed in [45]. We can interpret the dual solution π_n^c corresponding to the first-stage flow-balance equation (3.13e) as the marginal cost of serving an additional unit of forecasted demand at node n . Equivalently, the second-stage dual solution $\Pi_n^c(\omega)$ of (3.13i) can be interpreted as the marginal cost associated with adjustments in demand under scenario ω . Therefore, the following payment mechanism is appropriate for the canonical form.

Definition 4. Under scenario $\omega \in \Xi$, the market participants receive a payment given by

$$\rho_i^c(\omega) = \pi_{n(i)}^c x_i + \Pi_{n(i)}^c(\omega)(X_i(\omega) - x_i) \quad \forall i \in \mathcal{P}. \quad (\mathcal{R}^c)$$

The day-ahead decision x_i of an SP problem is hedged against uncertainty in real-time. Therefore, the first term captures the payments for providing the well-hedged solutions that are rectified in the second term by $\Pi_{n(i)}^c(\omega)x_i$. The payment corresponding to the second-stage quantity (i.e., $\Pi_{n(i)}^c(\omega)X_i$) can then be viewed purely as a spot-market trade. The following result is well known regarding the stochastic clearing problem in the canonical form.

Proposition 1. Let the incremental bids satisfy $\delta_i^+, \delta_i^- > 0, \forall i \in \mathcal{P}$. The optimal solutions of the canonical stochastic clearing model result in revenue adequacy for the ISO and cost recovery for all generators in expectation under pricing mechanism (\mathcal{R}^c) . Furthermore, the expected price distortion at node $n \in \mathcal{N}$ is bounded to the interval $[\max_{i \in \mathcal{P}(n)}\{-\delta_i^+\}, \min_{i \in \mathcal{P}(n)}\{\delta_i^-\}]$.

Proof. See Theorems 1 and 2 in [98] for the results pertaining to revenue adequacy and cost recovery in expectation. Under pricing mechanism (\mathcal{R}^c) , scenario-specific price distortion is given by $\mathbb{M}_n^c(\omega) = \pi_n^c - \Pi_n^c(\omega), \forall n \in \mathcal{N}, \omega \in \Omega$. Theorem 9 in [45] establishes the bounds on expected price distortion, i.e., $-\delta_i^+ \leq \mathbb{E}[\mathbb{M}_n^c(i)(\omega)] \leq \delta_i^-, \forall i \in \mathcal{P}$. \square

Notice the two critical features of the above pricing mechanism. Firstly, all elements necessary to compute the payment in (\mathcal{R}^c) can be extracted using the solutions reported from decomposition algorithms such as the L-shaped method. Secondly, the properties relating to revenue adequacy, cost recovery, and price distortions hold only in expectation. Furthermore, the first stage in the canonical formulation makes decisions based on the day-ahead information and then accounts for the real-time stochasticity only in the second stage. Due to this decision structure, the first-stage here-and-now decisions undergo a scenario-dependent correction in the second stage. Unfortunately, a generator's flexibility to undergo this correction is not reflected in the above pricing mechanism. In other words, the payments received by generators depend only on the optimal dual solutions corresponding to the flow

balance equations (possibly viewed as the stochastic location marginal prices). They do not account for the generator's flexibility to offer second-stage/real-time corrections. In the following, we present SP formulations that explicitly can price this flexibility while retaining computability.

3.3.2 Mean-vector Stochastic Programming Model

We now present an equivalent formulation of (3.11) and its dual, the mean-vector SP model, as follows:

$$\text{Primal: } \min \sum_{\omega \in \Omega} p(\omega) (c^\top x^m(\omega) + d^\top y^m(\omega)), \quad (3.14a)$$

$$\text{s.t. } Ax^m(\omega) = b, \quad \forall \omega \in \Omega, \quad (3.14b)$$

$$Cx^m(\omega) + Dy^m(\omega) = r(\omega) \quad \forall \omega \in \Omega, \quad (3.14c)$$

$$x^m(\omega) = \sum_{\omega' \in \Omega} p(\omega') x^m(\omega') \quad \forall \omega \in \Omega. \quad (3.14d)$$

Using the dual multipliers $(\pi^m(\omega), \Pi^m(\omega), \mu(\omega))$ of (3.14b), (3.14c), and (3.14d), respectively, we can write the dual of (3.14) as follows:

$$\text{Dual: } \max \sum_{\omega \in \Omega} (b^\top \pi^m(\omega) + r^\top(\omega) \Pi^m(\omega)), \quad (3.15a)$$

$$\begin{aligned} \text{s.t. } & A^\top \pi^m(\omega) + C^\top \Pi^m(\omega) + (1 - p(\omega)) \mu(\omega) \\ & - \sum_{\substack{\omega' \in \Omega \\ \omega' \neq \omega}} p(\omega') \mu(\omega') = p(\omega) c, \quad \forall \omega \in \Omega \end{aligned} \quad (3.15b)$$

$$D^\top \Pi^m(\omega) = p(\omega) d \quad \forall \omega \in \Omega. \quad (3.15c)$$

Notice the changes in the first-stage decisions. They are scenario-dependent. This scenario dependency distinguishes the mean-vector formulation from the canonical formulation, and as such the first-stage decisions are unimplementable. To resolve this issue, we introduce the non-anticipativity constraints to the first-stage decisions. The non-anticipativity constraints can take two different forms, and in the mean-vector formulation, we utilize the form stated in (3.14d). The idea of this form is to set all the scenario-dependent first-stage decisions to

their mean value. In this formulation, all constraints are required to hold almost surely.

Since (3.11) and (3.14) are equivalent formulations, that is, at optimality we have $x^c = x^m(\omega)$ and $y^c(\omega) = y^m(\omega) \forall \omega \in \Omega$. Similarly, we can establish relationships between (3.12) and (3.15) variables.

Theorem 1. Let $(\pi^{c^*}, \Pi^{c^*}(\omega))$ be the optimal solution to (3.12) and $(\pi^{m^*}(\omega), \Pi^{m^*}(\omega), \mu^*(\omega))$ be the optimal solution to (3.15). These solutions satisfy

$$i \quad \Pi^{c^*}(\omega) = \Pi^{m^*}(\omega), \quad \forall \omega \in \Omega.$$

$$ii \quad \pi^{c^*} = \sum_{\omega \in \Omega} \pi^{m^*}(\omega);$$

Proof. Let $(\pi^{c^*}, \Pi^{c^*}(\omega))$ be the optimal solution to (3.12) and $(\pi^{m^*}(\omega), \Pi^{m^*}(\omega), \mu^*(\omega))$ be the optimal solution to (3.15). Constraint (3.12c) is equal to (3.15c). Therefore, a solution that satisfies one constraint satisfies the other. Hence, $\Pi^{c^*}(\omega) = \Pi^{m^*}(\omega), \forall \omega \in \Omega$.

Consider the constraint (3.12b).

$$A^\top \pi^{c^*} + \sum_{\omega \in \Omega} C^\top \Pi^{c^*}(\omega) = c, \quad \forall \omega \in \Omega.$$

By rearranging the terms, we get

$$\sum_{\omega \in \Omega} C^\top \Pi^{c^*}(\omega) = c - A^\top \pi^{c^*} \quad \forall \omega \in \Omega. \quad (3.16)$$

Now consider the constraint (3.15b).

$$A^\top \pi^m(\omega) + C^\top \Pi^m(\omega) + (1 - p(\omega))\mu(\omega) - \sum_{\substack{\omega' \in \Omega \\ \omega' \neq \omega}} p(\omega')\mu(\omega') = p(\omega)c, \quad \forall \omega \in \Omega.$$

By taking the sum over all $\omega \in \Omega$, we get

$$\sum_{\omega \in \Omega} A^\top \pi^m(\omega) + \sum_{\omega \in \Omega} C^\top \Pi^m(\omega) + \sum_{\omega \in \Omega} (1 - p(\omega))\mu(\omega) - \sum_{\omega \in \Omega} \left(\sum_{\substack{\omega' \in \Omega \\ \omega' \neq \omega}} p(\omega')\mu(\omega') \right) = \sum_{\omega \in \Omega} p(\omega)c.$$

Since $\Pi^{c^*}(\omega) = \Pi^{m^*}(\omega)$, we can substitute (3.16) on the left-hand side of the above equation.

Then we have

$$\sum_{\omega \in \Omega} A^\top \pi^m(\omega) + c - A^\top \pi^{c^*} + \sum_{\omega \in \Omega} (1 - p(\omega))\mu(\omega) - \sum_{\omega \in \Omega} \left(\sum_{\substack{\omega' \in \Omega \\ \omega' \neq \omega}} p(\omega')\mu(\omega') \right) = \sum_{\omega \in \Omega} p(\omega)c.$$

The right-hand side simplifies to c since the expected value of a constant is the constant itself. Then using simple algebraic operations we get

$$\begin{aligned} & \sum_{\omega \in \Omega} A^\top \pi^m(\omega) + c - A^\top \pi^{c^*} + \sum_{\omega \in \Omega} \mu(\omega) - \sum_{\omega \in \Omega} p(\omega)\mu(\omega) - \sum_{\omega \in \Omega} \left(\sum_{\substack{\omega' \in \Omega \\ \omega' \neq \omega}} p(\omega')\mu(\omega') \right) = c, \\ & \Rightarrow \sum_{\omega \in \Omega} A^\top \pi^m(\omega) - A^\top \pi^{c^*} + \sum_{\omega \in \Omega} \mu(\omega) - \sum_{\omega \in \Omega} (p(\omega)\mu(\omega) + \sum_{\substack{\omega' \in \Omega \\ \omega' \neq \omega}} p(\omega')\mu(\omega')) = 0, \\ & \Rightarrow \sum_{\omega \in \Omega} A^\top \pi^m(\omega) - A^\top \pi^{c^*} + \sum_{\omega \in \Omega} \mu(\omega) - \sum_{\omega \in \Omega} \sum_{\omega' \in \Omega} p(\omega')\mu(\omega') = 0, \\ & \Rightarrow \sum_{\omega \in \Omega} A^\top \pi^m(\omega) - A^\top \pi^{c^*} + \sum_{\omega \in \Omega} \mu(\omega) - \sum_{\omega \in \Omega} \mathbb{E}[\mu(\omega)] = 0. \end{aligned}$$

Consider (3.14d),

$$x^m(\omega) = \sum_{\omega \in \Omega} p(\omega)x^m(\omega).$$

Since $\mu(\omega)$ is the dual multiplier of (3.14d), from complementary slackness we have,

$$\mu(\omega) \left(x^m(\omega) - \sum_{\omega' \in \Omega} p(\omega')x^m(\omega') \right) = 0 \quad \forall \omega \in \Omega.$$

By taking sum over all $\omega \in \Omega$, we get

$$\begin{aligned}
& \sum_{\omega \in \Omega} \left(\mu(\omega) \left(x^m(\omega) - \sum_{\omega \in \Omega} p(\omega) x^m(\omega) \right) \right) = 0, \\
& \Rightarrow \sum_{\omega \in \Omega} \mu(\omega) x^m(\omega) - \sum_{\omega \in \Omega} \left(\mu(\omega) \sum_{\omega \in \Omega} p(\omega) x^m(\omega) \right) = 0, \\
& \Rightarrow \sum_{\omega \in \Omega} \mu(\omega) x^m(\omega) - \sum_{\omega \in \Omega} \sum_{\omega \in \Omega} \mu(\omega) p(\omega) x^m(\omega) = 0, \\
& \Rightarrow \sum_{\omega \in \Omega} x^m(\omega) \mu(\omega) - \sum_{\omega \in \Omega} \left(x^m(\omega) \sum_{\omega \in \Omega} p(\omega) \mu(\omega) \right) = 0, \\
& \Rightarrow \sum_{\omega \in \Omega} \left(x^m(\omega) \left(\mu(\omega) - \sum_{\omega \in \Omega} p(\omega) \mu(\omega) \right) \right) = 0.
\end{aligned}$$

When $\sum_{\omega \in \Omega} x^m(\omega) = 0 \ \forall \omega \in \Omega$, the non-anticipativity constraints become redundant. The only interesting case is when we have $x^m(\omega) \neq 0 \ \forall \omega \in \Omega$. Therefore, we get

$$\sum_{\omega \in \Omega} \mu(\omega) - \sum_{\omega \in \Omega} p(\omega) \mu(\omega) = 0.$$

By applying this to

$$\sum_{\omega \in \Omega} A^\top \pi^m(\omega) - A^\top \pi^{c^*} + \sum_{\omega \in \Omega} \mu(\omega) - \sum_{\omega \in \Omega} \mathbb{E}[\mu(\omega)] = 0,$$

we get

$$\begin{aligned}
& \sum_{\omega \in \Omega} A^\top \pi^m(\omega) - A^\top \pi^{c^*} = 0, \\
& \Rightarrow A^\top \left(\sum_{\omega \in \Omega} \pi^m(\omega) - \pi^{c^*} \right) = 0.
\end{aligned}$$

Since, $A^\top \neq 0$ (see (3.2)). we have,

$$\sum_{\omega \in \Omega} \pi^m(\omega) = \pi^{c^*}.$$

This completes the proof. \square

Now we present the extended (3.14) formulation for the two-settlement market problem as follows:

$$\min \sum_{i \in \mathcal{P}} c_i x_i(\omega) + \mathbb{E}[(c_i + \delta_i^+)(X_i(\omega) - x_i(\omega))_+ - (c_i - \delta_i^-)(X_i(\omega) - x_i(\omega))_-], \quad (3.17a)$$

$$\text{s.t. } x_i^{\min} \leq x_i(\omega) \leq x_i^{\max} \quad \forall i \in \mathcal{P}, \omega \in \Omega, \quad (3.17b)$$

$$f_{ij}^{\min} \leq f_{ij}(\omega) \leq f_{ij}^{\max} \quad \forall (i, j) \in \mathcal{L}, \omega \in \Omega, \quad (3.17c)$$

$$(f_{ij}(\omega))_{(i,j) \in \mathcal{L}} \in \mathcal{F}, \quad \forall \omega \in \Omega, \quad (3.17d)$$

$$\tau_n(f(\omega)) + \sum_{j \in \mathcal{P}(n)} x_j(\omega) = 0, \quad \forall n \in \mathcal{N}, \omega \in \Omega, \quad (3.17e)$$

$$\max\{X_i^{\min}, -X_i^{\text{avail}}(\omega)\} \leq X_i(\omega) \leq \min\{X_i^{\max}, X_i^{\text{avail}}(\omega)\} \quad \forall i \in \mathcal{P}, \omega \in \Omega, \quad (3.17f)$$

$$F_{ij}^{\min} \leq F_{ij}(\omega) \leq F_{ij}^{\max} \quad \forall (i, j) \in \mathcal{L}, \omega \in \Omega, \quad (3.17g)$$

$$(F_{ij}(\omega))_{(i,j) \in \mathcal{L}} \in \mathcal{F}, \quad \forall \omega \in \Omega, \quad (3.17h)$$

$$\begin{aligned} & \tau_n(F(\omega)) - \tau_n(f(\omega)) \\ & + \sum_{j \in \mathcal{P}(n)} (X_j(\omega) - x_j(\omega)) = 0, \quad \forall n \in \mathcal{N}, \omega \in \Omega, \end{aligned} \quad (3.17i)$$

$$x_i(\omega) - \mathbb{E}[x_i(\omega)] = 0 \quad \forall i \in \mathcal{P}, \omega \in \Omega, \quad (3.17j)$$

$$f_{ij}(\omega) - \mathbb{E}[f_{ij}(\omega)] = 0 \quad \forall (i, j) \in \mathcal{L}, \omega \in \Omega. \quad (3.17k)$$

The scenario-dependent variables allow the model to decompose into scenario-specific problems. Hence, we can take advantage of scenario decomposition algorithms, specifically, the Progressive Hedging (PH) method [56] to recover the desired duals in a computationally efficient manner.

3.3.2.1 Pricing Mechanism 2

We derive the second payment mechanism from the mean-vector formulation (3.17). Similar to (\mathcal{R}^c) , the second mechanism also includes a day-head component and a real-time component which are computed using the optimal dual solutions $(\pi^m(\omega), \Pi^m(\omega))$ of the respective flow-balance equations (3.17e) and (3.17i). However, unlike the previous

mechanism, we include a scenario-wise adjustment for the first-stage component using the dual solution $\mu^x(\omega)$ of (3.17j). We define this payment mechanism as follows.

Definition 5. Under scenario $\omega \in \Xi$, the market participants receive a payment as follows:

$$\rho_i^m(\omega) = (\pi_{n(i)}^m(\omega) + \mu_i^x(\omega))x_i(\omega) + \Pi_{n(i)}^m(\omega)(X_i(\omega) - x_i(\omega)) \quad \forall i \in \mathcal{P}. \quad (\mathcal{R}^m)$$

Here, μ_i^x is the dual corresponding to the non-anticipative constraint of the form in (3.17j) for the variable $x_i(\omega)$.

The following result captures the properties of (\mathcal{R}^m) .

Theorem 2. Let $\delta_i^+, \delta_i^- > 0 \quad \forall i \in \mathcal{P}$. If the optimal dual solutions obtained from the mean-vector formulation of the stochastic market clearing problem satisfy $\sum_{i \in \mathcal{P}} \mathbb{E}[\mu_i^{x^*}(\omega)]\mathbb{E}[x_i^*(\omega)] \leq 0$, then pricing mechanism (\mathcal{R}^m) yields revenue adequacy in expectation for the ISO. Furthermore, if generator $i \in \mathcal{G}$ satisfies $\mathbb{E}[\mu_i^{x^*}(\omega)] \geq 0$ for all $i \in \mathcal{G}$ then it achieves cost recovery in expectation. Finally, the scenario-specific price distortion defined as $\mathbb{M}_n(\omega)^m = \pi_{n(i)}^m(\omega) + \mu_i^x(\omega) - \Pi_{n(i)}^m(\omega)$ satisfies

$$\mathbb{M}_n(\omega)^m \in [-\delta_i^+, \delta_i^-] + p(\omega)\mu_i^x(\omega), \quad \forall i \in \mathcal{P}. \quad (3.18)$$

Proof. Proof: Consider the Lagrangian relaxation of (3.17).

$$\begin{aligned} \min \quad \mathbb{L}^m = & \mathbb{E} \left[\sum_{i \in \mathcal{P}} c_i x_i(\omega) + (c_i + \delta_i^+)(X_i(\omega) - x_i(\omega))_+ - (c_i - \delta_i^-)(X_i(\omega) - x_i(\omega))_- \right. \\ & - \sum_{n \in \mathcal{N}} \pi_n^m(\omega) \left(\tau_n(f(\omega)) + \sum_{j \in \mathcal{P}(n)} x_j(\omega) \right) \\ & - \sum_{n \in \mathcal{N}} \Pi_n^m(\omega) \left(\tau_n(F(\omega)) - \tau_n(f(\omega)) + \sum_{j \in \mathcal{P}(n)} (X_j(\omega) - x_j(\omega)) \right) \\ & \left. - \sum_{i \in \mathcal{P}} \mu_i^x(\omega) \left(x_i(\omega) - \mathbb{E}[x_i(\omega)] \right) - \sum_{(i,j) \in \mathcal{L}} \mu_{ij}^f(\omega) \left(f_{ij}(\omega) - \mathbb{E}[f_{ij}(\omega)] \right) \right]. \quad (3.19) \end{aligned}$$

Since \mathbb{L}^m is minimized over (3.1) and (3.5), the optimal solution $(x^*(\omega), X^*(\omega), f^*(\omega), F^*(\omega), \pi^{m^*}(\omega), \Pi^{m^*}(\omega), \mu^{x^*}(\omega), \mu^{f^*}(\omega))$ also minimizes the Lagrangian

relaxation with the optimal value \mathbb{L}^{m^*} . Notice that the solution obtained by setting $f(\omega) = 0$ and $F(\omega) = 0$ for all $\omega \in \Xi$ is a sub-optimal feasible solution. For such a solution we have $\mathbb{E}[f(\omega)] = 0$ and

$$\begin{aligned}\mathbb{L}^{m^*} &\leq \mathbb{E} \left[\sum_{i \in \mathcal{P}} c_i x_i^*(\omega) + (c_i + \delta_i^+)(X_i^*(\omega) - x_i^*(\omega))_+ - (c_i - \delta_i^-)(X_i^*(\omega) - x_i^*(\omega))_- \right. \\ &\quad - \sum_{n \in \mathcal{N}} \pi_n^{m^*} \left(\sum_{i \in P(n)} x_i^*(\omega) \right) - \sum_{n \in \mathcal{N}} \Pi_n^{m^*}(\omega) \left(\sum_{i \in P(n)} (X_i^*(\omega) - x_i^*(\omega)) \right) \\ &\quad \left. - \sum_{i \in \mathcal{P}} \mu_i^{x^*}(\omega) (x_i^*(\omega) - \mathbb{E}[x_i^*(\omega)]) \right].\end{aligned}$$

Substituting \mathbb{L}^{m^*} from (3.19) and rearranging the terms we obtain

$$\begin{aligned}-\mathbb{E} \left[\sum_{n \in \mathcal{N}} \pi_n^{m^*}(\omega) \tau_n(f^*(\omega)) + \Pi_n^{m^*}(\omega) (\tau_n(F^*(\omega)) - \tau_n(f^*(\omega))) \right. \\ \left. + \sum_{i \in \mathcal{L}} \mu_i^{f^*}(\omega) (f_i^*(\omega) - \mathbb{E}[f_i^*(\omega)]) \right] \leq 0.\end{aligned}$$

Since the optimal solution satisfies $f_i^*(\omega) - \mathbb{E}[f_i^*(\omega)] = 0$ for all $i \in \mathcal{L}, \omega \in \Omega$, the last term in the above inequality equates to zero. The optimal solution also satisfies $x_i^*(\omega) - \mathbb{E}[x_i^*(\omega)] = 0$. Using this we obtain

$$-\mathbb{E} \left[\sum_{n \in \mathcal{N}} \pi_n^{m^*} \tau_n(f) + \Pi_n^{m^*}(\omega) (\tau_n(F^*(\omega)) - \tau_n(f^*(\omega))) + \sum_{i \in \mathcal{P}} \mu_i^{x^*}(\omega) (x_i^*(\omega) - \mathbb{E}[x_i^*(\omega)]) \right] \leq 0.$$

Using the flow balance equations (3.17e) and (3.17i), we have

$$\begin{aligned}\mathbb{E} \left[\sum_{i \in \mathcal{P}} \left(\pi_{n(i)}^{m^*}(\omega) x_i^*(\omega) + \Pi_{n(i)}^{m^*}(\omega) (X_i^*(\omega) - x_i^*(\omega)) + \mu_i^{x^*}(\omega) (x_i^*(\omega) - \mathbb{E}[x_i^*(\omega)]) \right) \right] \leq 0. \\ \mathbb{E} \left[\sum_{i \in \mathcal{P}} \left(\pi_{n(i)}^{m^*}(\omega) x_i^*(\omega) + \Pi_{n(i)}^{m^*}(\omega) (X_i^*(\omega) - x_i^*(\omega)) + \mu_i^{x^*}(\omega) x_i^*(\omega) \right) \right. \\ \left. - \sum_{i \in \mathcal{P}} \mathbb{E}[\mu_i^{x^*}(\omega)] \mathbb{E}[x_i^*(\omega)] \right] \leq 0.\end{aligned}$$

Therefore, if we have $\sum_{i \in \mathcal{P}} \mathbb{E}[\mu_i^{x^*}(\omega)] \mathbb{E}[x_i^*(\omega)] \leq 0$ then, we obtain $\mathbb{E}[\sum_{i \in \mathcal{P}} \rho_i^m(\omega)] \leq 0$ which implies that pricing mechanism (R^m) is revenue adequate in expectation.

Since the problem is convex, the optimal dual values, $(\pi^{m^*}(\omega), \Pi^{m^*}(\omega), \mu^{x^*}(\omega), \mu^{xf^*}(\omega))$ satisfy

$$\begin{aligned}\mathbb{L}^{m^*} = & \min_{\substack{x(\omega), X(\omega) \\ f(\omega), F(\omega)}} \mathbb{E} \left[\sum_{i \in \mathcal{P}} c_i x_i(\omega) + (c_i + \delta_i^+)(X_i(\omega) - x_i(\omega))_+ - (c_i - \delta_i^-)(X_i(\omega) - x_i(\omega))_- \right. \\ & - \sum_{n \in \mathcal{N}} \pi_n^{m^*}(\omega) \left(\tau_n(f(\omega)) + \sum_{i \in P(n)} x_i(\omega) \right) \\ & - \sum_{n \in \mathcal{N}} \Pi_n^{m^*}(\omega) \left(\tau_n(F(\omega)) - \tau_n(f(\omega)) + \sum_{i \in P(n)} (X_i(\omega) - x_i(\omega)) \right) \\ & \left. - \sum_{i \in \mathcal{P}} \mu_i^{x^*}(\omega) (x_i(\omega) - \mathbb{E}[x_i(\omega)]) - \sum_{i \in \mathcal{L}} \mu_i^{f^*}(\omega) (f_i(\omega) - \mathbb{E}[f_i(\omega)]) \right].\end{aligned}$$

Notice that the optimization problem on the right-hand side of the above inequality decomposes into participant-specific optimization problems. Therefore,

$$\mathbb{L}^{m^*} = \sum_{i \in \mathcal{P}} \mathbb{E} \left[\min_{x_i(\omega), X_i(\omega)} \mathbb{L}_i^1(x_i(\omega), X_i(\omega)) \right] + \min_{f(\omega), F(\omega)} \mathbb{E} \left[\mathbb{L}_i^2(f(\omega), F(\omega)) \right].$$

Here, we define

$$\begin{aligned}\mathbb{L}_i^1(x_i(\omega), X_i(\omega)) = & c_i x_i(\omega) + (c_i + \delta_i^+)(X_i(\omega) - x_i(\omega))_+ - (c_i - \delta_i^-)(X_i(\omega) - x_i(\omega))_- \\ & - \pi_{n(i)}^{m^*}(\omega) x_i(\omega) - \Pi_{n(i)}^{m^*}(\omega) (X_i(\omega) - x_i(\omega)) \\ & - \mu_i^{x^*}(\omega) (x_i(\omega) - \mathbb{E}[x_i(\omega)]) \quad \forall i \in \mathcal{P}, \\ \mathbb{L}_i^2(f_i(\omega), F_i(\omega)) = & - \sum_{n \in \mathcal{N}} \pi_n^{m^*}(\omega) \tau_n(f(\omega)) - \sum_{n \in \mathcal{N}} \Pi_n^{m^*}(\omega) (\tau_n(F(\omega)) - \tau_n(f(\omega))) \\ & - \sum_{i \in \mathcal{L}} \mu_i^{f^*}(\omega) (f_i(\omega) - \mathbb{E}[f_i(\omega)]).\end{aligned}$$

Further, we can minimize \mathbb{L}^{m^*} by minimizing above functions separately for every participant. Now consider the Lagrangian $\mathbb{L}_i^1(x_i(\omega), X_i(\omega))$ and its optimal solution $(x_i^*(\omega), X^*(\omega))$. Since

(x_i^{\min}, X_i^{\min}) is a sub-optimal feasible solution, we have for all $i \in \mathcal{P}$

$$\begin{aligned} \mathbb{E}[\mathbb{L}_i^1(x_i^*(\omega), X_i^*(\omega))] &\leq \mathbb{E}\left[c_i x_i^{\min} + (c_i + \delta_i^+)(X_i^{\min} - x_i^{\min})_+ - (c_i - \delta_i^-)(X_i^{\min} - x_i^{\min})_- \right. \\ &\quad \left. - \pi_{n(i)}^{m^*}(\omega)x_i^{\min} - \Pi_{n(i)}^{m^*}(\omega)(X_i^{\min} - x_i^{\min}) - \mu_i^{x^*}(\omega)(x_i^{\min} - \mathbb{E}[x_i^{\min}])\right]. \end{aligned}$$

Substituting $\mathbb{L}_i^1(x_i^*(\omega), X_i^*(\omega))$ and rearranging the terms, we obtain

$$\begin{aligned} &\mathbb{E}\left[c_i x_i^*(\omega) + (c_i + \delta_i^+)(X_i^*(\omega) - x_i^*(\omega))_+ - (c_i - \delta_i^-)(X_i^*(\omega) - x_i^*(\omega))_- \right. \\ &\quad \left. - \left(c_i x_i^{\min} + (c_i + \delta_i^+)(X_i^{\min} - x_i^{\min})_+ - (c_i - \delta_i^-)(X_i^{\min} - x_i^{\min})_-\right)\right] \\ &\leq \mathbb{E}\left[(\pi_{n(i)}^{m^*}(\omega) + \mu_i^{x^*}(\omega))x_i^*(\omega) + \Pi_{n(i)}^{m^*}(\omega)(X_i^*(\omega) - x_i^*(\omega))\right] - \mathbb{E}[\mu_i^{x^*}(\omega)]\mathbb{E}[x_i^*(\omega)] \\ &\quad - \mathbb{E}_1\left[\pi_{n(i)}^{m^*}(\omega) + \mu_i^{x^*}(\omega)\right]x_i^{\min} + \Pi_{n(i)}^{m^*}(\omega)(X_i^{\min} - x_i^{\min}) + \mathbb{E}[\mu_i^{x^*}(\omega)]\mathbb{E}[x_i^{\min}(\omega)]. \end{aligned}$$

If the startup costs are sufficiently covered through the uplifts paid by the commitment problem, then we can focus on payment settled using the clearing problem studied here. In this case, we have

$$\begin{aligned} &\mathbb{E}\left[c_i x_i^*(\omega) + (c_i + \delta_i^+)(X_i^*(\omega) - x_i^*(\omega))_+ - (c_i - \delta_i^-)(X_i^*(\omega) - x_i^*(\omega))_-\right] \\ &\leq \mathbb{E}\left[(\pi_{n(i)}^{m^*}(\omega) + \mu_i^{x^*}(\omega))x_i^*(\omega) + \Pi_{n(i)}^{m^*}(\omega)(X_i^*(\omega) - x_i^*(\omega))\right] - \mathbb{E}[\mu_i^{x^*}(\omega)]\mathbb{E}[x_i^*(\omega)]. \end{aligned}$$

Using (3.7) and (\mathcal{R}^m) in the above inequality, we obtain $\mathbb{E}[\rho_i^m(\omega) - \varphi_i(\omega)] \geq 0$ whenever $\mathbb{E}[\mu_i^{x^*}(\omega)]\mathbb{E}[x_i^*(\omega)] \geq 0$. Note that if $\mathbb{E}[\mu_i^{x^*}(\omega)] \geq 0$ for all $i \in \mathcal{G}$, the latter condition holds for all generators implying that they recover their costs in expectation.

We next show the price distortion properties. Notice that

$$\begin{aligned} &c_i x_i(\omega) + (c_i + \delta_i^+)(X_i(\omega) - x_i(\omega))_+ - (c_i - \delta_i^-)(X_i(\omega) - x_i(\omega))_- \\ &= c_i X_i(\omega) + (\delta_i^+ + \delta_i^-)(X_i(\omega) - x_i(\omega))_+ - \delta_i^-(X_i(\omega) - x_i(\omega)) \end{aligned}$$

Using the above relationship in \mathbb{L}^m , the partial Lagrangian with respect to day-ahead quan-

ity $x_i(\omega)$ at the stationary point can be written as follows:

$$\begin{aligned} 0 &\in \partial_{x_i(\omega)} \mathbb{L}^m = (\delta_i^+ + \delta_i^-) \partial_{x_i(\omega)} (X_i(\omega) - x_i(\omega))_+ + \delta_i^- - (\pi_{n(i)}^m(\omega) \\ &\quad - \Pi_{n(i)}^m(\omega) + (1 - p(\omega))\mu_i^x(\omega)) \\ &\Rightarrow \frac{-\delta_i^- + (\pi_{n(i)}^m(\omega) - \Pi_{n(i)}^m(\omega) + (1 - p(\omega))\mu_i^x(\omega))}{\delta_i^+ + \delta_i^-} \in \partial_{x_i(\omega)} (X_i(\omega) - x_i(\omega))_+. \end{aligned}$$

Since,

$$\partial_{x_i(\omega)} (X_i(\omega) - x_i(\omega))_+ = \begin{cases} -1, & \text{if } X_i(\omega) > x_i(\omega) \\ 0, & \text{if } X_i(\omega) < x_i(\omega) \\ [-1, 0] & \text{if } X_i(\omega) = x_i(\omega) \end{cases}.$$

We have

$$\begin{aligned} -1 &\leq \frac{-\delta_i^- + (\pi_{n(i)}^m(\omega) - \Pi_{n(i)}^m(\omega) + (1 - p(\omega))\mu_i^x(\omega))}{\delta_i^+ + \delta_i^-} \leq 0 \\ &\Rightarrow -\delta_i^+ + p(\omega)\mu_i^x(\omega) \leq (\pi_{n(i)}^m(\omega) + \mu_i^x(\omega)) - \Pi_{n(i)}^m(\omega) \leq \delta_i^- + p(\omega)\mu_i^x(\omega) \\ &\qquad\qquad\qquad \forall i \in \mathcal{P}, \omega \in \Omega. \end{aligned}$$

This completes the proof. \square

The mean-vector formulation reveals hidden dual information not available in the canonical model. This dual information allows us to design pricing mechanism \mathcal{R}^m that adjusts day-ahead and real-time components in every scenario. However, \mathcal{R}^m can achieve only conditional revenue adequacy and cost recovery in expectation which cannot be guaranteed for every instance. On the other hand, \mathcal{R}^m has price distortion bounds for every scenario as opposed to the expected price distortion bounds in (\mathcal{R}^c) . These bounds depend on the scenario probability and their corresponding non-anticipativity dual. For extreme scenarios, that is, low probability scenarios, the price distortion bounds stay closer to the interval $[-\delta^+, \delta^-]$ depending on the value of the non-anticipativity dual. For higher probability scenarios, the price distortion bounds move away from the interval $[-\delta^+, \delta^-]$ depending on the value of the

non-anticipativity dual. Notice that, in either case, the width of the interval remains the same, $(\delta^+ + \delta^-)$.

3.3.3 State-vector Stochastic Programming Model

The next equivalent model, the state-vector model, utilizes the second form of the non-anticipativity representation. In this method, the scenario-dependent first-stage decisions are tied together using an additional decision vector. We can state the primal and the dual forms of state-vector formulation as follows:

$$\text{Primal: } \min \sum_{\omega \in \Omega} p(\omega) (c^\top x^s(\omega) + d^\top y^s(\omega)), \quad (3.20a)$$

$$\text{s.t. } Ax^s(\omega) = b, \quad \forall \omega \in \Omega, \quad (3.20b)$$

$$Cx^s(\omega) + Dy^s(\omega) = r(\omega) \quad \forall \omega \in \Omega, \quad (3.20c)$$

$$x^s(\omega) = \chi \quad \forall \omega \in \Omega. \quad (3.20d)$$

Using the dual multipliers $(\pi^s(\omega), \Pi^s(\omega), \sigma(\omega))$ of (3.20b), (3.20c), and (3.20d), respectively, we can write the dual of (3.20) as follows:

$$\text{Dual: } \max \sum_{\omega \in \Omega} (b^\top \pi^s(\omega) + r^\top(\omega) \Pi^s(\omega)), \quad (3.21a)$$

$$\text{s.t. } A^\top \pi^s(\omega) + C^\top \Pi^s(\omega) + \sigma(\omega) = p(\omega)c, \quad \forall \omega \in \Omega \quad (3.21b)$$

$$D^\top \Pi^s(\omega) = p(\omega)d \quad \forall \omega \in \Omega. \quad (3.21c)$$

$$\sum_{\omega \in \Omega} \sigma(\omega) = 0. \quad (3.21d)$$

Since (3.20) is equivalent to previous models, we can state the relationships between primal decision variables as follows:

$$\text{i } x^c = x^m(\omega) = x^s(\omega), \quad \forall \omega \in \Omega;$$

$$\text{ii } y^c(\omega) = y^m(\omega) = y^s(\omega).$$

Furthermore, we can establish the dual variable relationships.

Theorem 3. Let $(\pi^{c*}, \Pi^{c*}(\omega))$ be the optimal solution to (3.12), $(\pi^{m*}(\omega), \Pi^{m*}(\omega), \mu^*(\omega))$ be

the optimal solution to (3.15), and $(\pi^{s^*}(\omega), \Pi^{s^*}(\omega), \sigma^*(\omega))$ be the optimal solution to (3.21). These solutions satisfy

$$i \sum_{\omega \in \Omega} \sigma^* = 0 ;$$

$$ii \quad \Pi^{c^*}(\omega) = \Pi^{m^*}(\omega) = \Pi^{s^*}(\omega), \quad \forall \omega \in \Omega;$$

$$iii \quad \pi^{c^*} = \sum_{\omega \in \Omega} \pi^{m^*}(\omega) = \sum_{\omega \in \Omega} \pi^{s^*}(\omega);$$

$$iv \quad If \pi^{m^*}(\omega) = \pi^{s^*}(\omega), then \sigma^*(\omega) = \mu^*(\omega) - \mathbb{E}[\mu^*(\omega)].$$

Proof. From the dual feasibility constraint (3.21d), we have

$$\sum_{\omega \in \Omega} \sigma^* = 0.$$

Furthermore, constraint (3.15c) is equal to (3.21c). Therefore, a solution that satisfies one constraint satisfies the other. Hence, $\Pi^{s^*}(\omega) = \Pi^{m^*}(\omega), \forall \omega \in \Omega$. Using Theorem 1 part i we have

$$\Pi^{c^*}(\omega) = \Pi^{s^*}(\omega) = \Pi^{m^*}(\omega), \quad \forall \omega \in \Omega.$$

Now consider the constraint (3.21b).

$$A^\top \pi^{s^*}(\omega) + C^\top \Pi^{s^*}(\omega) + \sigma^*(\omega) = p(\omega)c, \quad \forall \omega \in \Omega.$$

By taking the sum over all $\omega \in \Omega$, we get

$$\sum_{\omega \in \Omega} A^\top \pi^{s^*}(\omega) + \sum_{\omega \in \Omega} C^\top \Pi^{s^*}(\omega) + \sum_{\omega \in \Omega} \sigma^*(\omega) = \sum_{\omega \in \Omega} p(\omega)c$$

Since $\Pi^{c^*}(\omega) = \Pi^{s^*}(\omega)$, we can substitute (3.16) in the above equation. Then we have

$$\sum_{\omega \in \Omega} A^\top \pi^{s^*}(\omega) + c - A^\top \pi^{c^*} + \sum_{\omega \in \Omega} \sigma^*(\omega) = \sum_{\omega \in \Omega} p(\omega)c$$

The right-hand side simplifies to c since the expected value of a constant is the constant itself. Therefore, we get

$$\begin{aligned} & \sum_{\omega \in \Omega} A^\top \pi^{s^*}(\omega) + c - A^\top \pi^{c^*} + \sum_{\omega \in \Omega} \sigma^*(\omega) = c. \\ \Rightarrow & \sum_{\omega \in \Omega} A^\top \pi^{s^*}(\omega) - A^\top \pi^{c^*} + \sum_{\omega \in \Omega} \sigma^*(\omega) = 0. \end{aligned}$$

From (3.21d) we have $\sum_{\omega \in \Omega} \sigma(\omega) = 0$. Thus,

$$\begin{aligned} & \sum_{\omega \in \Omega} A^\top \pi^{s^*}(\omega) - A^\top \pi^{c^*} = 0. \\ \Rightarrow & A^\top \left(\sum_{\omega \in \Omega} \pi^{s^*}(\omega) - \pi^{c^*} \right) = 0. \end{aligned}$$

Since $A^\top \neq 0$, we have

$$\sum_{\omega \in \Omega} \pi^{s^*}(\omega) = \pi^{c^*}$$

Combining this result with Theorem 1 part ii we get

$$\pi^{c^*} = \sum_{\omega \in \Omega} \pi^{m^*}(\omega) = \sum_{\omega \in \Omega} \pi^{s^*}(\omega)$$

Consider the constraint (3.21b).

$$A^\top \pi^{s^*}(\omega) + C^\top \Pi^{s^*}(\omega) + \sigma^*(\omega) = p(\omega)c, \quad \forall \omega \in \Omega.$$

By rearranging the terms, we get

$$C^\top \Pi^{s^*}(\omega) = p(\omega)c - A^\top \pi^{s^*}(\omega) - \sigma^*(\omega) \quad \forall \omega \in \Omega. \quad (3.22)$$

Now consider the constraint (3.15b).

$$A^\top \pi^{m^*}(\omega) + C^\top \Pi^{m^*}(\omega) + (1 - p(\omega))\mu^*(\omega) - \sum_{\substack{\omega' \in \Omega \\ \omega' \neq \omega}} p(\omega')\mu^*(\omega') = p(\omega)c, \quad \forall \omega \in \Omega.$$

Using algebraic operations we can simplify this into

$$A^\top \pi^{m^*}(\omega) + C^\top \Pi^{m^*}(\omega) + \mu^*(\omega) - p(\omega)\mu^*(\omega) - \sum_{\substack{\omega' \in \Omega \\ \omega' \neq \omega}} p(\omega')\mu^*(\omega') = p(\omega)c, \quad \forall \omega \in \Omega.$$

The last two terms on the left hand side together represents the expected value of $\mu^*(\omega)$. Therefore,

$$A^\top \pi^{m^*}(\omega) + C^\top \Pi^{m^*}(\omega) + \mu^*(\omega) - \mathbb{E}[\mu^*(\omega)] = p(\omega)c, \quad \forall \omega \in \Omega.$$

Since $\Pi^{s^*}(\omega) = \Pi^{m^*}(\omega)$, we can substitute (3.22). Then we have

$$\begin{aligned} A^\top \pi^{m^*}(\omega) + p(\omega)c - A^\top \pi^{s^*}(\omega) - \sigma^*(\omega) + \mu^*(\omega) - \mathbb{E}[\mu^*(\omega)] &= p(\omega)c, \quad \forall \omega \in \Omega, \\ \Rightarrow A^\top \pi^{m^*}(\omega) - A^\top \pi^{s^*}(\omega) - \sigma^*(\omega) + \mu^*(\omega) - \mathbb{E}[\mu^*(\omega)] &= 0, \quad \forall \omega \in \Omega, \end{aligned}$$

Hence, if $\pi^{m^*}(\omega) = \pi^{s^*}(\omega)$ then

$$\sigma^*(\omega) = \mu^*(\omega) - \mathbb{E}[\mu^*(\omega)].$$

This completes the proof. \square

Next we present the extended state-vector two-settlement problem as follows:

$$\min \sum_{i \in \mathcal{P}} c_i x_i(\omega) + \mathbb{E}[(c_i + \delta_i^+)(X_i(\omega) - x_i(\omega))_+ - (c_i - \delta_i^-)(X_i(\omega) - x_i(\omega))_-], \quad (3.23a)$$

$$\text{s.t. } x_i^{\min} \leq x_i(\omega) \leq x_i^{\max} \quad \forall i \in \mathcal{P}, \omega \in \Omega, \quad (3.23b)$$

$$f_{ij}^{\min} \leq f_{ij}(\omega) \leq f_{ij}^{\max} \quad \forall (i, j) \in \mathcal{L}, \omega \in \Omega, \quad (3.23c)$$

$$(f_{ij}(\omega))_{(i,j) \in \mathcal{L}} \in \mathcal{F}, \quad \forall \omega \in \Omega, \quad (3.23d)$$

$$\tau_n(f(\omega)) + \sum_{j \in \mathcal{P}(n)} x_j(\omega) = 0, \quad \forall n \in \mathcal{N}, \omega \in \Omega, \quad (3.23e)$$

$$\max\{X_i^{\min}, -X_i^{\text{avail}}(\omega)\} \leq X_i(\omega) \leq \min\{X_i^{\max}, X_i^{\text{avail}}(\omega)\} \quad \forall i \in \mathcal{P}, \omega \in \Omega, \quad (3.23f)$$

$$F_{ij}^{\min} \leq F_{ij}(\omega) \leq F_{ij}^{\max} \quad \forall (i, j) \in \mathcal{L}, \omega \in \Omega, \quad (3.23g)$$

$$(F_{ij}(\omega))_{(i,j) \in \mathcal{L}} \in \mathcal{F}, \quad \forall \omega \in \Omega, \quad (3.23h)$$

$$\begin{aligned} & \tau_n(F(\omega)) - \tau_n(f(\omega)) \\ & + \sum_{j \in \mathcal{P}(n)} (X_j(\omega) - x_j(\omega)) = 0, \quad \forall n \in \mathcal{N}, \omega \in \Omega, \end{aligned} \quad (3.23i)$$

$$x_i(\omega) - \chi_i^x = 0 \quad \forall i \in \mathcal{P}, \omega \in \Omega, \quad (3.23j)$$

$$f_{ij}(\omega) - \chi_{ij}^f = 0 \quad \forall (i, j) \in \mathcal{L}, \omega \in \Omega. \quad (3.23k)$$

Similar to the previous model, the state-vector model can decompose into scenario problems. Thus, the PH method provides computationally efficient solution method for this model. Due to part *iv* of Theorem 3, we can use the optimal dual solution extracted from the PH method to compute the non-anticipativity dual of the state-vector formulation.

3.3.4 Pricing Mechanism 3

We derive the third payment mechanism from the state-vector formulation (3.23). Similar to previous payment mechanisms, this mechanism also includes a day-head component and a real-time component which are computed using the optimal dual solutions $(\pi^s(\omega), \Pi^s(\omega))$ of the respective flow-balance equations (3.23e) and (3.23i). Furthermore, like in (\mathcal{R}^m) , we include a scenario-wise adjustment for the first-stage component using the dual solution

$\sigma^x(\omega)$ of (3.23j). We define this payment mechanism as follows:

Definition 6. Under scenario $\omega \in \Xi$, the market participants receive a payment given by

$$\rho_i^s(\omega) = (\pi_{n(i)}^s(\omega) + \sigma_i^x(\omega))x_i(\omega) + \Pi_{n(i)}^s(\omega)(X_i(\omega) - x_i(\omega)) \quad \forall i \in \mathcal{P}. \quad (\mathcal{R}^s)$$

Here, $\sigma_i^x(\omega)$ is the dual corresponding to the non-anticipativity constraint of the form in (3.20d) for the variable $x_i(\omega)$.

Notice that the payment mechanism differs from (\mathcal{R}^m) only in its use of $\sigma_i^x(\omega)$ instead of $\mu_i^x(\omega)$. Furthermore, the day-ahead component in this pricing mechanism is scenario-dependent that satisfies $\mathbb{E}[(\pi_{n(i)}^s(\omega) + \sigma_i^x(\omega))] = \pi_{n(i)}^c$ (due to Theorem 3, parts *i* and *iv*). In other words, the day-ahead component of (\mathcal{R}^m) aligns in expectation with the day-ahead component of (\mathcal{R}^c) . The clairvoyant problem can identify the best dispatch plan for a given scenario. With the aim of hedging against uncertainty, the SP optimal dispatch deviates from the best scenario-specific dispatch. The quantity $\sigma_i^x(\omega)x_i(\omega)$ included in (\mathcal{R}^s) allows us to reflect the value offered by a participant i to attain a well-hedged stochastic solution in their payment. For this pricing mechanism, the scenario-specific price distortion is given by $\mathbb{M}_n^s(\omega) = \pi_n^s(\omega) + \sigma_i^x(\omega) - \Pi_n^s(\omega)$, $\forall n \in \mathcal{N}, \omega \in \Omega$. This pricing mechanism exhibits the following characteristics.

Theorem 4. Under the assumption that $\delta_i^+, \delta_i^- > 0 \quad \forall i \in \mathcal{P}$, the payment mechanism (\mathcal{R}^s) , computed using the optimal solutions of the (3.23), yield revenue adequacy in expectation for the ISO and cost recovery under every scenario for all generators. Furthermore, the scenario-specific price distortion satisfies

$$-\delta_i^+ \leq \mathbb{M}_{n(i)}^s(\omega) \leq \delta_i^- \quad \forall i \in \mathcal{P}, \omega \in \Omega.$$

Proof. Consider the following Lagrangian relaxation of the (3.23).

$$\begin{aligned} \mathbb{L}^s = & \mathbb{E} \left[\sum_{i \in \mathcal{P}} c_i x_i(\omega) + (c_i + \delta_i^+)(X_i(\omega) - x_i(\omega))_+ - (c_i - \delta_i^-)(X_i(\omega) - x_i(\omega))_- \right. \\ & - \sum_{n \in \mathcal{N}} \pi_n^s(\omega) \left(\tau_n(f(\omega)) + \sum_{i \in P(n)} x_i(\omega) \right) \\ & - \sum_{n \in \mathcal{N}} \Pi_n^s(\omega) \left(\tau_n(F(\omega)) - \tau_n(f(\omega)) + \sum_{i \in P(n)} (X_i(\omega) - x_i(\omega)) \right) \\ & \left. - \sum_{i \in \mathcal{P}} \sigma_i^x(\omega) (x_i(\omega) - \chi_i^x) - \sum_{i \in \mathcal{L}} \sigma_i^f(\omega) (f_i(\omega) - \chi_i^f) \right]. \end{aligned} \quad (3.24)$$

Since \mathbb{L}^s is minimized over (3.1) and (3.5), the optimal solution $(x_i^*(\omega), X_i^*(\omega), \chi_i^{x*}, f_i^*(\omega), F_i^*(\omega), \chi_i^{f*}, \pi_n^{s*}(\omega), \Pi_n^{s*}(\omega), \sigma_i^{x*}, \sigma_i^{f*})$ also minimizes the Lagrangian relaxation. Let \mathbb{L}^{s*} be the value of the Lagrangian at the optimal solution. Further since, $(x_i^*(\omega), X_i^*(\omega), \chi_i^{x*}, 0, 0, \chi_i^{f*}, \pi_n^{s*}(\omega), \Pi_n^{s*}(\omega), \sigma_i^{x*}, \sigma_i^{f*})$ (obtained by setting $f(\omega) = 0$ and $F(\omega) = 0$ for all $\omega \in \Xi$) is a sub-optimal feasible solution, we have

$$\begin{aligned} \mathbb{L}^{s*} \leq & \mathbb{E} \left[\sum_{i \in \mathcal{P}} c_i x_i^*(\omega) + (c_i + \delta_i^+)(X_i^*(\omega) - x_i^*(\omega))_+ - (c_i - \delta_i^-)(X_i^*(\omega) - x_i^*(\omega))_- \right. \\ & - \sum_{n \in \mathcal{N}} \pi_n^{s*}(\omega) \left(\sum_{i \in P(n)} x_i^*(\omega) \right) - \sum_{n \in \mathcal{N}} \Pi_n^{s*}(\omega) \left(\sum_{i \in P(n)} (X_i^*(\omega) - x_i^*(\omega)) \right) \\ & \left. - \sum_{i \in \mathcal{P}} \sigma_i^{x*}(\omega) (x_i^*(\omega) - \chi_i^{x*}) + \sum_{i \in \mathcal{L}} \sigma_i^{f*}(\omega) \chi_i^{f*} \right]. \end{aligned}$$

Substituting \mathbb{L}^{s*} from (3.24) on the left-hand side of the above and rearranging the terms, we obtain

$$-\mathbb{E} \left[\sum_{n \in \mathcal{N}} \pi_n^{s*}(\omega) \tau_n(f^*(\omega)) + \Pi_n^{s*}(\omega) (\tau_n(F^*(\omega)) - \tau_n(f^*(\omega))) + \sum_{i \in \mathcal{L}} \sigma_i^{f*}(\omega) f_i^*(\omega) \right] \leq 0.$$

Since, $f_i^*(\omega) = \chi_i^{f^*} \forall i \in \mathcal{L}, \omega \in \Omega$

$$\begin{aligned} & -\mathbb{E}\left[\sum_{n \in \mathcal{N}} \pi_n^{s^*}(\omega) \tau_n(f^*(\omega)) + \Pi_n^{s^*}(\omega)(\tau_n(F^*(\omega)) - \tau_n(f^*(\omega)))\right] + \mathbb{E}\left[\sum_{i \in \mathcal{L}} \sigma_i^{f^*}(\omega)\right] \chi_i^{f^*} \leq 0, \\ \Rightarrow & -\mathbb{E}\left[\sum_{n \in \mathcal{N}} \pi_n^{s^*}(\omega) \tau_n(f^*(\omega)) + \Pi_n^{s^*}(\omega)(\tau_n(F^*(\omega)) - \tau_n(f^*(\omega)))\right] \leq 0. \end{aligned}$$

In the second inequality, we have used $\mathbb{E}\left[\sum_{i \in \mathcal{L}} \sigma_i^{f^*}(\omega)\right] = 0$, due to Theorem 3 *i*. Similarly, since $\mathbb{E}\left[\sum_{i \in \mathcal{P}} \sigma_i^{x^*}(\omega)\right] = 0$ (also from Theorem 3 *i*), we have

$$-\mathbb{E}\left[\sum_{n \in \mathcal{N}} \pi_n^{s^*}(\omega) \tau_n(f^*(\omega)) + \Pi_n^{s^*}(\omega)(\tau_n(F^*(\omega)) - \tau_n(f^*(\omega)))\right] + \mathbb{E}\left[\sum_{i \in \mathcal{P}} \sigma_i^{x^*}(\omega)\right] \chi_i^{x^*} \leq 0.$$

Using the flow balance equations (3.23e) and (3.23i), and the state-vector form of the non-anticipativity constraint (3.23j) in the above inequality, we obtain

$$\mathbb{E}\left[\sum_{i \in \mathcal{P}} (\pi_{n(i)}^{s^*}(\omega) + \sigma_i^{x^*}(\omega)) x_i(\omega) + \Pi_{n(i)}^{s^*}(\omega)(X_i^*(\omega) - x_i^*(\omega))\right] \leq 0.$$

The above implies that $\mathbb{E}\left[\sum_{i \in \mathcal{P}} \rho_i^s(\omega)\right] \leq 0$, thereby, establishing the revenue adequacy of (\mathcal{R}^s) .

Since the problem is convex, the optimal dual values, $(\pi_n^{s^*}(\omega), \Pi_n^{s^*}(\omega), \sigma_i^{x^*}, \sigma_i^{f^*})$ satisfy

$$\begin{aligned} \mathbb{L}^{s^*} = \min_{\substack{x(\omega), X(\omega) \\ s^x, f(\omega), F(\omega), s^f}} & \mathbb{E}\left[\sum_{i \in \mathcal{P}} c_i x_i(\omega) + (c_i + \delta_i^+)(X_i(\omega) - x_i(\omega))_+ - (c_i - \delta_i^-)(X_i(\omega) - x_i(\omega))_- \right. \\ & - \sum_{n \in \mathcal{N}} \pi_n^{s^*}(\omega)(\tau_n(f(\omega)) + \sum_{i \in P(n)} x_i(\omega)) \\ & - \sum_{n \in \mathcal{N}} \Pi_n^{s^*}(\omega)(\tau_n(F(\omega)) - \tau_n(f(\omega)) + \sum_{i \in P(n)} (X_i(\omega) - x_i(\omega))) \\ & \left. - \sum_{i \in \mathcal{P}} \sigma_i^{x^*}(\omega)(x_i(\omega) - \chi_i^x) - \sum_{i \in \mathcal{L}} \sigma_i^{f^*}(\omega)(f_i(\omega) - \chi_i^f)\right]. \end{aligned}$$

Notice that the optimization problem on the right-hand side of the above inequality decom-

poses into participant-specific optimization problems. Therefore,

$$\mathbb{L}^{s^*} = \sum_{i \in \mathcal{P}} \mathbb{E} \left[\min_{x_i(\omega), X_i(\omega), \chi_i^x} \mathbb{L}_i^1(x_i(\omega), X_i(\omega), \chi_i^x) \right] + \min_{f(\omega), F(\omega), \chi^f} \mathbb{E}[\mathbb{L}^2(f(\omega), F(\omega), \chi^f)],$$

where, we define

$$\begin{aligned} \mathbb{L}_i^1(x_i(\omega), X_i(\omega), \chi_i^x) &= c_i x_i(\omega) + (c_i + \delta_i^+)(X_i(\omega) - x_i(\omega))_+ - (c_i - \delta_i^-)(X_i(\omega) - x_i(\omega))_- \\ &\quad - \pi_{n(i)}^{s^*}(\omega) x_i(\omega) - \Pi_{n(i)}^{s^*}(\omega)(X_i(\omega) - x_i(\omega)) - \sigma_i^{x^*}(\omega)(x_i(\omega) - \chi_i^x) \\ &\qquad \forall i \in \mathcal{P}, \end{aligned}$$

$$\begin{aligned} \mathbb{L}_i^2(f_i(\omega), F_i(\omega), \chi_i^f) &= - \sum_{n \in \mathcal{N}} \pi_n^{s^*}(\omega) \tau_n(f(\omega)) - \sum_{n \in \mathcal{N}} \Pi_n^{s^*}(\omega)(\tau_n(F(\omega)) - \tau_n(f(\omega))) \\ &\quad - \sum_{i \in \mathcal{L}} \sigma_i^{f^*}(\omega)(f_i(\omega) - \chi_i^f), \end{aligned}$$

for all $\omega \in \Xi$. Further, we can minimize \mathbb{L}^{s^*} by minimizing above functions separately for every participant and $\omega \in \Xi$. Now consider the Lagrangian $\mathbb{L}^1(x_i(\omega), X_i(\omega), \chi_i^x)$ and its optimal solution $(x_i^*(\omega), X_i^*(\omega), \chi_i^{x^*})$. Since $(x_i^{\min}, X_i^{\min}, \chi_i^{x^*})$ is a sub-optimal feasible solution, we have

$$\begin{aligned} \mathbb{L}(x_i^*(\omega), X_i^*(\omega), \chi_i^{x^*}) &\leq c_i x_i^{\min} + (c_i + \delta_i^+)(X_i^{\min} - x_i^{\min})_+ - (c_i - \delta_i^-)(X_i^{\min} - x_i^{\min})_- \\ &\quad - \pi_{n(i)}^{s^*}(\omega) x_i^{\min} - \Pi_{n(i)}^{s^*}(\omega)(X_i^{\min} - x_i^{\min}) - \sigma_i^{x^*}(\omega)(x_i^{\min} - \chi_i^{x^*}). \end{aligned}$$

Substituting $\mathbb{L}(x_i^*(\omega), X_i^*(\omega), \chi_i^{x^*})$ and rearranging the terms, we obtain

$$\begin{aligned} &c_i x_i^*(\omega) + (c_i + \delta_i^+)(X_i^*(\omega) - x_i^*(\omega))_+ - (c_i - \delta_i^-)(X_i^*(\omega) - x_i^*(\omega))_- \\ &\quad - \left(c_i x_i^{\min} + (c_i + \delta_i^+)(X_i^{\min} - x_i^{\min})_+ - (c_i - \delta_i^-)(X_i^{\min} - x_i^{\min})_- \right) \\ &\leq (\pi_{n(i)}^{s^*}(\omega) + \sigma_i^{x^*}(\omega)) x_i(\omega) + \Pi_{n(i)}^{s^*}(\omega)(X_i(\omega) - x_i(\omega)) \\ &\quad - \left(\pi_{n(i)}^{s^*}(\omega) + \sigma_i^{x^*}(\omega) \right) x_i^{\min} + \Pi_{n(i)}^{s^*}(\omega)(X_i^{\min} - x_i^{\min}). \end{aligned}$$

Once again, if the uplifts payments from unit commitment problem cover the minimum generation then, the above can be reduced to $\varphi_i(\omega) \leq \rho_i^s(\omega)$. This implies cost recovery for

all generators under every scenario $\omega \in \Xi$.

Finally, to establish the property of scenario-specific price distortion, notice that

$$\begin{aligned} c_i x_i(\omega) + (c_i + \delta_i^+)(X_i(\omega) - x_i(\omega))_+ - (c_i - \delta_i^-)(X_i(\omega) - x_i(\omega))_- \\ = c_i X_i(\omega) + (\delta_i^+ + \delta_i^-)(X_i(\omega) - x_i(\omega))_+ - \delta_i^-(X_i(\omega) - x_i(\omega)) \end{aligned}$$

Using the above relation in the Lagrangian \mathbb{L}^s in (3.24), the partial derivative of the Lagrangian with respect to day-ahead quantity $x_i(\omega)$ at the stationary point can be written as follows:

$$(\delta_i^+ + \delta_i^-) \partial_{x_i(\omega)}(X_i(\omega) - x_i(\omega))_+ + \delta_i^- - (\pi_{n(i)}^s(\omega) - \Pi_{n(i)}^s(\omega) + \sigma_i^x(\omega)).$$

Since $0 \in \partial_{x_i(\omega)} \mathbb{L}^s$, we have

$$\Rightarrow \frac{-\delta_i^- + (\pi_{n(i)}^s(\omega) - \Pi_{n(i)}^s(\omega) + \sigma_i^x(\omega))}{\delta_i^+ + \delta_i^-} \in \partial_{x_i(\omega)}(X_i(\omega) - x_i(\omega))_+.$$

Note that

$$\partial_{x_i(\omega)}(X_i(\omega) - x_i(\omega))_+ = \begin{cases} -1, & \text{if } X_i(\omega) > x_i(\omega) \\ 0, & \text{if } X_i(\omega) < x_i(\omega) \\ [-1, 0] & \text{if } X_i(\omega) = x_i(\omega). \end{cases}$$

This implies that

$$\begin{aligned} -1 \leq \frac{-\delta_i^- + (\pi_{n(i)}^s(\omega) - \Pi_{n(i)}^s(\omega) + \sigma_i^x(\omega))}{\delta_i^+ + \delta_i^-} \leq 0, \\ \Rightarrow -\delta_i^+ \leq \pi_{n(i)}^s(\omega) + \sigma_i^x(\omega) - \Pi_{n(i)}^s(\omega) \leq \delta_i^- \quad \forall i \in \mathcal{P}, \omega \in \Omega. \end{aligned}$$

This completes the proof. \square

Similar to the mean-vector formulation, the state-vector formulation also uncovers dual information not available in the canonical model. Using this dual information, we design

pricing mechanism \mathcal{R}^s that adjusts day-ahead and real-time components in every scenario. \mathcal{R}^s achieves revenue adequacy in expectation without any conditions like in \mathcal{R}^c . The advantage of \mathcal{R}^s is that it achieves cost recovery for every generator under every scenario without any conditions, unlike in \mathcal{R}^c and \mathcal{R}^m . In addition, price distortion are bounded within the $[-\delta^+, \delta^-]$ for every scenario without disruption unlike in the previous pricing mechanisms.

3.4 Experiments

In this section, we demonstrate the properties of all the pricing mechanisms presented in section 3.3.

3.4.1 Test System

We adopted a six-node system from [98] and [45], depicted in Figure 3.1 along with system characteristics, to illustrate the results. The system operates six buses connecting six generators and a load. Of the six generators, two are inflexible generators connected at bus 1 and 3, respectively; two are wind generators connected at bus 2 and 4, respectively; and two hydrothermal generators connected at bus 5. Both thermal generators have maximum capacity of 100MW and a generation cost of \$40 and \$45 per MW, respectively. We assume that the cost of generation for wind generators is zero. For the hydrothermal generators, the unit cost of generation are \$42 and \$80, respectively. The parenthetical terms are the negative and positive deviation price, respectively.

The line connecting buses 1 and 6 has a maximum capacity of 150MW and the remaining lines are uncapacitated. Further, we assume all lines are lossless and have equal reactance. That is, $\frac{1}{6}$ of the electricity generated in thermal 1 flow through line (1, 2) and the remaining $\frac{5}{6}$ flow through the line (1, 6). The single load which is connected bus 6, and is assumed to be firm with a demand of 264MW. We assume the wind generation to be a random quantity that can realize any scenario from the possible set (30, 50, 60, 70, 90) with equal probability. Thus, there are 25 total scenarios. Note that we use 90MW, the maximum possible output, as the first-stage capacity limit of the wind generators. The two flexible hydro generators can increase or decrease their generation in the real-time market with deviation costs to mitigate the impact of the wind generation uncertainty.

We implemented the models in C++ and solved them using CPLEX 12.9 solver. We

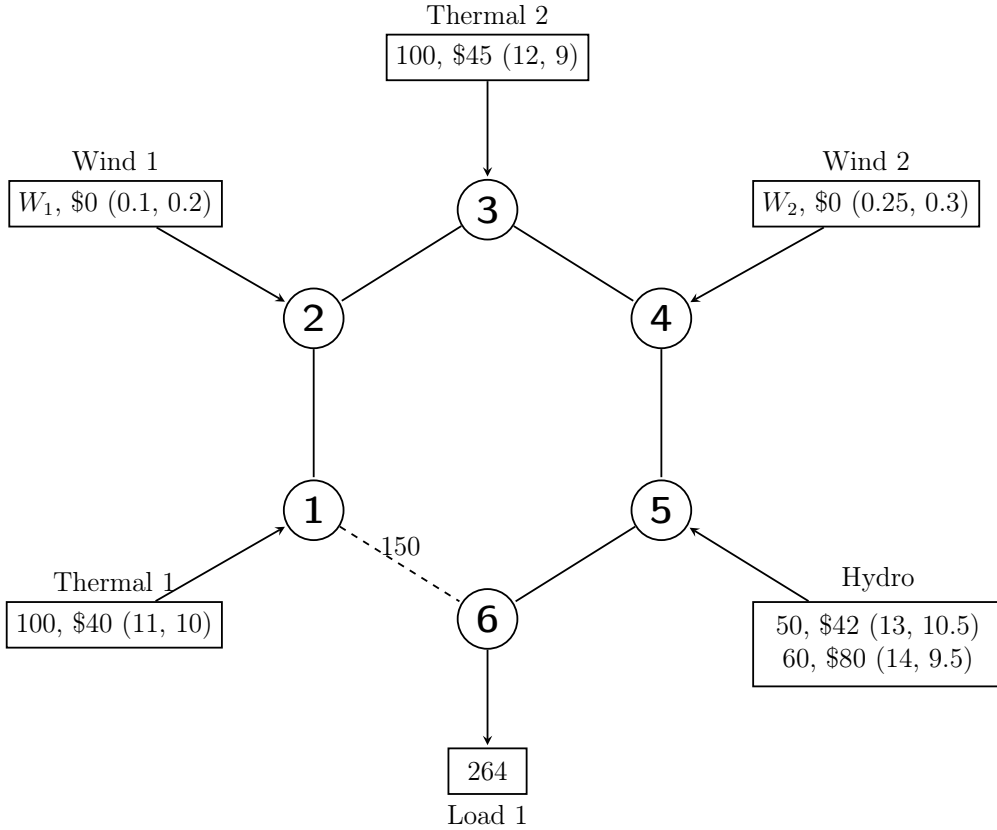


Figure 3.1: Network diagram of six-node system.

used an Intel Core i3 machine with a 2.20 GHz processor and 8GB RAM to conduct the experiments.

3.4.1.1 Relationships Between Dual Optimal Solutions

First, we summarize the dual solutions of the three models in Table 3.1. The day-ahead (DA) location marginal prices (LMP) of canonical model, the expected DA LMP of mean-vector model, and the expected DA LMP of state-vector model have similar values in Table 3.1 providing numerical evidence for Theorem 3 *iii*. The canonical formulation does not have scenario-dependent first-stage decisions. Therefore, the first-stage flow-balance constraints are scenario independent and hence their duals. On the other hand, the two alternative models, mean-vector and state-vector models have scenario-dependent first-stage decisions. Therefore, we have scenario-dependent first-stage flow-balance duals. However, the scenario-dependent flow balance equation duals agree in expectation to the canonical duals. The last

Table 3.1: Summary of dual solutions from different SP models.

	Canonical	Mean-vector	State-vector	
	DA LMP	Expected DA LMP	Expected DA LMP	Expected NA duals
Thermal 1	40	40	40	-2.22E-15
Wind 1	42.5	42.66	42.5	-3.33E-16
Thermal 2	45	45.16	45	-1.33E-15
Wind 2	47.5	47.66	47.5	-1.11E-16
Hydro 1	50	50.16	50	0
Hydro 2	50	50.16	50	0
Load 1	52.5	52.66	52.5	-2.22E-15

column of Table 3.1 shows that the non-anticipativity duals of state-vector formulation (3.23) are 0 in expectation for all market participants. This result provides numerical corroboration to our Theorem 3 i.

3.4.1.2 Performance of Pricing Mechanism \mathcal{R}^m

Next, we focus on the results from the mean-vector formulation and pricing mechanism \mathcal{R}^m . Recall that, in Theorem 2, to achieve revenue adequacy in expectation, the mean-vector solutions have to satisfy $\sum_{i \in \mathcal{P}} \mathbb{E}[\mu_i^{x^*}(\omega)] \mathbb{E}[x_i^*(\omega)] \leq 0$. However, this condition was not met in our numerical results. Therefore, we cannot conclude revenue adequacy in expectation under \mathcal{R}^m . In our experiments the net payment for the ISO was 72343.9 (a positive quantity) indicating that the payments made to the generator exceed those received from the load.

Furthermore, generators achieve cost recovery in expectation if $\mathbb{E}[\mu_i^{x^*}(\omega)] \geq 0$. We summarise the cost recovery results for \mathcal{R}^m in figure 3.2. The left vertical axis and the bar graph in Figure 3.2 represents the expected non-anticipativity duals for generators, and the right vertical axis is the cost or payment (in dollars). Notice that for generators Wind 1, Thermal 2, and Hydro 1, the expected non-anticipativity duals are positive, meaning that they satisfy the necessary condition for cost recovery in expectation. Therefore, for those generators, we can observe that the payments are higher than their costs. In other words, they achieve cost recovery in expectation. Also, notice that Hydro 2 achieves cost recovery in expectation even without satisfying the condition. This indicates that the identified condition is necessary but not sufficient. For Thermal 1 and Wind 2, the condition is not met and they fail to recover



Figure 3.2: Results illustrating cost recovery in expectation under \mathcal{R}^m .

costs (costs are higher than payments).

3.4.1.3 Performance of Pricing Mechanism \mathcal{R}^s

In the state-vector form, we focus on three crucial results. We begin with our discussion on cost recovery under every scenario for all generators. Notice that in Figure 3.3, for generators Thermal 1 and Thermal 2, the cost and payment are the same in all scenarios, and they are constant even with the scenario adjustment in the payment structure \mathcal{R}^s . This is an encouraging result since Thermal 1 and Thermal 2 are inflexible generators. If we do not expect any changes in the real-time generation, the payments also should reflect the same unchanged prices. Two wind generators are making profits under most scenarios due to their low generation costs. We can see similar results in [98] and [45] for wind generators under pricing mechanism \mathcal{R}^c . Hydro 1 is making a profit under a few scenarios and getting enough payment to cover their costs in others. For Hydro 2, costs and payments are the same for all scenarios.

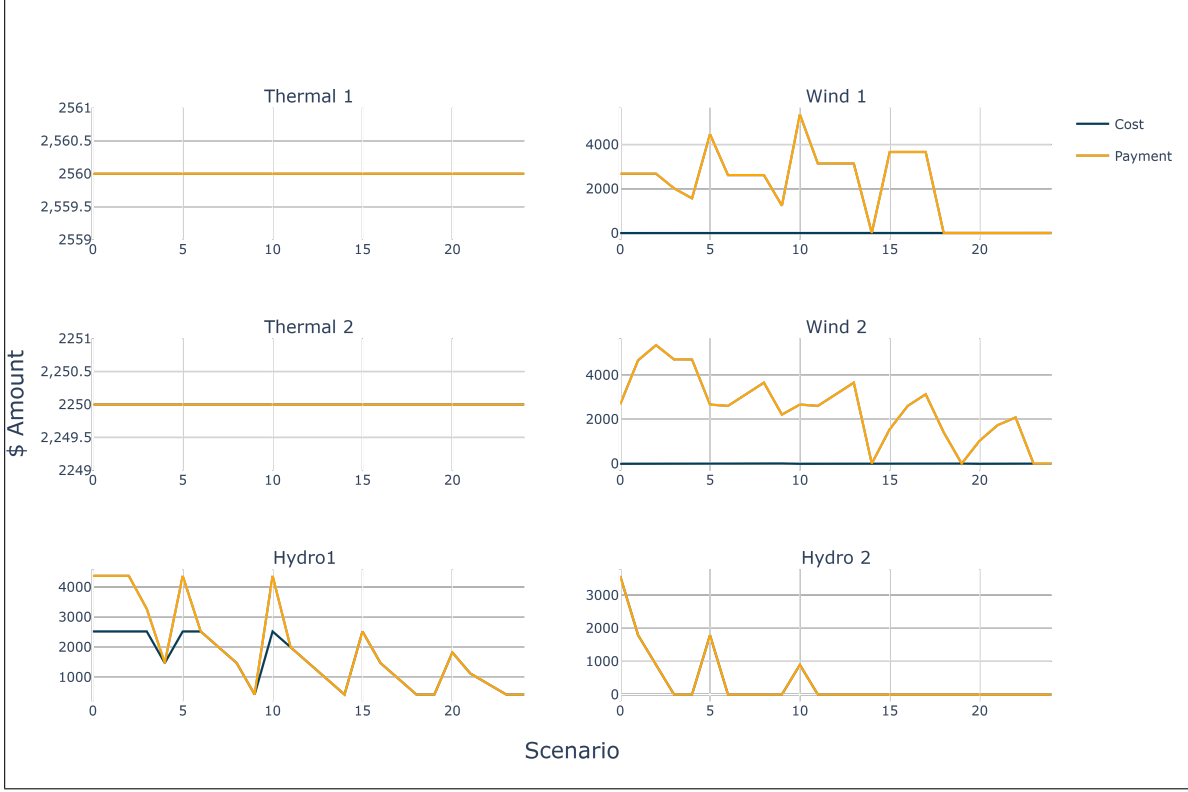


Figure 3.3: State-vector cost recovery by scenario.

Revenue adequacy is a vital property for a pricing mechanism since it guarantees that ISO will not face financial deficits. Under pricing mechanism \mathcal{R}^s , we showed that this is possible in expectation. For generators, Thermal 1, Wind 1, Thermal 2, Wind 2, Hydro 1, and Hydro 2, the expected payments are \$2560, \$2040.41, \$2250, \$2475.59, \$1926, and \$358, respectively. Therefore, the total expected payment is \$11610. The expected amount received from the load is \$13860. Since the received amount is greater than the total payment, this shows the revenue adequacy in expectation under pricing mechanism \mathcal{R}^s .

The final result in this section is for the price distortion under pricing mechanism \mathcal{R}^s . Figure 3.4 depicts all the price distortions for all the generators under every scenario. Recall that we define price distortion as the difference between the day-ahead unit payment and the real-time unit payment. Our results in Theorem 4 indicate that these quantities are bounded by their deviation penalties $(-\delta_i^+, \delta_i^-)$. This property is reflected in numerical results presented in Figure 3.4 for all generators.

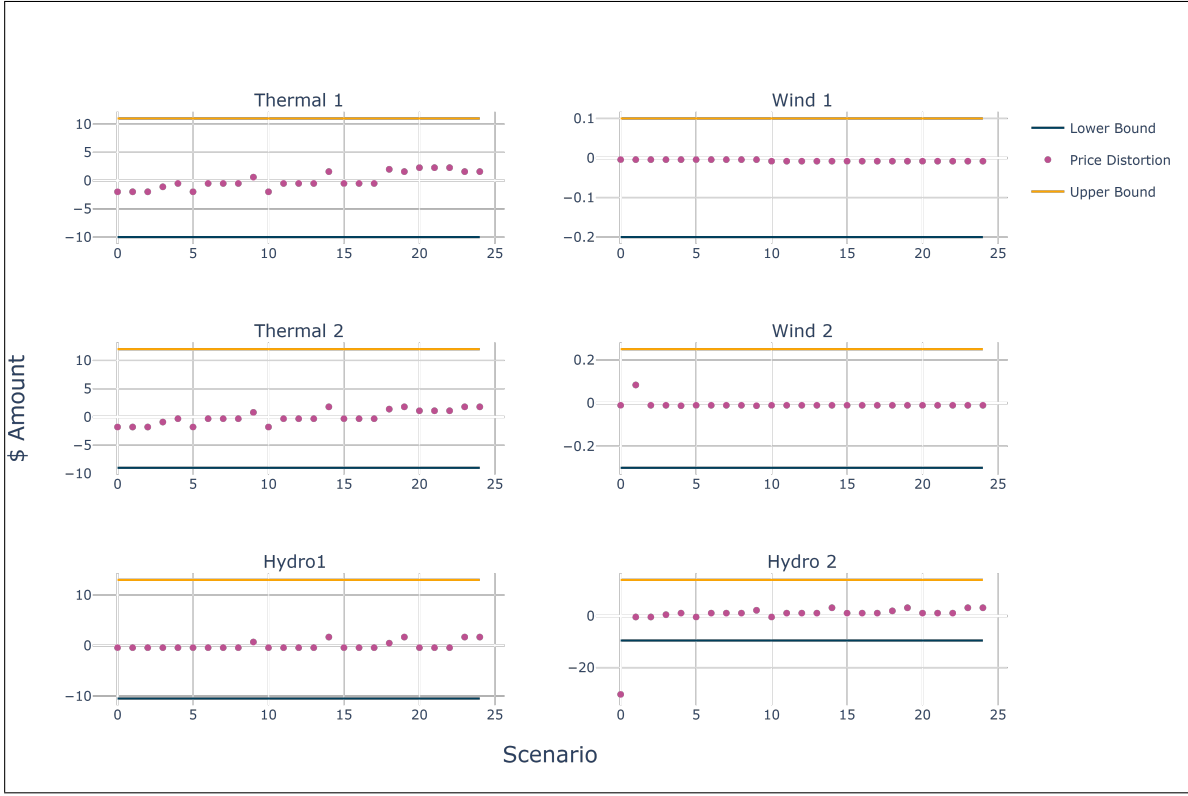


Figure 3.4: State-vector price distortion by scenario.

3.5 Conclusion

In this chapter, our focus was on emphasizing the advantages of alternative SP models, namely, mean-vector and state-vector models, for the electricity market clearing problem. While the canonical SP model is capable of capturing the stochasticity in the real-time market, it fails to make adjustments to the day-ahead market based on real-time outcomes. This inability is especially evident in the day-ahead flow balance duals since they are equal for all scenarios. Flow balance duals, which are often viewed as locational marginal price, are a crucial component of developing pricing mechanisms for the electricity market. Therefore, being unable to apprehend these dual values restrict the development of proper pricing mechanisms.

To address this issue, we developed electricity market clearing models based on the non-anticipativity concept in SP. The non-anticipativity constraints in an SP model allow the model to have scenario-dependent first-stage decisions, in our case, day-ahead decisions.

As a result, the model has scenario-dependent day-ahead flow balance and hence scenario-dependent duals. These scenario-dependent day-ahead duals can adjust the real-time fluctuations while keeping the day-ahead primal decisions intact. Furthermore, they helped prove pricing mechanism properties such as cost recovery and price distortion for every scenario.

The two alternative SP models, mean-vector and state-vector, allowed us to develop two pricing mechanisms, \mathcal{R}^m and \mathcal{R}^s , respectively. We showed that pricing mechanism \mathcal{R}^m yields revenue adequacy in expectation for the system operator if the condition in Theorem 2 is satisfied. Furthermore, a generator achieves cost recovery in expectation if its non-anticipativity duals are non-negative in expectation. We also developed scenario-specific bounds for the price distortion under pricing mechanism \mathcal{R}^m .

We also showed the revenue adequacy for the system operator in expectation for pricing mechanism \mathcal{R}^s without any conditions. Furthermore, we proved cost recovery for every generator under every scenario without any conditions. This is a significant result in terms of real-world application since it guarantees that generators do not lose money under any circumstances. Then we defined bounds for the price distortion for every scenario using the deviation penalties. In other words, we can control the price distortion by setting appropriate deviation penalties. The scenario-wise price distortion results were made possible by the non-anticipativity constraints in the two models.

In Theorem 3, we proved the dual relationships between all SP models: canonical, means-vector, and state-vector. Using Theorem 3 *iv*, we can obtain the state-vector results using the mean-vector formulation solutions. These results can hugely improve the pricing problems faced by the system operators while retaining the computational capabilities. Furthermore, they can improve the confidence of the generators and provide fair prices for the consumers.

Chapter 4

Multiagent Optimization for Coordinated Transmission-distribution System

4.1 Introduction

The smart grid is a concept that came as a solution to the outdated conventional power grid. The rapid growth of electricity demand causes reliability issues for the conventional power grid, and the old technology troubles integrating new technologies such as renewable energy and distributed energy resources (DER). The smart grid was formally recognized in the Energy Independence and Security Act of 2007. The act “Declares it is the policy of the United States to support modernization of the nation’s electricity transmission and distribution system to maintain a reliable and secure electricity infrastructure that can meet future demand growth and to achieve specified characteristics of a Smart Grid.” (<https://www.congress.gov/bill/110th-congress/house-bill/6>). The purpose of the smart grid is to improve reliability, security, and efficiency and to integrate renewable energy into the power system. To achieve this, a smart grid provides timely information and control to the consumer. These changes forced the utilities to innovate and incorporate new technologies into their operations.

The most significant advantage of the smart grid is that it allows two-way communication between the power system and consumers as opposed to one-way communication in the conventional power grid. As seen in earlier chapters, the conventional power grid has a central authority (the ISO). They make all decisions and all communication must go through them. Consumers have no control over any decisions. The smart grid changes this by enabling consumers to participate in the electricity market through DER, such as rooftop solar. Thus, they can decide according to their needs and determine when to sell or buy depending on the prices. However, we need an efficient communication system to perform these smart grid operations.

4.1.1 Multiagent markets

There are multiple DSs within a TS. The DS operations usually follow TS decisions. Therefore the DS decisions must be coordinated with TS decisions. A sequential sampling-based optimization algorithm has been proposed in [99]. The authors considered a main grid with multiple microgrids with renewable generation and modeled the problem using a two-stage SP.

In addition, each DS deals with the TS in different locations. That is, DSs get different purchasing prices depending on their connected TS bus. Further, DSs also generate electricity that can be sold to the TS. This creates competition between DSs to sell and buy electricity even though the decisions are made independently.

When all the participants make individual decisions achieving an equilibrium can be a daunting task. These are known as noncooperative games in the literature [100]. These settings are common in power systems, communication systems, and transportation networks. In a noncooperative game, every participant optimizes their strategy in a feasible set specific to that participant given others' strategies. The Nash equilibrium is a set of strategies for all players such that no player can improve their strategy unilaterally by deviating from it [100]. We can find the noncooperative game application in power systems in [101], [102].

4.1.2 Best Response Schemes

A player selecting their best strategy given the other decisions is known as the Best Response (BR) scheme [103], and [104]. To achieve the best strategy for all the players, all players must apply their BR scheme repeatedly [105]. The BR schemes can be viewed as a protocol that shares minimum information to achieve equilibrium for all players. A discussion on solution algorithms for stochastic BR schemes is in [106]. An inexact generalization of the BR scheme has been proposed in [107]. Further, to solve two-stage non-cooperative games, a few variants of BR schemes have been used in [108].

BR schemes do not always guarantee a Nash equilibrium. This is true even for potential games in which all player strategies can be modeled using a single objective function, with convex potential functions [109]. Furthermore, [109] shows that the guaranteed convergence is achievable by adding a regularized quadratic proximal term to the objective functions of

all players. Further, for generalized potential games, which do not require private feasible regions for subproblems, unlike in standard games, it introduces regularized Gauss-Seidel BR schemes and shows that a limit point is a Nash equilibrium for player-specific convex subproblems.

When developing BR schemes or, equivalently, block coordinate-descent (BCD) schemes, the order of selection in which the player-specific problems are solved plays a crucial role. In [110], this is introduced as the block selection and done in a cyclical order. Convergence of these algorithms has been studied in [111] for both convex and nonconvex problems. [112] has employed a randomized block selection method for BCD schemes. [113] has studied the strongly convex BCD schemes and has shown that it converges linearly.

The main contributions of this chapter are as follows.

1. *Coordination system.* We develop a framework that captures the smart grid operations of multiple DSs that interact with one another through markets. We simultaneously update both electricity exchanges and price changes at the markets using an inverse demand curve. We model this framework as a noncooperative game. The DSs optimize their operation individually, only sharing their best strategy with others reducing the communication complexity. We use SOCP relaxation to model the DS operations.
2. *Algorithms and results* We develop three best-response schemes to identify the Nash equilibrium solution of the noncooperative game. To guarantee the convergence to Nash equilibrium, we add regularized quadratic proximal term to control the step size at each iteration. We analyze the performance of the algorithms through computational experiments conducted using two test data sets. We provide numerical results that provide empirical evidence of convergence of DS strategies and prices at the markets.

The rest of the chapter is organized as follows. In Section 4.2, we introduce the market setting and the optimization model for each individual DS. We discuss the mathematical structure of the overall problem in section 4.2.2. Then we develop algorithms in section 4.3. Finally, in section 4.4 we numerically analyze the performance of the algorithms using two test sets.

4.2 Market Setting and Models

In this section, we present the details of the market setting. First, we describe DS operations at a single DS and then describe the entire system setting with multiple DSs and markets.

We consider a setup comprising of multiple geographically separated DSs. We denote these DSs by the set \mathcal{N} . The DSs can exchange electricity with TS through a set of interconnection lines, \mathcal{I} connected to transmission buses \mathcal{M} . We refer to the TS buses that are connected to the DS as "markets". The following figure depicts an instance of the market setting that we are considering. Notice that DSs are not connected to one another directly. That is, they cannot share information or electricity between themselves.

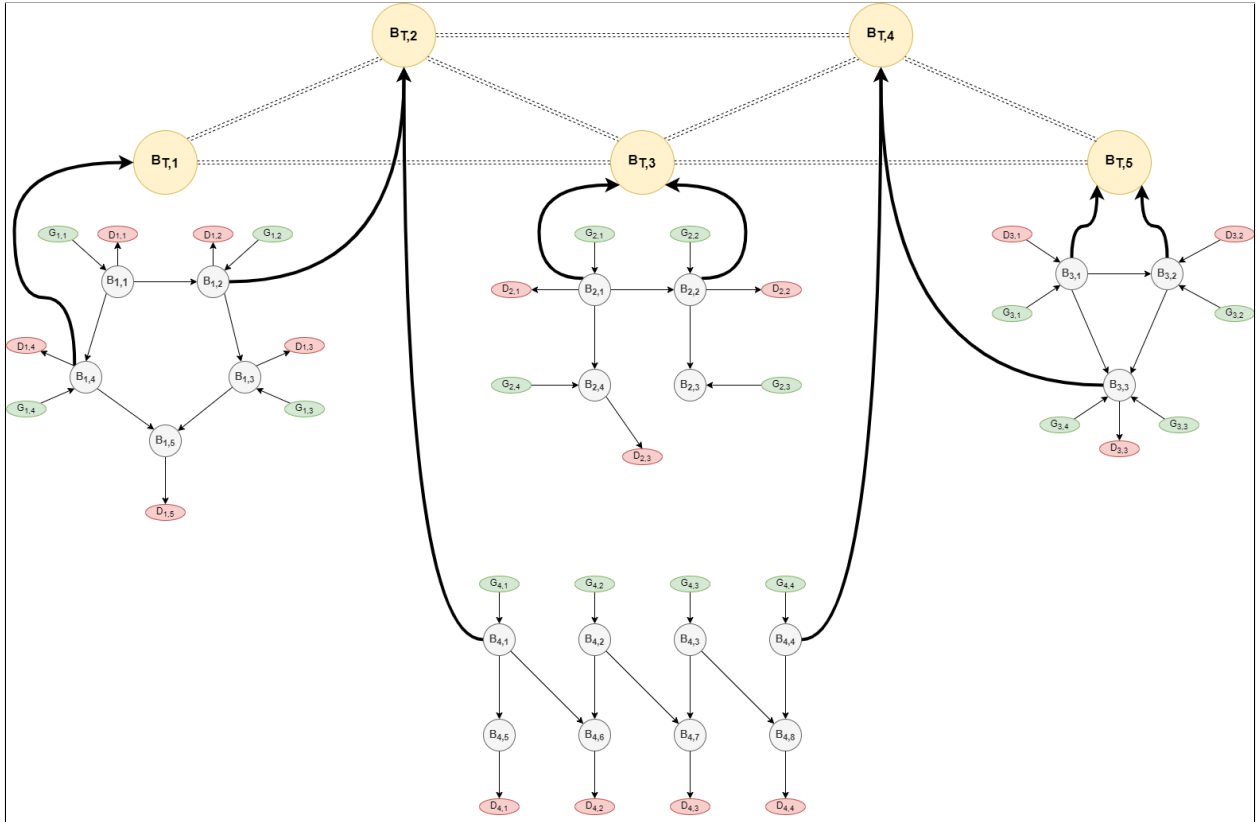


Figure 4.1: Market setting

4.2.1 DS optimization problem

Operations inside a DS are independent. Therefore, now we focus on an individual DS problem. For DS $n \in \mathcal{N}$, we denote the set of buses by \mathcal{B}_n and the set of lines by \mathcal{L}_n . We denote the set of distributed energy resources (DER) by \mathcal{G}_n that are small modular energy generators. These include photovoltaics, wind turbines, combustion turbines, etc. We denote the active and reactive generation from a DER $i \in \mathcal{G}_n$ by $p_{n,i}^g$ and $q_{n,i}^g$. These quantities are limited by their capacities captured by the intervals $[p_{n,i}^{g,\min}, p_{n,i}^{g,\max}]$ and $[q_{n,i}^{g,\min}, q_{n,i}^{g,\max}]$, respectively. That is,

$$p_{n,i}^{g,\min} \leq p_{n,i}^g \leq p_{n,i}^{g,\max} \quad \forall i \in \mathcal{G}_n, \quad (4.1a)$$

$$q_{n,i}^{g,\min} \leq q_{n,i}^g \leq q_{n,i}^{g,\max} \quad \forall i \in \mathcal{G}_n. \quad (4.1b)$$

Furthermore, we assume that there is electricity demand at every bus $i \in \mathcal{B}_n$ denoted by $p_{n,i}^d$ and $q_{n,i}^d$, the active and reactive components, respectively.

Power flows within a distribution system are nonlinear and nonconvex functions of bus voltages V_i . We express the complex voltage $V_{n,i}$ at bus i in its rectangular form, i.e., $V_{n,i} = e_{n,i} + \mathbf{i}f_{n,i}$ where $\mathbf{i} = \sqrt{-1}$. To model these power flows, we use the nodal admittance matrix of the system that has a component $Y_{n,ij} = G_{n,ij} + \mathbf{i}B_{n,ij}$ for every line $(i, j) \in \mathcal{L}_n$. Here, $G_{n,ii} = g_{n,ii} - \sum_{j \neq i} G_{n,ij}$, $B_{n,ii} = b_{n,ii} - \sum_{j \neq i} B_{n,ij}$ with $g_{n,ii}$ denoting the shunt conductance and $b_{n,ii}$ denoting the susceptance at bus $i \in \mathcal{B}_n$. We use $c_{n,ii} = e_{n,i}^2 + f_{n,i}^2$ to denote the squared voltage magnitude $|V_{n,i}|^2$. Further, we denote the real and the imaginary parts of the voltage product $V_{n,i}V_{n,j}$ by $c_{n,ij} = e_{n,i}e_{n,j} + f_{n,i}f_{n,j}$ and $s_{n,ij} = e_{n,i}f_{n,j} - e_{n,j}f_{n,i}$, respectively. To address computational challenges associated with nonconvexity of power flows, we adopt the convex second-order cone programming relaxation of the power flows from [114]. This

relaxation is captured by the following

$$p_{n,i}^f = G_{n,ii}c_{n,ii} + \sum_{j:(i,j) \in \mathcal{L}_n} (G_{n,ij}c_{n,ij} - B_{n,ij}s_{n,ij}) \quad \forall i \in \mathcal{B}_n \quad (4.2a)$$

$$q_{n,i}^f = -B_{n,ii}c_{n,ii} + \sum_{j:(i,j) \in \mathcal{L}_n} (-B_{n,ij}c_{n,ij} - G_{n,ij}s_{n,ij}) \quad \forall i \in \mathcal{B}_n \quad (4.2b)$$

$$c_{n,ij} = c_{n,ji}, \quad s_{n,ij} = -s_{n,ji}, \quad (i, j) \in \mathcal{L}_n, \quad (4.2c)$$

$$c_{n,ij}^2 + s_{n,ij}^2 \leq c_{n,ii}c_{n,jj}, \quad (i, j) \in \mathcal{L}_n, \quad (4.2d)$$

$$(V_{n,i}^{\min})^2 \leq c_{n,ii} \leq (V_{n,i}^{\max})^2, \quad i \in \mathcal{B}_n. \quad (4.2e)$$

In the above, we use $p_{n,i}^f$ and $q_{n,i}^f$ to denote the active and reactive parts of the net power imported via the distribution lines connected at bus i .

The power flow balance at each bus is captured by the following equations:

$$\sum_{j \in \mathcal{G}_{n,i}} p_{n,j}^g - \sum_{j \in \mathcal{B}_{n,i}} p_{n,j}^d - p_{n,i}^f = 0, \quad \forall i \in \mathcal{B}_n, \quad (4.3a)$$

$$\sum_{j \in \mathcal{G}_{n,i}} q_{n,j}^g - \sum_{j \in \mathcal{B}_{n,i}} q_{n,j}^d + q_{n,i}^f = 0, \quad \forall i \in \mathcal{B}_n. \quad (4.3b)$$

The objective of the DS optimization model is to minimize the total system cost. We use a quadratic function to capture the cost of a single generator using two parameters, α and β . Thus, the total cost of the system is as follows:

$$f_n(p_n^g) = \sum_{i \in \mathcal{G}_n} \alpha_i (p_{n,i}^g)^2 + \beta_i p_{n,i}^g$$

The aim of distribution system operator is to satisfy demand at all buses at minimum generation cost while ensuring that the power flows obey the physical laws. The following

second-order cone program captures this requirement:

$$\min \sum_{i \in \mathcal{G}_n} \alpha(p_{n,i}^g)^2 + \beta p_{n,i}^g \quad (4.4a)$$

$$\text{s.t. } \sum_{j \in \mathcal{G}_{n,i}} p_{n,j}^g - \sum_{j \in \mathcal{B}_{n,i}} p_{n,j}^d = G_{n,ii} c_{n,ii} + \sum_{j:(i,j) \in \mathcal{L}_n} (G_{n,ij} c_{n,ij} - B_{n,ij} s_{n,ij}) \quad \forall i \in \mathcal{B}_n \quad (4.4b)$$

$$\sum_{j \in \mathcal{G}_{n,i}} q_{n,j}^g - \sum_{j \in \mathcal{B}_{n,i}} q_{n,j}^d = -B_{n,ii} c_{n,ii} + \sum_{j:(i,j) \in \mathcal{L}_n} (-B_{n,ij} c_{n,ij} - G_{n,ij} s_{n,ij}) \quad \forall i \in \mathcal{B}_n \quad (4.4c)$$

$$(V_{n,i}^{\min})^2 \leq c_{n,ii} \leq (V_{n,i}^{\max})^2, \quad i \in \mathcal{B}_n, \quad (4.4d)$$

$$c_{n,ij} = c_{n,ji}, \quad s_{n,ij} = s_{n,ji}, \quad (i, j) \in \mathcal{L}_n, \quad (4.4e)$$

$$c_{n,ij}^2 + s_{n,ij}^2 \leq c_{n,ii} c_{n,jj}, \quad (i, j) \in \mathcal{L}_n, \quad (4.4f)$$

$$p_{n,i}^{g,\min} \leq p_{n,i}^g \leq p_{n,i}^{g,\max} \quad \forall i \in \mathcal{G}_n, \quad (4.4g)$$

$$q_{n,i}^{g,\min} \leq q_{n,i}^g \leq q_{n,i}^{g,\max} \quad \forall i \in \mathcal{G}_n. \quad (4.4h)$$

We denote the solution vector of the above program by x_n and its' feasible region by \mathcal{X}_n .

Thus, the model in (4.4) can be states succinctly as follows:

$$\min\{f_n(x_n) | x_n \in \mathcal{X}_n\}. \quad (4.5)$$

It is worthwhile to note that optimization problem solved at individual DS is a convex program.

4.2.2 Mathematical Structure

Now we introduce the interconnection set \mathcal{I} to the DS market setting. We denote the interconnection set that belongs to the n^{th} DS by \mathcal{I}_n . An element $(i, m) \in \mathcal{I}_n$ has $i \in \mathcal{B}_n$ and $m \in \mathcal{M}$ and hence, $\mathcal{I} = \cup_{n \in \mathcal{N}} \mathcal{I}_n$. We use the decision variable y_{im} to denote the transaction amount on interconnection line $(i, m) \in \mathcal{I}$. A positive value of y_{im} implies the DS is selling electricity at market m , while a negative value implies buying. Thus, the total transaction amount s_m at a market m , can compute as follows:

$$s_m = \sum_{i:(i,m) \in \mathcal{I}} y_{im}. \quad (4.6)$$

At an individual market, a inverse demand curve determines the transaction price. In other words, when there is more supply than demand within a market, the price goes down, and when the demand is higher, the price goes up. We treat the TS day-ahead locational marginal price (LMP), μ_m , as the initial price for a market and γ_m as the rate at which the price changes with the demand/supply. Figure 4.7 depicts the price action of a market, and we compute the price, $\rho_m(s_m)$, as follows:

$$\rho_m(s_m) = \mu_m - \gamma_m s_m. \quad (4.7)$$

Notice that price can have negative values when the transaction amount surpasses a certain

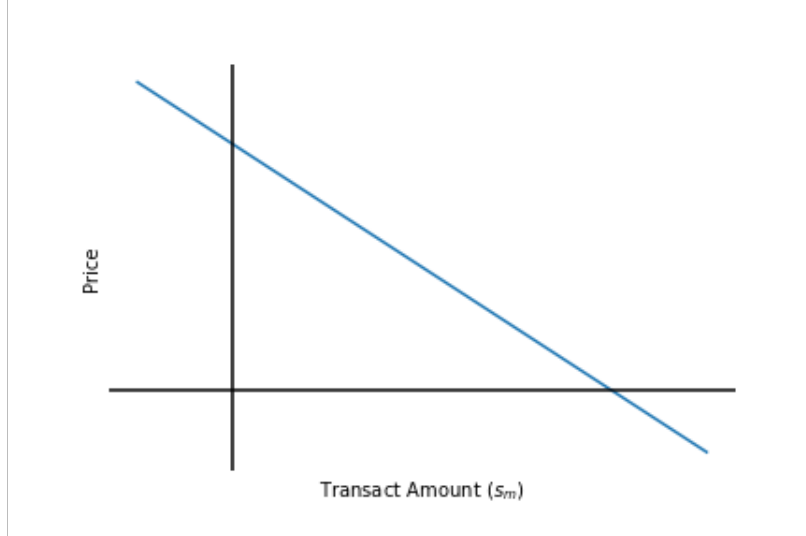


Figure 4.2: Demand inverse curve

level. Beyond that level, DS must pay to sell their electricity (see [115] for an example). Similarly, when demand exceeds supply, prices increase beyond their initial LMP.

The new set of decision variables, y , affects the objective function and the flow balance constraints (4.4b). We assume that the interconnection power flows have high voltages. Therefore, we only consider the active power flow on them. The updated active flow balance

constraint is as follows:

$$\sum_{j \in \mathcal{G}_{n,i}} p_{n,j}^g - \sum_{j \in \mathcal{B}_{n,i}} p_{n,j}^d + \sum_{m:(i,m) \in \mathcal{I}_n} y_{im} = G_{n,ii} c_{n,ii} + \sum_{j:(i,j) \in \mathcal{L}_n} (G_{n,ij} c_{n,ij} - B_{n,ij} s_{n,ij}) \quad \forall i \in \mathcal{B}_n.$$

Similarly, selling and buying electricity from the TS affects the objective function. The updated objective function is as follows:

$$\min f_n(x_n) - \sum_{(i,m) \in \mathcal{I}_n} (\mu_m - \gamma_m s_m) y_{im}.$$

By substituting (4.6), we get

$$f_n(x_n) - \sum_{(i,m) \in \mathcal{I}_n} \left(\mu_m - \gamma_m \sum_{j:(j,m) \in \mathcal{I}} y_{jm} \right) y_{im}.$$

We can simplify this to

$$f_n(x_n) - \sum_{(i,m) \in \mathcal{I}_n} \left(\mu_m - \gamma_m \left(\sum_{j:(j,m) \in \mathcal{I} \setminus \mathcal{I}_n} y_{jm} + \sum_{j:(j,m) \in \mathcal{I}_n} y_{jm} \right) \right) y_{im}.$$

Notice that the above objective function depends on others' decisions. However, each distribution system optimize their operations individually. We will use $\mathbf{x} := (x_n)_{\forall n \in \mathcal{N}}$ to denote the solution vector across all the DS. Furthermore, we denote others' solutions by $\mathbf{x}_{-n} = (x_{n'})_{n' \in \mathcal{N} \setminus \{n\}}$. using these notations, we can state the DS optimization model that accounts for transactions with the markets more generally as follows:

$$\min \{f_n(x_n; \mathbf{x}_{-n}) | x_n \in \mathcal{X}_n\}.$$

Note that, the feasible region for a DS only depends on its properties and decisions. It does not interact with other DSs' decisions. Therefore, the feasible region for DS is private. The interaction occurs only through the objective function. To update the objective function, we need others' decisions, \mathbf{x}_{-n} . However, once a DS solves the optimization problem and decides on its strategy, other DSs may want to adjust theirs. Therefore, it desirable for DSs to reach a consensus. Under these circumstances, the problem becomes a standard Nash

game [100], and therefore the consensus strategy for all the DSs is a Nash equilibrium, which we formally define next.

Definition 7. A tuple \mathbf{x}^* is a Nash equilibrium if

$$f_n(x_n^*; \mathbf{x}_{-n}^*) \leq f_n(x_n; \mathbf{x}_{-n}^*) \quad \forall x_n \in \mathcal{X}_n,$$

for all $n = 1, \dots, N$.

Under this definition, a DS cannot improve its objective unilaterally by deviating from the Nash equilibrium x_n^* . In the next section we present solutions strategies to identify such points.

4.3 Proximal BR Algorithms

In this section, we present algorithms that conduct the iterative process leading to Nash equilibrium points. In our solution algorithms, every DS updates its strategy independently, given the other's decisions. Such algorithms are known as the best response schemes [116]. However, there is no guarantee that the best response schemes always converge to a Nash equilibrium. An example illustrating this deficiency of best response schemes can be found in [109]. To overcome this there have been suggestion to incorporate a proximal term the objective function [109, 117]. The resulting proximal BR algorithm has been shown to generate a sequence of solutions that converge to Nash equilibrium when the DS-specific optimization problems are convex. Motivated by these previous works we employ a proximal objective function given by:

$$\min f_n(x_n; \mathbf{x}_{-n}^k) + \frac{\mu}{2} \|x_n - x_n^{k-1}\|^2, \quad (4.8)$$

where k is the iteration index. We denote the optimal solution by x_n^k . The proximal parameter $\mu > 0$ which is an input the algorithm controls the deviation from the previous optimal solution x_n^{k-1} .

Two components dominate the performance of a BR scheme, the order of the problems solved and the updating time of the solution vector \mathbf{x} . The order of selecting a DS can

be either cyclic or random. Similarly, there are two ways to update the decision vector \mathbf{x} , immediate and coordinated. Based on these two components, we next present three variants of the proximal BR algorithms.

4.3.1 Cyclic Order Coordinated Updates

We develop the first algorithm by solving the DS problems in cyclical order, and we perform coordinated updates. That is, DS problems are solved in the same order in every iteration. However, the coordinated update, the solution vector \mathbf{x}^k and the market prices get updated only after solving all the DS problems. This algorithm is stated in Algorithm 2. The algorithm takes all DSs, markets, and interconnection information as inputs. Between

Algorithm 2 Cyclic order coordinated updates

- 1: **Input:** DS $\mathcal{N} = \{1, 2, \dots, N\}$, Markets $\mathcal{M} = \{1, 2, \dots, M\}$, Inter connections $\mathcal{I} = \cup_{n \in \mathcal{N}} \mathcal{I}_n$, $\mu > 0$, $k \leftarrow 0$.
 - 2: **while** Stopping criteria not met **do**
 - 3: **for** $n = 1$ to N **do**
 - 4: Setup objective for n^{th} DS using $\rho_m(s_m^{k-1}) \forall m \in \mathcal{M}$ as shown in (4.8).
 - 5: Solve and extract solutions
 - 6: **end for**
 - 7: Using $\mathbf{x}^k = (x_1^k, x_2^k, \dots, x_N^k)$, update the prices at all markets as:
$$\rho_m(s_m^k) = \mu_m - \gamma_m s_m^k \quad \forall m \in \mathcal{M}.$$
 - 8: $k \leftarrow k + 1$.
 - 9: **end while**
-

lines 3 and 6, we setup the objective function, solve the optimization problems separately and store the solution in their respective vector x_n^k for all individual DS problems. Notice that prices at markets connected to a specific DS are used in updating its objective function.

After solving all the DS problems, in line 7, we update the market information using the consolidated decision vector \mathbf{x}^k , which affects the objective functions of DS models. We run the algorithm for a prespecified termination condition. It is worthwhile to note that the price updates are carried out once per iteration.

4.3.2 Cyclic Order Immediate Updates

The second algorithm also solves the DS problems in a cyclical order. However, we perform market price updates immediately after solving every DS problem. The algorithmic steps are shown in Algorithm 3. Similar to algorithm 2, the second algorithm takes the same

Algorithm 3 Cyclic order immediate updates

- 1: **Input:** DS $\mathcal{N} = \{1, 2, \dots, N\}$, Markets $\mathcal{M} = \{1, 2, \dots, M\}$, Inter connections $\mathcal{I} = \cup_{n \in \mathcal{N}} \mathcal{I}_n$, $\mu > 0$, $k \leftarrow 0$.
 - 2: **while** Stopping criteria not met **do**
 - 3: **for** $n = 1$ to N **do**
 - 4: Using $\mathbf{x}_{-n}^{k,n} = (x_1^k, x_2^k, \dots, x_{n-1}^k, x_{n+1}^{k-1}, \dots, x_N^{k-1})$, update the prices at all markets as:
 - $$\rho_m(s_m^{k,n}) = \mu_m - \gamma_m s_m^{k,n} \quad \forall m \in \mathcal{M}.$$
 - 5: Setup objective for n^{th} DS using $\rho_m(s_m^{k,n})$ as shown in (4.8).
 - 6: Solve and extract solutions
 - $$x_n^k \in \arg \min f_n(x_n; \mathbf{x}_{-n}^k) + \frac{\mu}{2} \|x_n - x_n^{k-1}\|^2.$$
 - 7: **end for**
 - 8: $k \leftarrow k + 1$.
 - 9: **end while**
-

inputs and runs until a prespecified termination condition is met. Notice that the algorithm updates the consolidated decision vector $\mathbf{x}_n^{k,n}$ vector before solving every individual DS problem in line 4. We capture this distinction by using an addition superscript in the notation of the consolidated decisions vector ($\mathbf{x}_n^{k,n}$ as opposed to \mathbf{x}_n^k in Algorithm 2). This change

results in multiple (N times in each iteration) updates to the market prices. Consequently, the objective function of each DS model reflects the latest price information. Then in line 6, each DS model solves for their optimal solutions.

4.3.3 Random Order Immediate Updates

The last algorithm we develop works similarly to the previous algorithm, except that the order of solving the DS problems is selected randomly in each iteration. When we use coordinated update, the order of solving the problems has the same effect in both cyclic and random order. They lead to the same algorithm. Therefore, when random ordering is employed we only focus on immediate updates. This procedure is shown in Algorithm 4.

Algorithm 4 Random order immediate updates

```

1: Input: DS  $\mathcal{N} = \{1, 2, \dots, N\}$ , Markets  $\mathcal{M} = \{1, 2, \dots, M\}$ , Inter connections  $\mathcal{I} = \cup_{n \in \mathcal{N}} \mathcal{I}_n$ ,  $\mu > 0$ ,  $k \leftarrow 0$ .
2: while Stopping criteria not met do
3:   Generate a random permutation,  $\mathcal{P} = (p_1, p_2, \dots, p_N)$ .
4:   for  $n = 1$  to  $N$  do
5:     Using  $\mathbf{x}_{-n}^{k,n} = (x_{j:p_j < n}^k, x_{j:p_j > n}^{k-1})$ , update the prices at all markets as:

$$\rho_m(s_m^{k,n}) = \mu_m - \gamma_m s_m^{k,n} \quad \forall m \in \mathcal{M}.$$

6:     Setup objective for  $n^{th}$  DS using  $\rho_m(s_m^{k,n})$  as shown in (4.8).
7:     Solve and extract solutions

$$x_n^k \in \arg \min f_n(x_n; \mathbf{x}_{-n}^k) + \frac{\mu}{2} \|x_n - x_n^{k-1}\|^2.$$

8:   end for
9:    $k \leftarrow k + 1$ 
10: end while

```

The difference between algorithms 3 and 4 is in line 3. That is, in algorithm 4 we pick a random permutation to determine the order of solving the DS optimization problems. A

the beginning of the n^{th} round, we have solved optimization problems for DSs indexed by p_1, p_2, \dots, p_n . Therefore, we have their optimal solutions $x_{j:p_j < n}^k$ identified in iteration k . However, we only have the optimal solutions from the previous iteration for DSs indexed by p_{n+1}, \dots, p_N , that is, $x_{j:p_j > n}^{k-1}$. The resulting consolidated vector $\mathbf{x}_{-n}^{k,n}$ is used in computing the market prices in line 5. The rest of the steps are exactly similar to the case of cyclical order immediate updates.

4.4 Experiments

In this section, we present the computational results of the three variants of proximal BR algorithm presented in section 4.3. We first present the setting use for our case study and then share the numerical results.

4.4.1 Problem Settings

For our numerical experiments, we design two market settings. The first setting has three markets and 3 DSs. The second setting has three markets and 6 DSs. We modify the test systems IEEE-9, IEEE-14, and IEEE-30 to create our DSs (see [118]). Interconnection details of the three DSs setting are given in the table 4.1. Interconnection details of the

Table 4.1: Three DSs setting interconnection setting.

	DS 1	DS 2	DS 3
Market 1	4	-	5
Market 2	4, 6	-	6
Market 3	-	7	9

six DSs setting are given in the table 4.2. In tables 4.1 and 4.2, a non-empty cell value represents an interconnection between the corresponding market and the specific bus(es) in the DS. Multiple values represent multiple connections between the two entities. The value inside the cell is the bus ID that the interconnection originated. For example, in table 4.2, the bottom right cell value of 4 indicates an interconnection between Market 3 and Bus-4 of

Table 4.2: Six DSs setting interconnection setting.

	DS 1	DS 2	DS 3	DS 4	DS 5	DS 6
Market 1	4	-	5	4	2	-
Market 2	4, 6	-	6	-	3	-
Market 3	-	7	9	5	1	4

DS 6. In addition, we assume there are no connections between the DSs. To represent the higher prices at TS, we set the initial unit prices at each market as \$5000, \$4000, and \$6000, respectively. These are the μ value in (4.7). Values for γ in (4.7) are 100, 150, and 200 for markets 1, 2, and 3, respectively.

We implemented the algorithms in Julia 1.7.2. We used the PowerModels package in Julia to build SOCP relaxation models and solved them using Ipopt 3.14.10 solver. We used an Intel Core i3 machine with a 2.20 GHz processor and 8GB RAM to conduct the experiments.

4.4.2 Performance of the Algorithms

We tested the performance of the three algorithms using the two market settings. A summary of the results is in Table 4.3.

We tested the performance of the three algorithms with different values of the proximal parameter μ . Note that at the optimal solution, the effect of the proximal term diminishes. However, due to the precision of decimals, there can be slight changes. The effects are significant when the value of μ is large. Recall that our objective is to minimize the total market cost.

In each row of the table 4.3, Algorithm 3, that is, cyclic and immediate update algorithm, outperform the other two algorithms in terms of the number of iterations and time. Also, notice that for six DSs system, cyclic and coordinated update algorithm (Algorithm 2) do not converge to a solution after 100 iterations. These results indicate that immediate updates are more suitable than coordinated updates. In addition, we can notice the increase in the number of iterations with the value of μ , especially in six DSs system with Algorithm 4.

Next, we present the convergence results of the interconnection lines.

Table 4.3: Summary of performance of cyclical order coordinated updates (CC), cyclical order immediate updates (CI), and random order immediate updates (RI).

(a) Three DS setting.

mu	Algorithm 1: CC			Algorithm 1: CI			Algorithm 1: RI		
	Iters.	Objective	Time	Iters.	Objective	Time	Iters.	Objective	Time
0	22	982.2	17.15	13	982.2	9.7	18	982.2	13.26
0.125	24	982.63	16.84	13	982.5	9.44	18	982.48	12.64
0.25	26	983.05	18.82	13	982.79	9.94	18	982.76	13.42
0.5	23	983.88	16.29	13	983.36	10.1	19	983.29	14.09
1	26	985.45	19.11	13	984.42	10.46	18	984.29	13.32
2	23	988.27	16.36	14	986.22	10.14	18	985.98	14
4	22	992.71	16.55	14	988.68	9.93	19	988.18	14.19
8	22	997.2	16.43	14	989.43	10.41	19	988.42	13.74
16	23	991.7	18.07	15	977.18	10.76	20	975.1	16.06
32	26	939.63	19.58	20	914.13	14.17	21	909.76	15.6

(b) Six DS setting.

mu	Algorithm 1: CC			Algorithm 1: CI			Algorithm 1: RI		
	Iters.	Objective	Time	Iters.	Objective	Time	Iters.	Objective	Time
0	100+	-	-	19	8659.39	26.96	22	8659.39	30.17
0.125	100+	-	-	19	8660.35	28.46	24	8659.64	33.01
0.25	100+	-	-	19	8661.29	27.22	22	8659.89	31.02
0.5	100+	-	-	19	8663.16	26.7	22	8660.37	30.74
1	100+	-	-	19	8666.84	26.64	23	8661.3	31.93
2	100+	-	-	19	8673.86	26.43	23	8663	31.65
4	100+	-	-	20	8686.73	27.89	23	8665.85	31.7
8	100+	-	-	19	8708.19	26.15	23	8669.47	31.64
16	100+	-	-	19	8736.91	26.05	24	8669.69	32.81
32	100+	-	-	21	8753.97	29.09	25	8649.17	33.6

4.4.3 Convergence of Inter Connections

In three DSs setting, there are seven interconnections from DSs to the 3 markets. We depict the convergence of these interconnections in figure 4.3. Note that we chose $\mu = 2$ and algorithm two results for the following discussions. Notice that one of the interconnections from DS 1 to market 2 (purple line) converges at a negative value. This indicates that DS 1 buys electricity from market 2. The other interconnection from DS 1 to market 2 converges

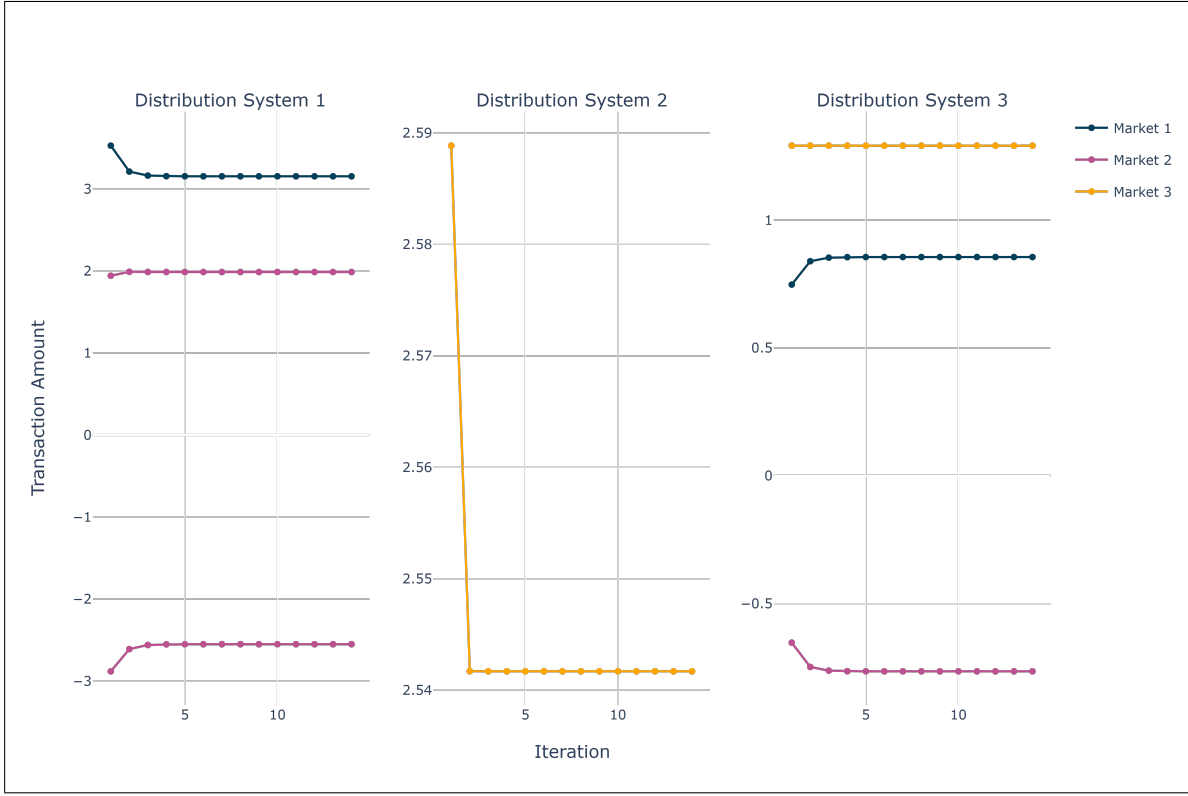


Figure 4.3: Convergence of Interconnections

at positive values indicating DS 1 sells electricity to market 2. These results show that within a single DS, the system operator has the freedom to buy and sell electricity from and to markets. These decisions purely depend on the prices of DS buses. We can observe similar buying and selling of electricity in DS 3. This allows market arbitrage, meaning a DS can increase its income by buying from cheap markets and selling to expensive markets. However, a DS cannot do this indefinitely because cheap markets become expensive when buying electricity, and expensive markets become cheap due to the inverse demand curve. Also, market arbitrage is possible only if a DS has multiple interconnections. Therefore, it incentivizes the DS to operate multiple connections to markets.

4.4.4 Market Prices

Next, we present market price convergence for three DS setting in figure 4.4. The yellow lines of figure 4.4 corresponds to the six DS setting, and the purple lines correspond to the three DS setting. We can observe that for the six DS setting, the prices are settling at lower

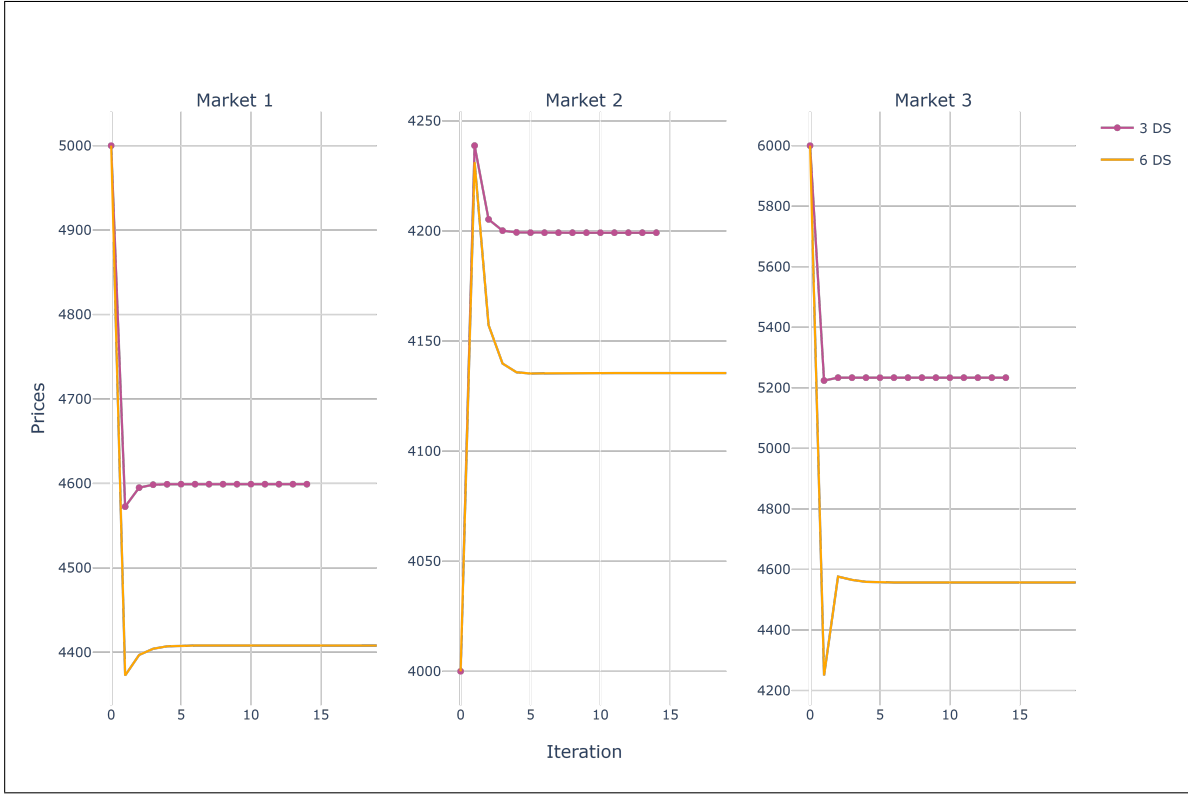


Figure 4.4: Market prices.

values than for the three DS setting. This indicates that when more DSSs are available for the coordination systems, meaning more generation is available, the prices decrease. Lower prices at markets are beneficial to consumers. This encourages the policymakers to force DS to participate in the system.

In six DS setting, final prices are \$4407.96, \$4135.46, and \$4556.96 for markets 1, 2, and 3, respectively. These converged prices have changed from their initial prices of \$5000, \$4000, and \$6000, respectively. This implies that when there is enough electricity available from DSSs, the market prices are getting closer to one another, even without any connections between markets. These similar prices are helpful in providing fair prices to consumers.

4.5 Conclusions

In this chapter, we introduced a coordination system for decentralized smart grid operation. We showed that our system allows individual distribution systems to make their strategies independently while sharing only a limited information. Independent strategizing

allows distribution systems to keep their competitive advantage. Furthermore, the setting does not require every system to be fully cooperative. Distribution systems only have to share their best response to the other systems' strategies. Therefore, the communication complexity is much less and efficient. Also, it allows the individual system details, such as generator capacities, ramping rates, generation costs, DS network topology, and other vital information to be private.

In addition, we developed three algorithms to achieve the Nash equilibrium for the system. We guarantee the convergence to a Nash equilibrium by adding a regularized quadratic proximal term to every DSs' objective function. The proximal term controls the step size in every iteration. Our numerical results show that when the weight of the proximal term μ is increased, it takes a longer time to converge to a Nash equilibrium.

We showed the numerical results for these algorithms using two test sets. Comparing the algorithm performance reveals that immediate updates outperform the coordinated update algorithm. Out of the three algorithms, the immediate update and cyclic order algorithm gave the best results in terms of time and number of iterations. We observed that it is advantageous to have multiple connections from one DS to multiple markets. Also, the benefits of the system increase when more DSs participate. We discussed the importance of the coordinated system from the consumer's, the policymakers', and the distribution system operators' points of view.

Chapter 5

Conclusion

In this dissertation, we discussed the electricity market operations and pricing from an Operations Research (OR) point of view. We emphasized the advantages of using OR techniques, such as stochastic programming (SP). We presented a brief introduction to stochastic programming in chapter 1

Our primary focus was on the electricity market clearing problem. We discussed the challenges of integrating large-scale renewable resources. The stochasticity of renewable resources such as wind and solar diminishes the usefulness of deterministic models, which are used in practice. The nature of the problem setup allowed us to apply two-stage stochastic programming to model the electricity market clearing model. To represent the stochasticity in the model, SP uses a set of scenarios. While we assumed we had a finite set of scenarios (finite support) to develop our models, the theory and the analyses developed in this dissertation holds for the continuous support case as well, in which case we must resort to stochastic convex programming methods.

The quality of SP models depends on the quality of the scenarios. Therefore, we must develop near-realistic scenarios to achieve a realistic solution. Therefore, in chapter 2, we developed wind generation scenarios using wind-speed time series data. To develop multivariate time series, we utilized the spatio-temporal correlation of wind speeds in wind farms located in close proximity. We demonstrate that the wind speed time series are nonstationary, and hence, regular time series methods cannot directly apply to build models. Therefore we presented a nonparametric change point based method to simulate wind speed time series. The change point detection method identifies a point as a change point when there is a disruption to the covariance structure of the series.

The identified change points separate the time series into stationary segments. We presented parametric and nonparametric methods to build models for each segment. Then we

used the models to simulate the series for each part separately and add them together to obtain the whole simulation. Finally, we used the simulated series in an electricity market clearing model. We showed the high volatility in electricity prices where we observed the change points in the original wind-speed time series.

In chapter 3, we developed alternative SP models for the electricity market clearing problem. We showed the incapabilities of the canonical model in capturing the stochasticity in the first-stage decisions. We addressed this issue using the notion of non-anticipativity in SP. It is important to note that electricity market clearing models decide market operations decisions. The pricing decisions are derived from the dual solutions of the model. Therefore, we do not have any control over the pricing decisions in the model.

The two alternative SP models allowed us to develop proper pricing mechanisms for the market participants. While state-vector formulation provides better pricing mechanisms properties, mean-vector formulation is efficient in obtaining solutions (progressive hedging). In theorem 3, we showed that it is possible to reconstruct state-vector solutions using mean-vector solutions. Therefore, pricing mechanism \mathcal{R}^s has both computational and application advantages. The main benefit of \mathcal{R}^s is that it guarantees cost recovery for every generator under every scenario. Pricing mechanisms \mathcal{R}^m and \mathcal{R}^s both achieve revenue adequacy in expectation and provide bounds for the price distortion for every scenario. These properties are crucial in convincing generators and ISOs to adopt such pricing mechanisms.

Finally, in chapter 4, we developed a coordination system for distribution systems and markets to exchange electricity. We presented a system that achieves the Nash equilibrium while sharing minimum information. Reluctant to sharing information is typical behavior in practice, making this setting more suitable for such an environment. Another advantage of this system is that every participant makes their decisions separately while adapting to others' decisions. Thus, the system is suitable for distributed computing.

We developed three algorithms to solve the system, and according to numerical results, DS must update their solutions immediately after they solve the problem. This helps the algorithm to converge equilibrium quickly. We guarantee convergence by adding a quadratic proximal term to every DS objective function. In addition, we showed that it is beneficial to operate more than one interconnection to the DS. For the system operator and consumers,

it is more beneficial to have more DS as they help to reduce prices significantly.

BIBLIOGRAPHY

- [1] A.-J. Perea-Moreno, M. Ángel Perea-Moreno, Q. Hernandez-Escobedo, and F. Manzano-Agugliaro, “Towards forest sustainability in mediterranean countries using biomass as fuel for heating,” *Journal of Cleaner Production*, vol. 156, pp. 624 – 634, 2017. [1](#)
- [2] S. Meredith. (2022) Oil opec+ to cut oil production by 2 million barrels per day to shore up prices, defying u.s. pressure. [Online]. Available: <https://www.cnbc.com/2022/10/05/oil-opec-imposes-deep-production-cuts-in-a-bid-to-shore-up-prices.html> [1](#)
- [3] H. Ziady. (2022) Opec announces the biggest cut to oil production since the start of the pandemic. [Online]. Available: <https://www.cnn.com/2022/10/05/energy/opec-production-cuts> [1](#)
- [4] Electricity in the united states. [Online]. Available: <https://www.eia.gov/energyexplained/electricity/electricity-in-the-us.php> [2](#)
- [5] (2021) Eia projects renewables share of u.s. electricity generation mix will double by 2050. [Online]. Available: <https://www.eia.gov/todayinenergy/detail.php?id=46676> [2, 40](#)
- [6] Y. Kumar, J. Ringenberg, S. S. Depuru, V. K. Devabhaktuni, J. W. Lee, E. Nikolaidis, B. Andersen, and A. Afjeh, “Wind energy: Trends and enabling technologies,” *Renewable and Sustainable Energy Reviews*, vol. 53, pp. 209–224, 2016. [2, 13](#)
- [7] E. Erik, M. Milligan, and B. Kirby, “Operating reserves and variable generation,” *NREL Technical Report*, Aug. 2011. [2, 13](#)
- [8] M. Carrión and J. M. Arroyo, “A computationally efficient mixed-integer linear formulation for the thermal unit commitment problem,” *IEEE Transactions on power systems*, vol. 21, no. 3, pp. 1371–1378, 2006. [5](#)
- [9] New England ISO, “Market operations: Manual m-11,” Tech. Rep., October 2018, retrieved from https://www.iso-ne.com/static-assets/documents/2018/10/manual_11_market_operations_rev55_20181004.pdf. [5](#)
- [10] California ISO, “Business practice manual for market operations,” Tech. Rep., October 2017, retrieved from <https://www.caiso.com/rules/Pages/BusinessPracticeManuals/Default.aspx>.

[Online]. Available:
<https://www.caiso.com/rules/Pages/BusinessPracticeManuals/Default.aspx> 5

- [11] L. L. Garver, “Power generation scheduling by integer programming-development of theory,” *Transactions of the American Institute of Electrical Engineers. Part III: Power Apparatus and Systems*, vol. 81, no. 3, pp. 730–734, 1962. 5
- [12] B. Knueven, J. Ostrowski, and J.-P. Watson, “On mixed-integer programming formulations for the unit commitment problem,” *INFORMS Journal on Computing*, vol. 32, no. 4, pp. 857–876, 2020. 5
- [13] J. Ostrowski, M. F. Anjos, and A. Vannelli, “Tight mixed integer linear programming formulations for the unit commitment problem,” *IEEE Transactions on Power Systems*, vol. 27, no. 1, pp. 39–46, 2011. 5
- [14] P. A. Ruiz, C. R. Philbrick, E. Zak, K. W. Cheung, and P. W. Sauer, “Uncertainty management in the unit commitment problem,” *IEEE Transactions on Power Systems*, vol. 24, no. 2, pp. 642–651, 2009. 5
- [15] A. Papavasiliou, S. S. Oren, and R. P. O’Neill, “Reserve requirements for wind power integration: A scenario-based stochastic programming framework,” *IEEE Transactions on Power Systems*, vol. 26, no. 4, pp. 2197–2206, 2011. 5
- [16] K. Cheung, D. Gade, C. Silva-Monroy, S. M. Ryan, J.-P. Watson, R. J.-B. Wets, and D. L. Woodruff, “Toward scalable stochastic unit commitment,” *Energy Systems*, vol. 6, no. 3, pp. 417–438, 2015. 5
- [17] A. Tuohy, P. Meibom, E. Denny, and M. O’Malley, “Unit commitment for systems with significant wind penetration,” *IEEE Transactions on power systems*, vol. 24, no. 2, pp. 592–601, 2009.
- [18] A. Sturt and G. Strbac, “Efficient stochastic scheduling for simulation of wind-integrated power systems,” *IEEE transactions on Power Systems*, vol. 27, no. 1, pp. 323–334, 2011.
- [19] J. Wang, J. Wang, C. Liu, and J. P. Ruiz, “Stochastic unit commitment with sub-hourly dispatch constraints,” *Applied energy*, vol. 105, pp. 418–422, 2013. 5
- [20] Q. Wang, Y. Guan, and J. Wang, “A chance-constrained two-stage stochastic program for unit commitment with uncertain wind power output,” *IEEE transactions on power systems*, vol. 27, no. 1, pp. 206–215, 2011. 5
- [21] D. Bertsimas, E. Litvinov, X. A. Sun, J. Zhao, and T. Zheng, “Adaptive robust optimization for the security constrained unit commitment problem,” *IEEE transactions on power systems*, vol. 28, no. 1, pp. 52–63, 2012. 5
- [22] Q. P. Zheng, J. Wang, and A. L. Liu, “Stochastic optimization for unit commitment—a review,” *IEEE Transactions on Power Systems*, vol. 30, no. 4, pp. 1913–1924, 2014. 6

- [23] B. F. Hobbs, M. H. Rothkopf, R. P. O'Neill, and H.-p. Chao, *The next generation of electric power unit commitment models*. Springer Science & Business Media, 2006, vol. 36. [6](#)
- [24] S. S. Reddy and P. Bijwe, “Day-ahead and real time optimal power flow considering renewable energy resources,” *International Journal of Electrical Power & Energy Systems*, vol. 82, pp. 400–408, 2016. [6](#)
- [25] S. Choi, “Practical coordination between day-ahead and real-time optimization for economic and stable operation of distribution systems,” *IEEE Transactions on Power Systems*, vol. 33, no. 4, pp. 4475–4487, 2017. [6](#)
- [26] T. Schulze and K. McKinnon, “The value of stochastic programming in day-ahead and intra-day generation unit commitment,” *Energy*, vol. 101, pp. 592–605, 2016. [6](#)
- [27] E. Bjørndal, M. Bjørndal, K. Midthun, and A. Tomasgard, “Stochastic electricity dispatch: A challenge for market design,” *Energy*, vol. 150, pp. 992–1005, 2018. [6](#)
- [28] H. Gangammanavar, S. Sen, and V. M. Zavala, “Stochastic optimization of sub-hourly economic dispatch with wind energy,” *IEEE Transactions on Power Systems*, vol. 31, no. 2, pp. 949–959, 2015. [6](#)
- [29] Y.-Y. Lee and R. Baldick, “A frequency-constrained stochastic economic dispatch model,” *IEEE Transactions on power systems*, vol. 28, no. 3, pp. 2301–2312, 2013. [6](#)
- [30] A. Lorca and X. A. Sun, “Adaptive robust optimization with dynamic uncertainty sets for multi-period economic dispatch under significant wind,” *IEEE Transactions on Power Systems*, vol. 30, no. 4, pp. 1702–1713, 2014. [6](#)
- [31] H. Zhong, Q. Xia, Y. Wang, and C. Kang, “Dynamic economic dispatch considering transmission losses using quadratically constrained quadratic program method,” *IEEE Transactions on Power Systems*, vol. 28, no. 3, pp. 2232–2241, 2013. [6](#)
- [32] H. Zhong, Q. Xia, C. Kang, M. Ding, J. Yao, and S. Yang, “An efficient decomposition method for the integrated dispatch of generation and load,” *IEEE Transactions on Power Systems*, vol. 30, no. 6, pp. 2923–2933, 2015. [6](#)
- [33] G. Bitran and R. Caldentey, “An overview of pricing models for revenue management,” *Manufacturing & Service Operations Management*, vol. 5, no. 3, pp. 203–229, 2003. [6](#)
- [34] A. Philpott and G. Pritchard, “Financial transmission rights in convex pool markets,” *Operations Research Letters*, vol. 32, no. 2, pp. 109–113, 2004. [7](#)
- [35] P. L. Joskow, “Competitive electricity markets and investment in new generating capacity,” *AEI-Brookings Joint Center Working Paper*, no. 06-14, 2006. [7](#)
- [36] R. P. O'Neill, P. M. Sotkiewicz, B. F. Hobbs, M. H. Rothkopf, and W. R. Stewart Jr, “Efficient market-clearing prices in markets with nonconvexities,” *European journal of operational research*, vol. 164, no. 1, pp. 269–285, 2005. [7](#)

- [37] G. Liberopoulos and P. Andrianesis, “Critical review of pricing schemes in markets with non-convex costs,” *Operations Research*, vol. 64, no. 1, pp. 17–31, 2016. [7](#)
- [38] D. A. Schiro, T. Zheng, F. Zhao, and E. Litvinov, “Convex hull pricing in electricity markets: Formulation, analysis, and implementation challenges,” *IEEE Transactions on Power Systems*, vol. 31, no. 5, pp. 4068–4075, 2015. [7](#)
- [39] R. Sioshansi, R. O’Neill, and S. S. Oren, “Economic consequences of alternative solution methods for centralized unit commitment in day-ahead electricity markets,” *IEEE Transactions on Power Systems*, vol. 23, no. 2, pp. 344–352, 2008. [7](#)
- [40] B. Eldridge, R. O’Neill, and B. F. Hobbs, “Near-optimal scheduling in day-ahead markets: pricing models and payment redistribution bounds,” *IEEE transactions on power systems*, vol. 35, no. 3, pp. 1684–1694, 2019. [7](#)
- [41] Y. M. Al-Abdullah, M. Abdi-Khorsand, and K. W. Hedman, “The role of out-of-market corrections in day-ahead scheduling,” *IEEE Transactions on Power Systems*, vol. 30, no. 4, pp. 1937–1946, 2014. [7](#)
- [42] S. Wong and J. D. Fuller, “Pricing energy and reserves using stochastic optimization in an alternative electricity market,” *IEEE Transactions on Power Systems*, vol. 22, no. 2, pp. 631–638, 2007. [7](#)
- [43] J. M. Morales, A. J. Conejo, K. Liu, and J. Zhong, “Pricing electricity in pools with wind producers,” *IEEE Transactions on Power Systems*, vol. 27, no. 3, pp. 1366–1376, 2012. [7](#)
- [44] G. Pritchard, G. Zakeri, and A. Philpott, “A single-settlement, energy-only electric power market for unpredictable and intermittent participants,” *Operations research*, vol. 58, no. 4-part-2, pp. 1210–1219, 2010. [7, 40, 41, 42, 49](#)
- [45] V. M. Zavala, K. Kim, M. Anitescu, and J. Birge, “A stochastic electricity market clearing formulation with consistent pricing properties,” *Operations Research*, vol. 65, no. 3, pp. 557–576, 2017. [7, 40, 42, 45, 49, 50, 71, 74](#)
- [46] R. Cory-Wright, A. Philpott, and G. Zakeri, “Payment mechanisms for electricity markets with uncertain supply,” *Operations Research Letters*, vol. 46, no. 1, pp. 116–121, 2018. [8](#)
- [47] G. Zakeri, G. Pritchard, M. BJORNDAL, and E. BJORNDAL, “Pricing wind: a revenue adequate, cost recovering uniform price auction for electricity markets with intermittent generation,” *INFORMS Journal on Optimization*, vol. 1, no. 1, pp. 35–48, 2019. [8](#)
- [48] J. Kazempour, P. Pinson, and B. F. Hobbs, “A stochastic market design with revenue adequacy and cost recovery by scenario: Benefits and costs,” *IEEE Transactions on Power Systems*, vol. 33, no. 4, pp. 3531–3545, 2018. [8, 40](#)

- [49] A. R. Ferguson and G. B. Dantzig, “The allocation of aircraft to routes—an example of linear programming under uncertain demand,” *Management science*, vol. 3, no. 1, pp. 45–73, 1956. [8](#)
- [50] A. Charnes, W. W. Cooper, and G. H. Symonds, “Cost horizons and certainty equivalents: an approach to stochastic programming of heating oil,” *Management science*, vol. 4, no. 3, pp. 235–263, 1958. [8](#)
- [51] A. Prékopa and T. Szántai, “An optimal regulation of a storage level with application to the water level regulation of a lake,” *European Journal of Operational Research*, vol. 3, no. 3, pp. 175–189, 1979. [8](#)
- [52] J. R. Birge and F. Louveaux, *Introduction to stochastic programming*. Springer Science & Business Media, 2011. [8](#)
- [53] A. Shapiro, D. Dentcheva, and A. Ruszczynski, *Lectures on stochastic programming: modeling and theory*. SIAM, 2021. [8](#)
- [54] S. W. Wallace and W. T. Ziemba, *Applications of stochastic programming*. SIAM, 2005. [8](#)
- [55] R. M. Van Slyke and R. Wets, “L-shaped linear programs with applications to optimal control and stochastic programming,” *SIAM Journal on Applied Mathematics*, vol. 17, no. 4, pp. 638–663, 1969. [10, 49](#)
- [56] R. T. Rockafellar and R. J.-B. Wets, “Scenarios and policy aggregation in optimization under uncertainty,” *Mathematics of operations research*, vol. 16, no. 1, pp. 119–147, 1991. [10, 55](#)
- [57] Y.-K. Wu and J.-S. Hong, “A literature review of wind forecasting technology in the world,” in *2007 IEEE Lausanne Power Tech*. IEEE, 2007, pp. 504–509. [13](#)
- [58] M. Khodayar and J. Wang, “Spatio-temporal graph deep neural network for short-term wind speed forecasting,” *IEEE Transactions on Sustainable Energy*, vol. 10, no. 2, pp. 670–681, 2018. [14](#)
- [59] O. B. Shukur and M. H. Lee, “Daily wind speed forecasting through hybrid KF-ANN model based on ARIMA,” *Renewable Energy*, vol. 76, pp. 637–647, 2015. [14](#)
- [60] J. Wang and J. Hu, “A robust combination approach for short-term wind speed forecasting and analysis—combination of the ARIMA (autoregressive integrated moving average), ELM (extreme learning machine), SVM (support vector machine) and lssvm (least square SVM) forecasts using a GPR (gaussian process regression) model,” *Energy*, vol. 93, pp. 41–56, 2015. [14](#)
- [61] P. Campbell and K. Adamson, “A novel approach to wind forecasting in the United Kingdom and Ireland,” *International Journal Of Simulation Systems*, vol. 6, no. 12-13, pp. 1–10, 2005. [14](#)

- [62] P. J. Brockwell and R. A. Davis, *Time Series: Theory and Methods*, 2nd ed., ser. Springer Series in Statistics. New York: Springer-Verlag, 1991. [14](#)
- [63] W. Wangdee and R. Billinton, “Considering load-carrying capability and wind speed correlation of WECS in generation adequacy assessment,” *IEEE Transactions on Energy Conversion*, vol. 21, no. 3, pp. 734–741, 2006. [14](#)
- [64] K. Xie and R. Billinton, “Considering wind speed correlation of WECS in reliability evaluation using the time-shifting technique,” *Electric Power Systems Research*, vol. 79, no. 4, pp. 687–693, 2009. [14](#)
- [65] J. L. Torres, A. Garcia, M. De Blas, and A. De Francisco, “Forecast of hourly average wind speed with arma models in navarre (spain),” *Solar energy*, vol. 79, no. 1, pp. 65–77, 2005. [14](#)
- [66] H. Lütkepohl, *New Introduction to Multiple Time Series Analysis*. Springer Publishing Company, Incorporated, 2007. [14](#), [18](#), [25](#)
- [67] X. De Luna and M. G. Genton, “Predictive spatio-temporal models for spatially sparse enviromental data,” *Statistica Sinica*, pp. 547–568, 2005. [14](#)
- [68] E. M. Constantinescu, V. M. Zavala, M. Rocklin, S. Lee, and M. Anitescu, “A computational framework for uncertainty quantification and stochastic optimization in unit commitment with wind power generation,” *IEEE Transactions on Power Systems*, vol. 26, no. 1, pp. 431–441, 2010. [14](#)
- [69] F. Van Hulle, J. O. Tande, K. Uhlen, L. Warland, M. Korpås, P. Meibom *et al.*, “Integrating wind: Developing europe’s power market for the large-scale integration of wind power,” *European Wind Energy Association, Brussels, Belgium, TradeWind final report*, 2009. [14](#)
- [70] M. S. Miranda and R. W. Dunn, “Spatially correlated wind speed modelling for generation adequacy studies in the UK,” in *2007 IEEE power engineering society general meeting*. IEEE, 2007, pp. 1–6. [15](#)
- [71] Y. Zhao, L. Ye, P. Pinson, Y. Tang, and P. Lu, “Correlation-constrained and sparsity-controlled vector autoregressive model for spatio-temporal wind power forecasting,” *IEEE Transactions on Power Systems*, vol. 33, no. 5, pp. 5029–5040, 2018. [15](#)
- [72] A. Papavasiliou, S. S. Oren, and I. Aravena, “Stochastic modeling of multi-area wind power production,” in *2015 48th Hawaii International Conference on System Sciences*. IEEE, 2015, pp. 2616–2626. [15](#), [16](#)
- [73] B. G. Brown, R. W. Katz, and A. H. Murphy, “Time series models to simulate and forecast wind speed and wind power,” *Journal of Applied Meteorology and Climatology*, vol. 23, no. 8, pp. 1184–1195, 1984. [15](#)

- [74] J. Olauson, M. Bergkvist, and J. Rydén, “Simulating intra-hourly wind power fluctuations on a power system level,” *Wind Energy*, vol. 20, no. 6, pp. 973–985, 2017. [16](#)
- [75] M. Koivisto, G. M. Jónsdóttir, P. Sørensen, K. Plakas, and N. Cutululis, “Combination of meteorological reanalysis data and stochastic simulation for modelling wind generation variability,” *Renewable Energy*, vol. 159, pp. 991–999, 2020. [16](#)
- [76] R. Friedrich and J. Peinke, “Description of a turbulent cascade by a Fokker-Planck equation,” *Physical Review Letters*, vol. 78, no. 5, p. 863, 1997. [16](#)
- [77] M. Ragwitz and H. Kantz, “Indispensable finite time corrections for Fokker-Planck equations from time series data,” *Physical Review Letters*, vol. 87, no. 25, p. 254501, 2001. [16](#)
- [78] R. R. Sundararajan and M. Pourahmadi, “Nonparametric change point detection in multivariate piecewise stationary time series,” *Journal of Nonparametric Statistics*, vol. 30, no. 4, pp. 926–956, 2018. [16](#), [23](#)
- [79] D. Brillinger, *Time Series*. Society for Industrial and Applied Mathematics, 2001. [16](#), [26](#)
- [80] C. Jentsch and S. Subba Rao, “A test for second order stationarity of a multivariate time series,” *Journal of Econometrics*, vol. 185, no. 1, pp. 124 – 161, 2015. [18](#)
- [81] M. Talih and N. Hengartner, “Structural learning with time-varying components: tracking the cross-section of financial time series,” *Journal of the Royal Statistical Society: Series B (Statistical Methodology)*, vol. 67, no. 3, pp. 321–341, 2005. [23](#)
- [82] V. Muggeo and G. Adelfio, “Efficient change point detection for genomic sequences of continuous measurements,” *Bioinformatics (Oxford, England)*, vol. 27, pp. 161–6, 11 2010. [23](#)
- [83] R. J. Bolton and D. J. Hand, “Statistical Fraud Detection: A Review,” *Statistical Science*, vol. 17, no. 3, pp. 235 – 255, 2002. [23](#)
- [84] J. Chen and A. K. Gupta, “Testing and locating variance changepoints with application to stock prices,” *Journal of the American Statistical association*, vol. 92, no. 438, pp. 739–747, 1997. [23](#)
- [85] L. Perreault, J. Bernier, B. Bobée, and E. Parent, “Bayesian change-point analysis in hydrometeorological time series. part 1. the normal model revisited,” *Journal of Hydrology*, vol. 235, no. 3, pp. 221–241, 2000. [23](#)
- [86] D. S. Matteson and N. A. James, “A nonparametric approach for multiple change point analysis of multivariate data,” *Journal of the American Statistical Association*, vol. 109, no. 505, pp. 334–345, 2014. [23](#)

- [87] P. Preuss, R. Puchstein, and H. Dette, “Detection of multiple structural breaks in multivariate time series,” *Journal of the American Statistical Association*, vol. 110, no. 510, pp. 654–668, 2015. [23](#)
- [88] D. S. Matteson and N. A. James, “A nonparametric approach for multiple change point analysis of multivariate data,” *Journal of the American Statistical Association*, vol. 109, no. 505, pp. 334–345, 2014. [23](#)
- [89] J.-P. Kreiss, “Bootstrap procedures for ar (∞) — processes,” in *Bootstrapping and Related Techniques: Proceedings of an International Conference, Held in Trier, FRG, June 4–8, 1990*, K.-H. Jöckel, G. Rothe, and W. Sendler, Eds. Berlin, Heidelberg: Springer Berlin Heidelberg, 1992, pp. 107–113. [25](#)
- [90] D. N. Politis and J. P. Romano, “The stationary bootstrap,” *Journal of the American Statistical Association*, vol. 89, no. 428, pp. 1303–1313, 1994. [26](#)
- [91] D. N. Politis and H. White, “Automatic block-length selection for the dependent bootstrap,” *Econometric Reviews*, vol. 23, pp. 53–70, 2004. [26](#)
- [92] W. S. Cleveland and S. J. Devlin, “Locally weighted regression: An approach to regression analysis by local fitting,” *Journal of the American Statistical Association*, vol. 83, no. 403, pp. 596–610, 1988. [26](#)
- [93] A. M. D. Livera, R. J. Hyndman, and R. D. Snyder, “Forecasting time series with complex seasonal patterns using exponential smoothing,” *Journal of the American Statistical Association*, vol. 106, no. 496, pp. 1513–1527, 2011. [27](#)
- [94] R. J. Hyndman, A. B. Koehler, R. D. Snyder, and S. Grose, “A state space framework for automatic forecasting using exponential smoothing methods,” *International Journal of forecasting*, vol. 18, no. 3, pp. 439–454, 2002. [27](#), [30](#)
- [95] R. D. Christie, “Power systems test case archive,” <http://www.ee.washington.edu/research/pstca/>, 08 1999, Accessed: 2015-08-01. [35](#)
- [96] PJM, “Pjm manual 11: Energy and ancillary services market operations,” Day-Ahead and Real-Time Market Operations, PJM, Tech. Rep., 2022. [42](#)
- [97] D. K. Molzahn, I. A. Hiskens *et al.*, “A survey of relaxations and approximations of the power flow equations,” 2019. [43](#)
- [98] G. Pritchard, G. Zakeri, and A. Philpott, “A single-settlement, energy-only electric power market for unpredictable and intermittent participants,” *Operations Research*, vol. 58, no. 4-part-2, pp. 1210–1219, 2010. [Online]. Available: <https://doi.org/10.1287/opre.1090.0800> [50](#), [71](#), [74](#)
- [99] S. Wang, H. Gangammanavar, S. D. Eksioğlu, and S. J. Mason, “Stochastic optimization for energy management in power systems with multiple microgrids,” *IEEE Transactions on Smart Grid*, vol. 10, no. 1, pp. 1068–1079, 2017. [79](#)

- [100] J. Nash, “Non-cooperative games,” *Annals of mathematics*, pp. 286–295, 1951. [79](#), [87](#)
- [101] A. Kannan, U. V. Shanbhag, and H. M. Kim, “Addressing supply-side risk in uncertain power markets: stochastic nash models, scalable algorithms and error analysis,” *Optimization Methods and Software*, vol. 28, no. 5, pp. 1095–1138, 2013. [79](#)
- [102] ——, “Strategic behavior in power markets under uncertainty,” *Energy Systems*, vol. 2, no. 2, pp. 115–141, 2011. [79](#)
- [103] D. Fudenberg, F. Drew, D. K. Levine, and D. K. Levine, *The theory of learning in games*. MIT press, 1998, vol. 2. [79](#)
- [104] T. Başar and G. J. Olsder, *Dynamic noncooperative game theory*. SIAM, 1998. [79](#)
- [105] N. Nisan, M. Schapira, G. Valiant, and A. Zohar, “Best-response mechanisms.” in *ICS*, 2011, pp. 155–165. [79](#)
- [106] J. Lei, U. V. Shanbhag, J.-S. Pang, and S. Sen, “On synchronous, asynchronous, and randomized best-response schemes for stochastic nash games,” *Mathematics of Operations Research*, vol. 45, no. 1, pp. 157–190, 2020. [79](#)
- [107] U. V. Shanbhag, J.-S. Pang, and S. Sen, “Inexact best-response schemes for stochastic nash games: Linear convergence and iteration complexity analysis,” in *2016 IEEE 55th Conference on Decision and Control (CDC)*. IEEE, 2016, pp. 3591–3596. [79](#)
- [108] J.-S. Pang, S. Sen, and U. V. Shanbhag, “Two-stage non-cooperative games with risk-averse players,” *Mathematical Programming*, vol. 165, no. 1, pp. 235–290, 2017. [79](#)
- [109] F. Facchinei, V. Piccialli, and M. Sciandrone, “Decomposition algorithms for generalized potential games,” *Computational Optimization and Applications*, vol. 50, no. 2, pp. 237–262, 2011. [79](#), [87](#)
- [110] D. d’Esopo, “A convex programming procedure,” *Naval Research Logistics Quarterly*, vol. 6, no. 1, pp. 33–42, 1959. [80](#)
- [111] P. Tseng, “Convergence of a block coordinate descent method for nondifferentiable minimization,” *Journal of optimization theory and applications*, vol. 109, no. 3, pp. 475–494, 2001. [80](#)
- [112] Y. Nesterov, “Efficiency of coordinate descent methods on huge-scale optimization problems,” *SIAM Journal on Optimization*, vol. 22, no. 2, pp. 341–362, 2012. [80](#)
- [113] P. Richtárik and M. Takáč, “Iteration complexity of randomized block-coordinate descent methods for minimizing a composite function,” *Mathematical Programming*, vol. 144, no. 1, pp. 1–38, 2014. [80](#)
- [114] B. Kocuk, S. S. Dey, and X. A. Sun, “Strong socp relaxations for the optimal power flow problem,” *Operations Research*, vol. 64, no. 6, pp. 1177–1196, 2016. [82](#)

- [115] S. Atakan, H. Gangammanavar, and S. Sen, “Towards a sustainable power grid: Stochastic hierarchical planning for high renewable integration,” *European Journal of Operational Research*, vol. 302, no. 1, pp. 381–391, 2022. [85](#)
- [116] T. Basar and G. J. Olsder, *Dynamic Noncooperative Game Theory*. SIAM, 1999, vol. 23. [87](#)
- [117] F. Facchinei and J.-S. Pang, “Nash equilibria: the variational approach,” *Convex optimization in signal processing and communications*, p. 443, 2010. [87](#)
- [118] R. D. Christie, “Power systems test case archive,” Online: <http://www.ee.washington.edu/research/pstca/>, 08 1999, Accessed: 2015-08-01. [91](#)
- [119] I. Dincer, “Renewable energy and sustainable development: a crucial review,” *Renewable and sustainable energy reviews*, vol. 4, no. 2, pp. 157–175, 2000.
- [120] H. Wang, Z. Lei, X. Zhang, B. Zhou, and J. Peng, “A review of deep learning for renewable energy forecasting,” *Energy Conversion and Management*, vol. 198, p. 111799, 2019.
- [121] R. H. Inman, H. T. Pedro, and C. F. Coimbra, “Solar forecasting methods for renewable energy integration,” *Progress in energy and combustion science*, vol. 39, no. 6, pp. 535–576, 2013.
- [122] G. Dany, “Power reserve in interconnected systems with high wind power production,” in *2001 IEEE Porto Power Tech Proceedings (Cat. No. 01EX502)*, vol. 4. IEEE, 2001, pp. 6–pp.
- [123] L. Dale, D. Milborrow, R. Slark, and G. Strbac, “Total cost estimates for large-scale wind scenarios in uk,” *Energy Policy*, vol. 32, no. 17, pp. 1949–1956, 2004.
- [124] F. Bouffard and F. D. Galiana, “Stochastic security for operations planning with significant wind power generation,” in *2008 IEEE Power and Energy Society General Meeting-Conversion and Delivery of Electrical Energy in the 21st Century*. IEEE, 2008, pp. 1–11.
- [125] M. V. Pereira and L. M. Pinto, “Multi-stage stochastic optimization applied to energy planning,” *Mathematical programming*, vol. 52, no. 1, pp. 359–375, 1991.
- [126] J. R. Birge, “Decomposition and partitioning methods for multistage stochastic linear programs,” *Operations research*, vol. 33, no. 5, pp. 989–1007, 1985.
- [127] A. L. Ott, “Experience with pjm market operation, system design, and implementation,” *IEEE Transactions on Power Systems*, vol. 18, no. 2, pp. 528–534, 2003.
- [128] P. R. Gribik, D. Chatterjee, N. Navid, and L. Zhang, “Dealing with uncertainty in dispatching and pricing in power markets,” in *2011 IEEE Power and Energy Society General Meeting*. IEEE, 2011, pp. 1–6.

- [129] E. Lorenz, J. Hurka, D. Heinemann, and H. G. Beyer, “Irradiance forecasting for the power prediction of grid-connected photovoltaic systems,” *IEEE Journal of selected topics in applied earth observations and remote sensing*, vol. 2, no. 1, pp. 2–10, 2009.
- [130] J. L. Torres, A. Garcia, M. De Blas, and A. De Francisco, “Forecast of hourly average wind speed with arma models in navarre (spain),” *Solar energy*, vol. 79, no. 1, pp. 65–77, 2005.
- [131] Y. Guo, C. Chen, and L. Tong, “Pricing multi-interval dispatch under uncertainty part i: Dispatch-following incentives,” *arXiv preprint arXiv:1911.05784*, 2019.
- [132] C. Chen, Y. Guo, and L. Tong, “Pricing multi-interval dispatch under uncertainty part ii: Generalization and performance,” *IEEE Transactions on Power Systems*, 2020.
- [133] C. A. Sima, G. C. Lazaroiu, V. Dumbrava, and M. Costoiu, “A deterministic approach for generation expansion planning optimization,” in *2018 IEEE PES Innovative Smart Grid Technologies Conference Europe (ISGT-Europe)*. IEEE, 2018, pp. 1–6.
- [134] J. O. Royset, “Good and bad optimization models: Insights from rockafellians,” in *Tutorials in Operations Research: Emerging Optimization Methods and Modeling Techniques with Applications*. INFORMS, 2021, pp. 131–160.
- [135] C. Jentsch and M. Pauly, “Testing equality of spectral densities using randomization techniques,” *Bernoulli*, vol. 21, no. 2, pp. 697–739, 2015.
- [136] J. Torres, A. García, M. De Blas, and A. De Francisco, “Forecast of hourly average wind speed with arma models in navarre (spain),” *Solar Energy*, vol. 79, no. 1, pp. 65–77, 2005. [Online]. Available: <https://www.sciencedirect.com/science/article/pii/S0038092X04002877>
- [137] R. Billinton, H. Chen, and R. Ghajar, “Time-series models for reliability evaluation of power systems including wind energy,” *Microelectronics Reliability*, vol. 36, no. 9, pp. 1253–1261, 1996.
- [138] H. Gangammanavar, “Multiple timescale stochastic optimization with application to integrating renewable resources in power systems,” Ph.D. dissertation, The Ohio State University, 2013.
- [139] M. A. Mohandes, T. O. Halawani, S. Rehman, and A. A. Hussain, “Support vector machines for wind speed prediction,” *Renewable energy*, vol. 29, no. 6, pp. 939–947, 2004.
- [140] M. Monfared, H. Rastegar, and H. M. Kojabadi, “A new strategy for wind speed forecasting using artificial intelligent methods,” *Renewable energy*, vol. 34, no. 3, pp. 845–848, 2009.

- [141] R. T. Rockafellar and R. J. Wets, “On the interchange of subdifferentiation and conditional expectation for convex functionals,” *Stochastics: An International Journal of Probability and Stochastic Processes*, vol. 7, no. 3, pp. 173–182, 1982.
- [142] S. Adak, “Time-dependent spectral analysis of nonstationary time series,” *Journal of the American Statistical Association*, vol. 93, no. 444, pp. 1488–1501, 1998.
- [143] H. R. Kunsch, “The Jackknife and the Bootstrap for General Stationary Observations,” *The Annals of Statistics*, vol. 17, no. 3, pp. 1217 – 1241, 1989. [Online]. Available: <https://doi.org/10.1214/aos/1176347265>
- [144] D. N. Politis and H. White, “Automatic block-length selection for the dependent bootstrap,” *Econometric Reviews*, vol. 23, no. 1, pp. 53–70, 2004. [Online]. Available: <https://doi.org/10.1081/ETC-120028836>
- [145] D. V. Hinkley, “Inference about the change-point in a sequence of random variables,” 1970.
- [146] J. P. Hennessey Jr, “Some aspects of wind power statistics,” *Journal of Applied Meteorology and Climatology*, vol. 16, no. 2, pp. 119–128, 1977.
- [147] J. M. Morales, R. Minguez, and A. J. Conejo, “A methodology to generate statistically dependent wind speed scenarios,” *Applied Energy*, vol. 87, no. 3, pp. 843–855, 2010.
- [148] A. Staid, J.-P. Watson, R. J.-B. Wets, and D. L. Woodruff, “Generating short-term probabilistic wind power scenarios via nonparametric forecast error density estimators,” *Wind Energy*, vol. 20, no. 12, pp. 1911–1925, 2017.
- [149] I. Rios, R. J. Wets, and D. L. Woodruff, “Multi-period forecasting and scenario generation with limited data,” *Computational Management Science*, vol. 12, no. 2, pp. 267–295, 2015.
- [150] F. J. Massey Jr, “The kolmogorov-smirnov test for goodness of fit,” *Journal of the American statistical Association*, vol. 46, no. 253, pp. 68–78, 1951.
- [151] A. M. Polansky, “Detecting change-points in Markov chains,” *Computational statistics & data analysis*, vol. 51, no. 12, pp. 6013–6026, 2007.
- [152] J. Chen and A. K. Gupta, *Parametric statistical change point analysis: with applications to genetics, medicine, and finance*. Springer Science & Business Media, 2011.
- [153] C. Jentsch and S. S. Rao, “A test for second order stationarity of a multivariate time series,” *Journal of Econometrics*, vol. 185, no. 1, pp. 124–161, 2015.
- [154] F. Abbaspourtorbati, A. J. Conejo, J. Wang, and R. Cherkaoui, “Pricing electricity through a stochastic non-convex market-clearing model,” *IEEE Transactions on Power Systems*, vol. 32, no. 2, pp. 1248–1259, 2016.

- [155] J. Zhao, T. Zheng, and E. Litvinov, “A multi-period market design for markets with intertemporal constraints,” *IEEE Transactions on Power Systems*, vol. 35, no. 4, pp. 3015–3025, 2019.
- [156] B. Hua, D. A. Schiro, T. Zheng, R. Baldick, and E. Litvinov, “Pricing in multi-interval real-time markets,” *IEEE Transactions on Power systems*, vol. 34, no. 4, pp. 2696–2705, 2019.
- [157] J. Higle and S. Sen, “Multistage stochastic convex programs: Duality and its implications,” *Annals of Operations Research*, vol. 142, pp. 129–146, 02 2006.
- [158] J. Kazempour, P. Pinson, and B. F. Hobbs, “A stochastic market design with revenue adequacy and cost recovery by scenario: Benefits and costs,” *IEEE Transactions on Power Systems*, vol. 33, no. 4, pp. 3531–3545, July 2018.
- [159] A. Daraeepour, D. Patino-Echeverri, and A. J. Conejo, “Economic and environmental implications of different approaches to hedge against wind production uncertainty in two-settlement electricity markets: A PJM case study,” *Energy Economics*, vol. 80, no. C, pp. 336–354, 2019. [Online]. Available: <https://ideas.repec.org/a/eee/eneeco/v80y2019icp336-354.html>
- [160] G. Zakeri, G. Pritchard, M. Bjorndal, and E. Bjørndal, “Pricing wind: A revenue adequate, cost recovering uniform price auction for electricity markets with intermittent generation,” *INFORMS Journal on Optimization*, vol. 1, 10 2018.
- [161] S. Martín, Y. Smeers, and J. A. Aguado, “A stochastic two settlement equilibrium model for electricity markets with wind generation,” *IEEE Transactions on Power Systems*, vol. 30, no. 1, pp. 233–245, Jan 2015.
- [162] M. Zugno and A. J. Conejo, “A robust optimization approach to energy and reserve dispatch in electricity markets,” *European Journal of Operational Research*, vol. 247, no. 2, pp. 659–671, 2015.
- [163] C. Jentsch and S. Subba Rao, “A test for second order stationarity of a multivariate time series,” *Journal of Econometrics*, vol. 185, no. 1, pp. 124 – 161, 2015.
- [164] R. R. Sundararajan and M. Pourahmadi, “Nonparametric change point detection in multivariate piecewise stationary time series,” *Journal of Nonparametric Statistics*, vol. 30, no. 4, pp. 926–956, 2018. [Online]. Available: <https://doi.org/10.1080/10485252.2018.1504943>
- [165] D. S. Matteson and N. A. James, “A nonparametric approach for multiple change point analysis of multivariate data,” *Journal of the American Statistical Association*, vol. 109, no. 505, pp. 334–345, 2014.
- [166] M. Garcia, H. Nagarajan, and R. Baldick, “Generalized convex hull pricing for the ac optimal power flow problem,” *IEEE Transactions on Control of Network Systems*, pp. 1–1, 2020.

- [167] R. Cory-Wright, A. Philpott, and G. Zakeri, “Payment mechanisms for electricity markets with uncertain supply,” *Operations Research Letters*, vol. 46, no. 1, pp. 116 – 121, 2018. [Online]. Available: <http://www.sciencedirect.com/science/article/pii/S016763771730305X>
- [168] H. Gangammanavar, S. Sen, and V. M. Zavala, “Stochastic optimization of sub-hourly economic dispatch with wind energy,” *IEEE Transactions on Power Systems*, vol. 31, no. 2, pp. 949–959, March 2016.
- [169] CAISO, “FERC order 764 compliance 15-minute scheduling and settlement,” *CAISO Report*, Mar. 2013.
- [170] R. T. Rockafellar and R. J. Wets, “Stochastic convex programming: relatively complete recourse and induced feasibility,” *SIAM Journal on Control and Optimization*, vol. 14, no. 3, pp. 574–589, 1976.
- [171] H. H. Bauschke, P. L. Combettes *et al.*, *Convex analysis and monotone operator theory in Hilbert spaces*. Springer, 2011, vol. 408.
- [172] C. Zalinescu, *Convex analysis in general vector spaces*. World scientific, 2002.
- [173] B. Wang and B. F. Hobbs, “A flexible ramping product: Can it help real-time dispatch markets approach the stochastic dispatch ideal?” *Electric Power Systems Research*, vol. 109, pp. 128–140, 2014.
- [174] Sources of greenhouse gas emissions. [Online]. Available: <https://www.epa.gov/ghgemissions/sources-greenhouse-gas-emissions#t1fn3>
- [175] N. Muralikrishnan, L. Jebaraj, and C. C. A. Rajan, “A comprehensive review on evolutionary optimization techniques applied for unit commitment problem,” *IEEE Access*, vol. 8, pp. 132 980–133 014, 2020.
- [176] R. P. O’Neill, T. Dautel, and E. Krall, “Recent iso software enhancements and future software and modeling plans,” *Federal Energy Regulatory Commission, Tech. Rep*, 2011.
- [177] J. Lei and U. V. Shanbhag, “Asynchronous schemes for stochastic and misspecified potential games and nonconvex optimization,” *Operations Research*, vol. 68, no. 6, pp. 1742–1766, 2020.
- [178] J. Driesen and F. Katiraei, “Design for distributed energy resources,” *IEEE power and energy magazine*, vol. 6, no. 3, pp. 30–40, 2008.
- [179] X. Fang, S. Misra, G. Xue, and D. Yang, “Smart grid—the new and improved power grid: A survey,” *IEEE communications surveys & tutorials*, vol. 14, no. 4, pp. 944–980, 2011.
- [180] S. K. Aggarwal, L. Saini, and A. Kumar, “Short term price forecasting in deregulated electricity markets: A review of statistical models and key issues,” *International Journal of Energy Sector Management*, 2009.

- [181] Y. Ye, D. Qiu, M. Sun, D. Papadaskalopoulos, and G. Strbac, “Deep reinforcement learning for strategic bidding in electricity markets,” *IEEE Transactions on Smart Grid*, vol. 11, no. 2, pp. 1343–1355, 2019.
- [182] A. S. Manne, “Waiting for the breeder,” *The Review of Economic Studies*, vol. 41, pp. 47–65, 1974.
- [183] G. Scutari and D. P. Palomar, “Mimo cognitive radio: A game theoretical approach,” *IEEE Transactions on Signal Processing*, vol. 58, no. 2, pp. 761–780, 2009.
- [184] J. Mays, D. P. Morton, and R. P. O’Neill, “Investment effects of pricing schemes for non-convex markets,” *European Journal of Operational Research*, vol. 289, no. 2, pp. 712–726, 2021.
- [185] New England ISO, “Business practices manual: Energy and operating reserve markets,” Tech. Rep., September 2017, retrieved from <https://www.misoenergy.org/legal/business-practice-manuals/>.
- [186] New York ISO, “Day-ahead scheduling manual,” Tech. Rep., October 2017. [Online]. Available: http://www.nyiso.com/public/webdocs/markets_operations/documents/Manuals_and_Guides/Manuals/Operations/dayahd_schd_mnl.pdf